

# Geometric Phases of the Uhlmann and Sjöqvist *et al* Types for $O(3)$ -Orbits of $n$ -Level Gibbsian Density Matrices

Paul B. Slater

ISBER, University of California, Santa Barbara, CA 93106-2150

e-mail: slater@itp.ucsb.edu, FAX: (805) 893-7995

(November 5, 2018)

We accept the implicit challenge of A. Uhlmann in his 1994 paper, “Parallel Lifts and Holonomy along Density Operators: Computable Examples Using  $O(3)$ -Orbits,” by, in fact, computing the holonomy invariants for rotations of certain  $n$ -level Gibbsian density matrices ( $n = 2, \dots, 11$ ). From these we derive, by the tracing operation, the associated geometric phases and visibilities, which we analyze and display. We then proceed analogously, implementing the alternative methodology presented by E. Sjöqvist *et al* in their letter, “Geometric Phases for Mixed States in Interferometry” (Phys. Rev. Lett. 85, 2845 [2000]). For the Uhlmann case, we are able to also compute several *higher-order* holonomy invariants. We compare the various geometric phases and visibilities for different values of  $n$ , and also directly compare the two forms of analysis. By setting one parameter ( $a$ ) in the Uhlmann analysis to zero, we find that the so-reduced form of the first-order holonomy invariant is simply equal to  $(-1)^{n+1}$  times the holonomy invariant in the Sjöqvist *et al* method. Additional phenomena of interest are reported too.

PACS Numbers 03.65.Vf, 05.30.-d, 05.70.-a

## Contents

<b>I</b>	<b>Introduction</b>	<b>1</b>
<b>II</b>	<b>Uhlmann geometric phases for Gibbsian <math>n</math>-level systems (<math>n = 2, \dots, 11</math>)</b>	<b>3</b>
<b>III</b>	<b>Uhlmann visibilities for Gibbsian <math>n</math>-level systems (<math>n = 2, \dots, 11</math>)</b>	<b>8</b>
<b>IV</b>	<b>Comparisons across Gibbsian <math>n</math>-level systems of Uhlmann geometric phases and visibilities</b>	<b>13</b>
<b>V</b>	<b>Higher-order Uhlmann holonomy invariants</b>	<b>16</b>
	A Traces of powers of Uhlmann holonomy invariants . . . . .	16
	B Cross-comparisons of Uhlmann holonomy invariants . . . . .	31
	C Eigenvalues of Uhlmann holonomy invariant for $n = 2, 3, 5$ . . . . .	32
<b>VI</b>	<b>Sjöqvist <i>et al</i> geometric phases for Gibbsian <math>n</math>-level systems (<math>n = 2, \dots, 11</math>)</b>	<b>41</b>
<b>VII</b>	<b>Sjöqvist <i>et al</i> visibilities for Gibbsian <math>n</math>-level systems (<math>n = 2, \dots, 11</math>)</b>	<b>48</b>
<b>VIII</b>	<b>Comparisons across Gibbsian <math>n</math>-level systems of Sjöqvist <i>et al</i> geometric phases and visibilities</b>	<b>53</b>
<b>IX</b>	<b>Direct comparisons of Uhlmann and Sjöqvist <i>et al</i> results</b>	<b>55</b>
<b>X</b>	<b>Summary</b>	<b>57</b>

## I. INTRODUCTION

In a recent paper, Sjöqvist *et al* [1] provided “a new formalism of the geometric phase for mixed states in the experimental context of quantum interferometry”. Only in passing, did these authors note that “Uhlmann was probably the first to address the issue of mixed state holonomy, but as a purely mathematical problem”.

Interested in possible (previously uninvestigated) relationships between the work of Sjöqvist *et al* [1] and that of Uhlmann [2,3], the present author compared the two approaches in terms of two spin- $\frac{1}{2}$  scenarios [4]. In the first of these, the spin- $\frac{1}{2}$  systems undergo unitary evolution along geodesic triangles [2], while in the second the unitary

evolution takes place along circular paths [3]. In [3], Uhlmann had also proposed an additional scenario, which was (initially) left unanalyzed in [4]. It involves “the Gibbsian states of the form”,

$$\rho = \frac{e^{\alpha \vec{n} \cdot \vec{J}}}{\text{trace } e^{\alpha \vec{n} \cdot \vec{J}}}, \quad (1)$$

which fill for a given value of  $\alpha$  a 2-sphere called  $\mathbf{S}_j^\alpha$  if  $\vec{n}$  runs through all directions in 3-space. Now, for the starting point of the unitary evolution, one sets  $\vec{n} = (0, 0, 1)$ , while  $\vec{n} = (0, \sin \theta, \cos \theta)$  is chosen as rotational axis. The curve of state evolution is given by

$$\phi \rightarrow U(\phi) \rho_0 U(-\phi), \quad U(\phi) = e^{-i\phi(\sin \theta J_y + \cos \theta J_z)}, \quad (2)$$

and the associated parallel lift of this curve with initial value  $\rho^{1/2}$  is

$$\phi \rightarrow U(\phi) \rho_0^{1/2} V(\phi), \quad V(\phi) = e^{i\phi \tilde{H}}, \quad (3)$$

where

$$\tilde{H} = \cos \theta J_z + a \sin \theta J_y, \quad \text{and} \quad a = \frac{1}{\cosh \frac{\alpha}{2}}. \quad (4)$$

It is possible to regard  $V(\phi)$  as a rotation with angle

$$\tilde{\phi} = \kappa \phi, \quad \kappa = \sqrt{\cos^2 \theta + a^2 \sin^2 \theta} \leq 1 \quad (5)$$

and rotation axis

$$\vec{\xi} = (0, \frac{\sin \theta}{\kappa}, \frac{a \cos \theta}{\kappa}). \quad (6)$$

The holonomy invariant can then be written as

$$(-1^{2j}) \rho_0^{1/2} e^{2\pi i \tilde{H}} \rho_0^{1/2} = (-1^{2j}) \rho_0^{1/2} e^{2\pi i \kappa} \vec{\xi} \cdot \vec{J} \rho_0^{1/2}. \quad (7)$$

(All the preceding equations are directly adopted from [2].)

In this paper, to begin, we compute the trace of this invariant (7) for all  $j = \frac{1}{2}, 1, \frac{3}{2}, \dots, \frac{9}{2}$ . We plot the arguments of these traces, that is the corresponding geometric phases  $(\gamma_j)$ , in Figs. 1 - 10 (sec. II), and their absolute values, that is the visibilities  $(\nu_j)$ , in Figs. 11 - 20 (sec. III). (For  $j = \frac{1}{2}$ , the results are equivalent to the first (non-Gibbsian) set of models in [2], which was compared with the analyses of Sjöqvist *et al* [1] in [4].) Let us note that the value  $\alpha = 0$  corresponds to the fully mixed (classical) state, while  $\alpha = \pm\infty$  correspond to pure states.

In sec. IV, we compare certain aspects of these results *across* the ten distinct values of  $n$ . All the various results up to this point can be considered as *first-order* in nature. In sec. V, on the other hand, we compute certain *higher-order* invariants. In secs. VI-VIII, we perform analyses precisely analogous to those in secs. II-IV, but now in terms not of the approach of Uhlmann to mixed state holonomy, but that of Sjöqvist *et al* [1]. In our final analytical section (sec. IX), before the summary (sec. X), we directly compare results obtained by the two different procedures.

One of our main findings is that if one sets the implicit parameter  $a$  in the Uhlmann holonomy invariant (7) to zero, then its resultant trace is simply equal to  $(-1)^{n+1}$  times the holonomy invariant [1, eq. (15)] yielded by the methodology of Sjöqvist *et al*.

## II. UHLMANN GEOMETRIC PHASES FOR GIBBSIAN $N$ -LEVEL SYSTEMS ( $N = 2, \dots, 11$ )

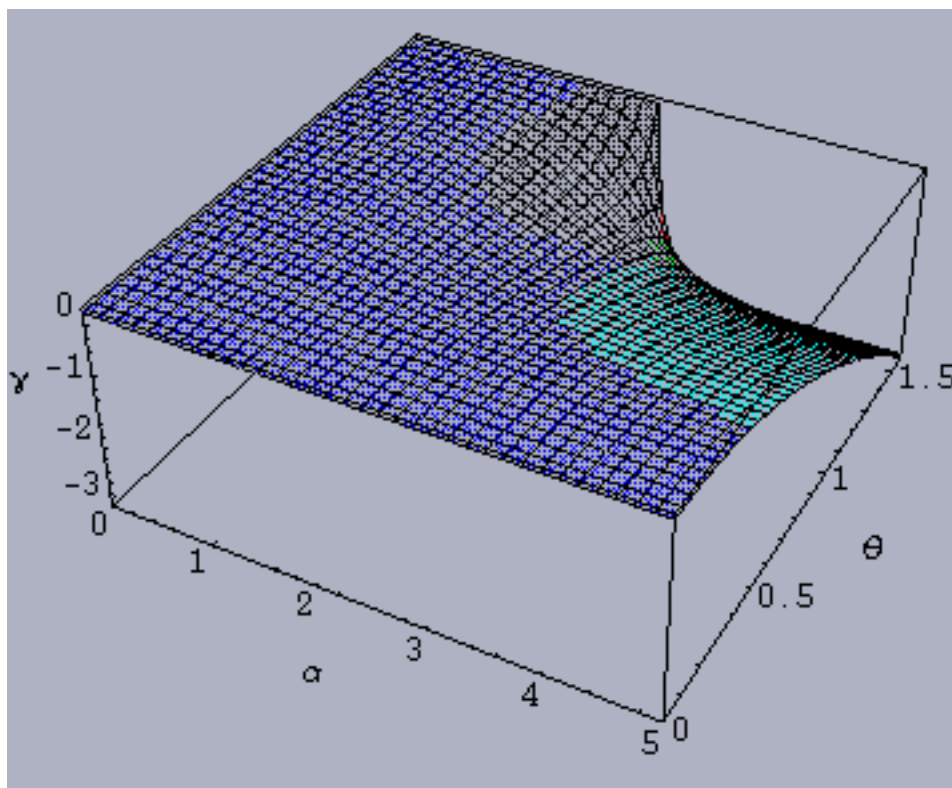


FIG. 1. Uhlmann geometric phase for Gibbsian spin- $\frac{1}{2}$  systems

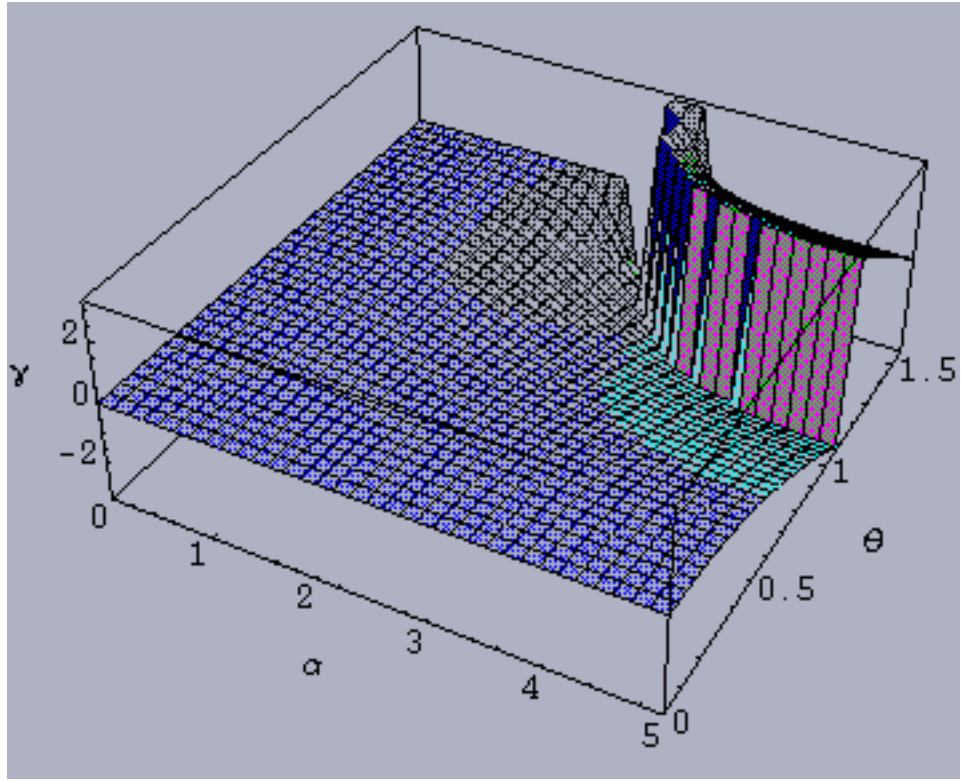


FIG. 2. Uhlmann geometric phase for Gibbsian spin-1 systems

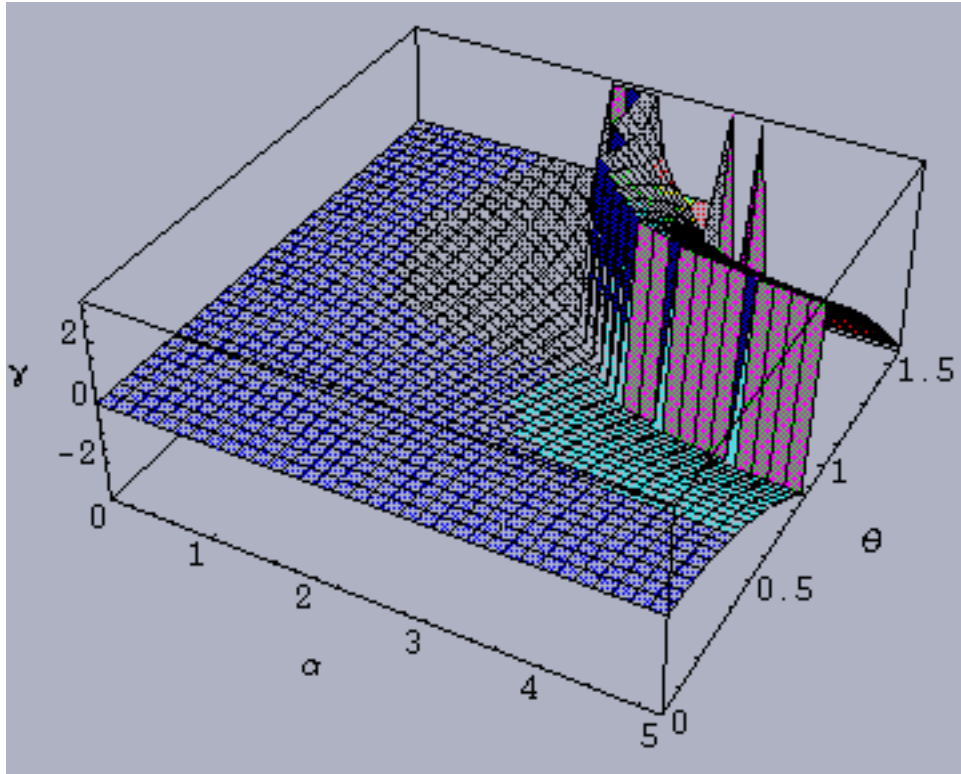


FIG. 3. Uhlmann geometric phase for Gibbsian spin- $\frac{3}{2}$  systems

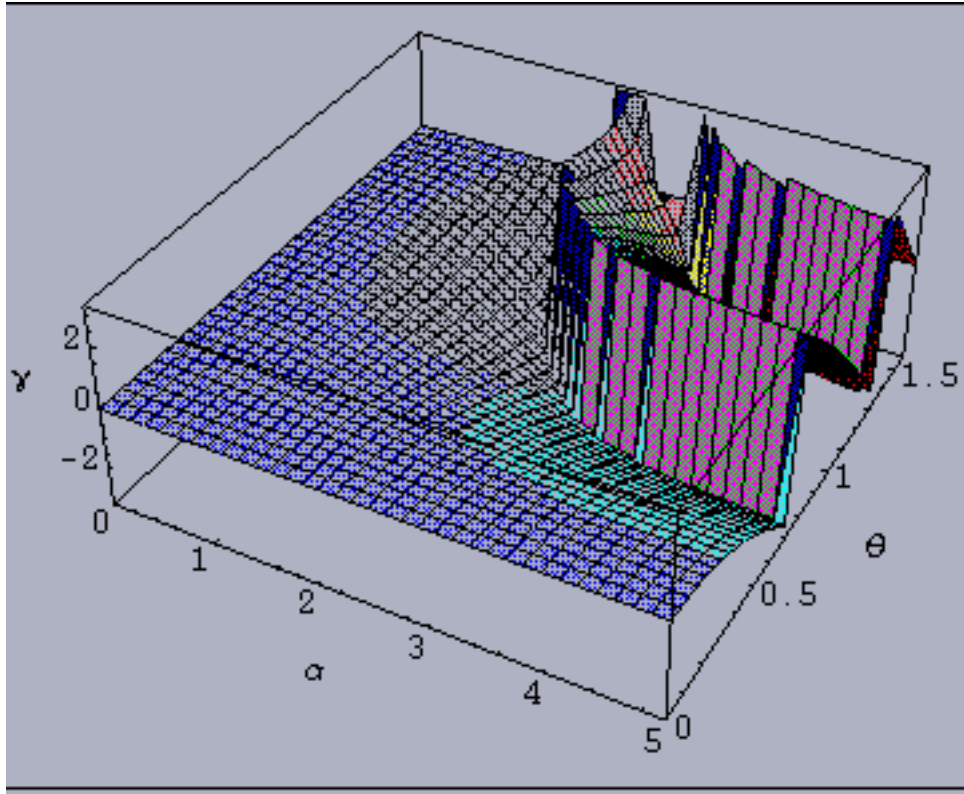


FIG. 4. Uhlmann geometric phase for Gibbsian spin-2 systems

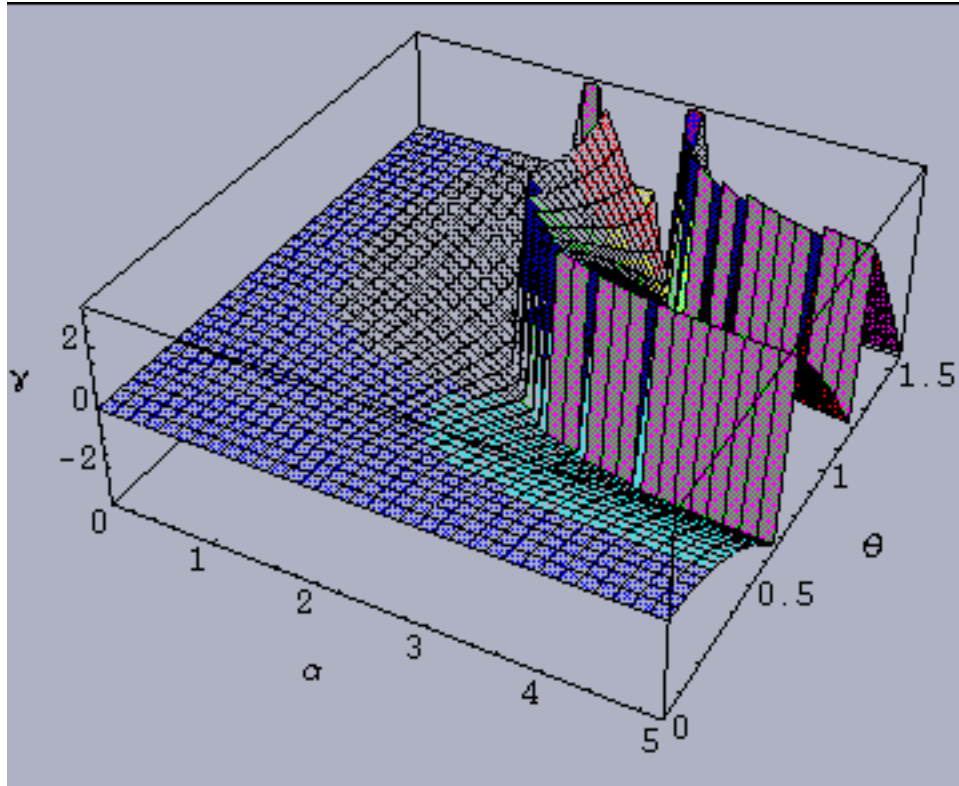


FIG. 5. Uhlmann geometric phase for Gibbsian spin- $\frac{5}{2}$  systems



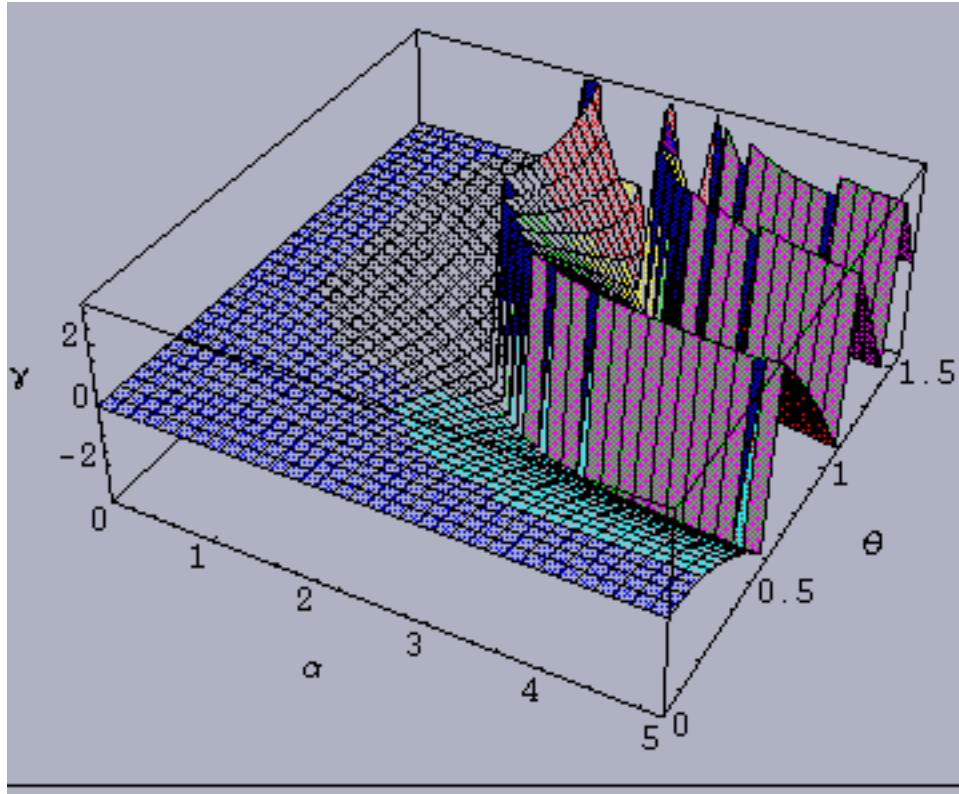


FIG. 6. Uhlmann geometric phase for Gibbsian spin-3 systems

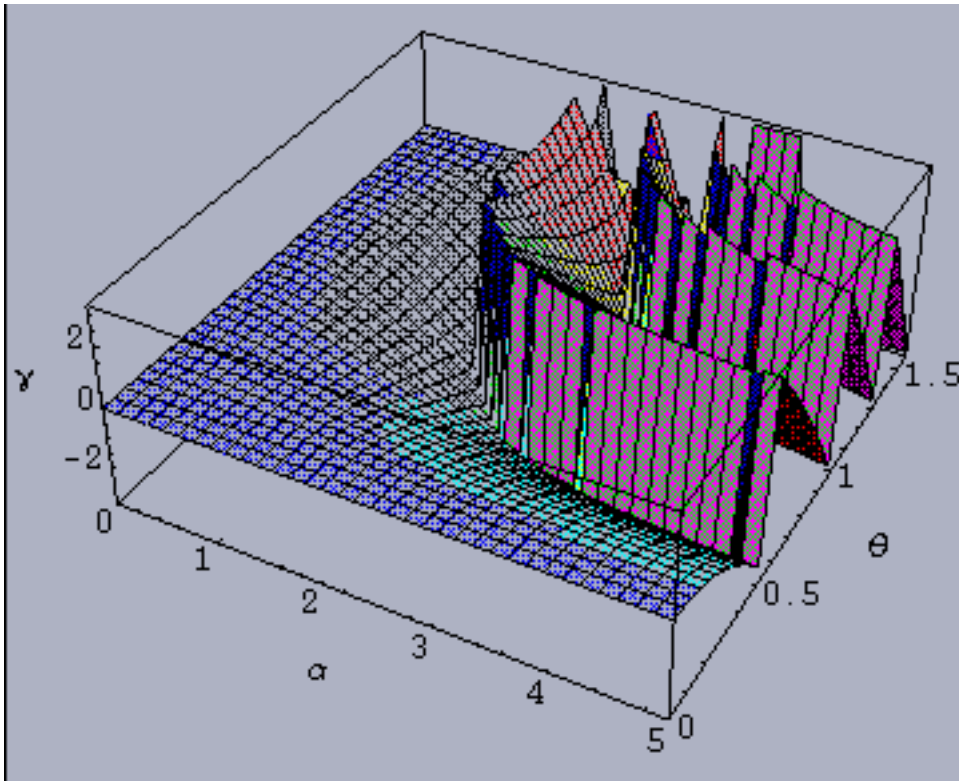


FIG. 7. Uhlmann geometric phase for Gibbsian spin- $\frac{7}{2}$  systems

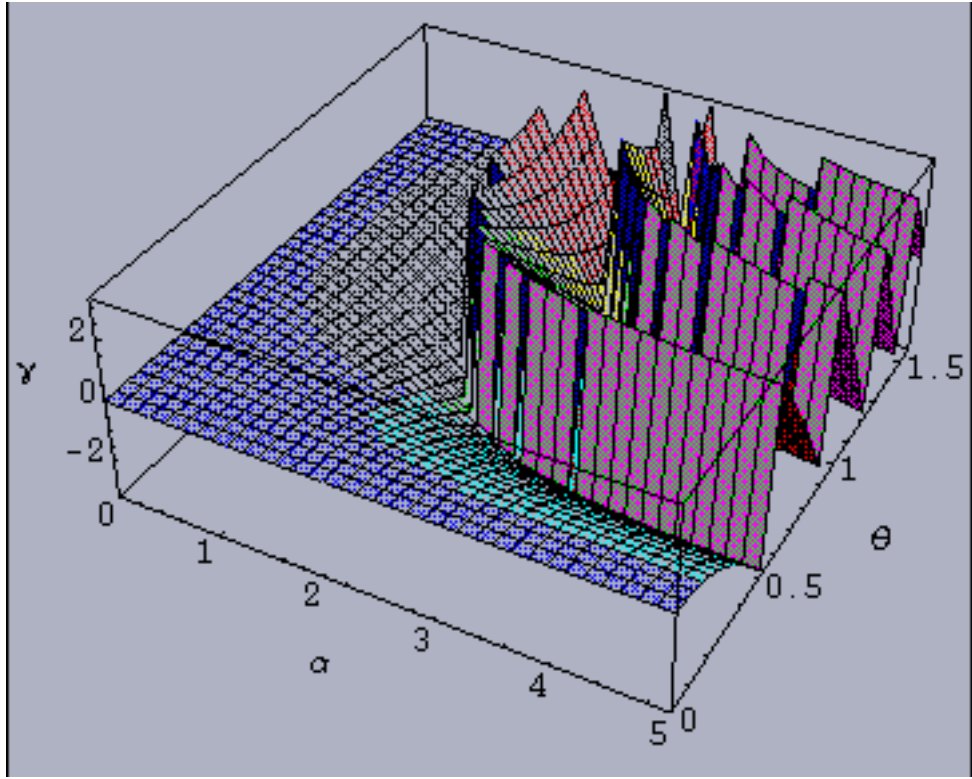


FIG. 8. Uhlmann geometric phase for Gibbsian spin-4 systems

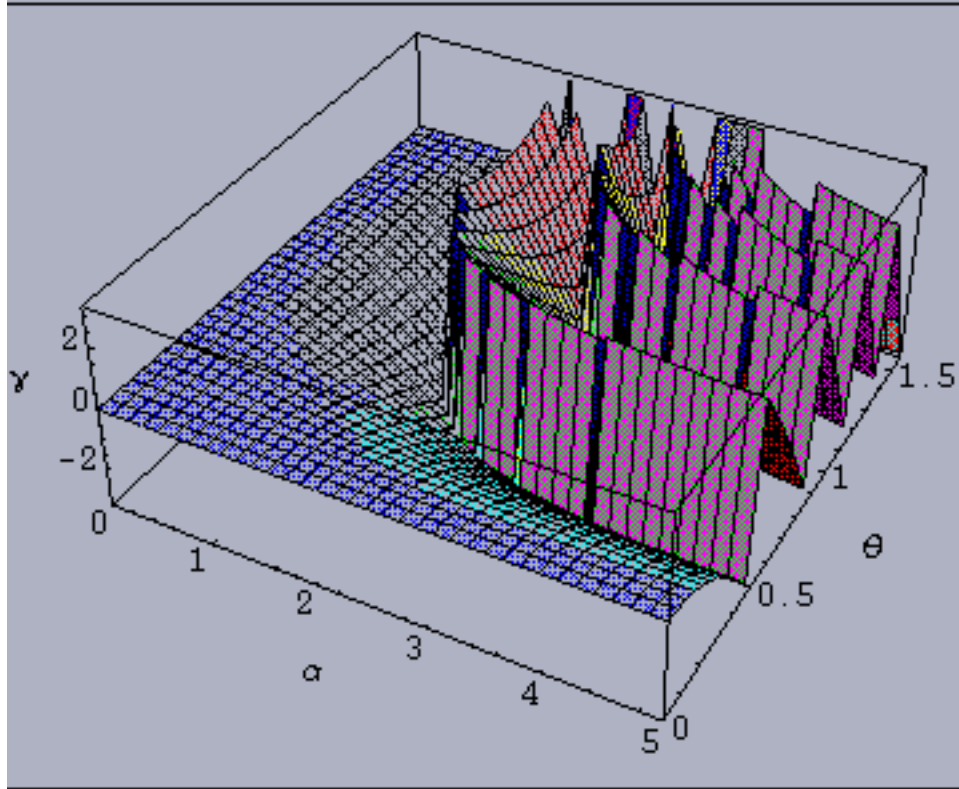


FIG. 9. Uhlmann geometric phase for Gibbsian spin- $\frac{9}{2}$  systems

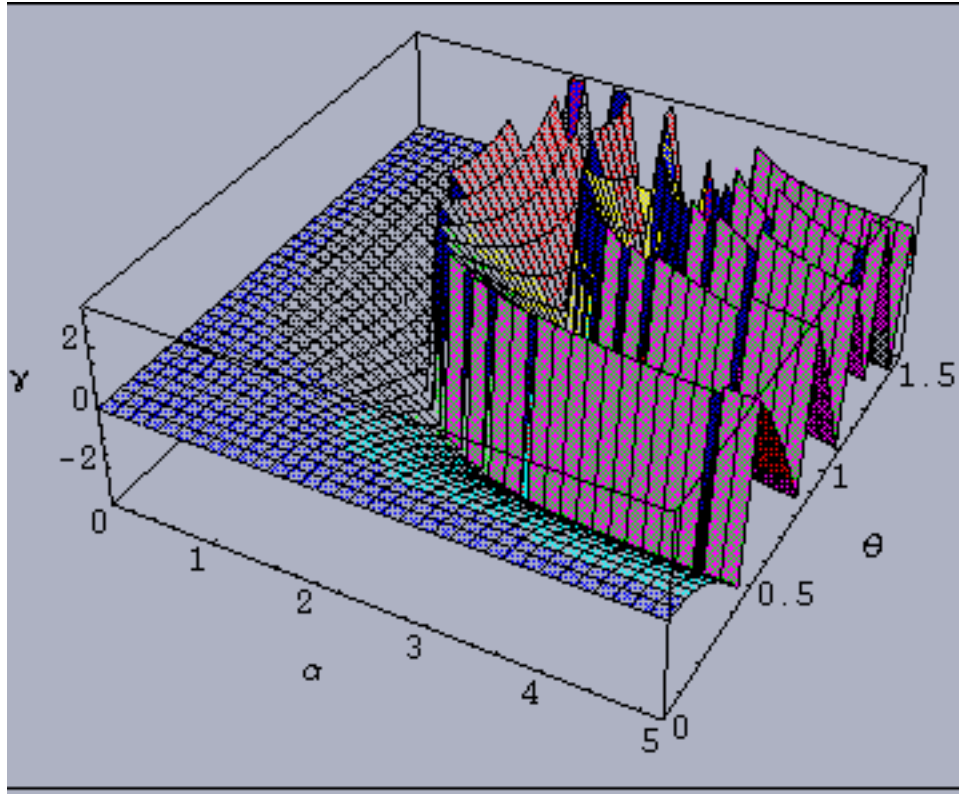


FIG. 10. Uhlmann geometric phase for Gibbsian spin-5 systems

### III. UHLMANN VISIBILITIES FOR GIBBSIAN $N$ -LEVEL SYSTEMS ( $N = 2, \dots, 11$ )

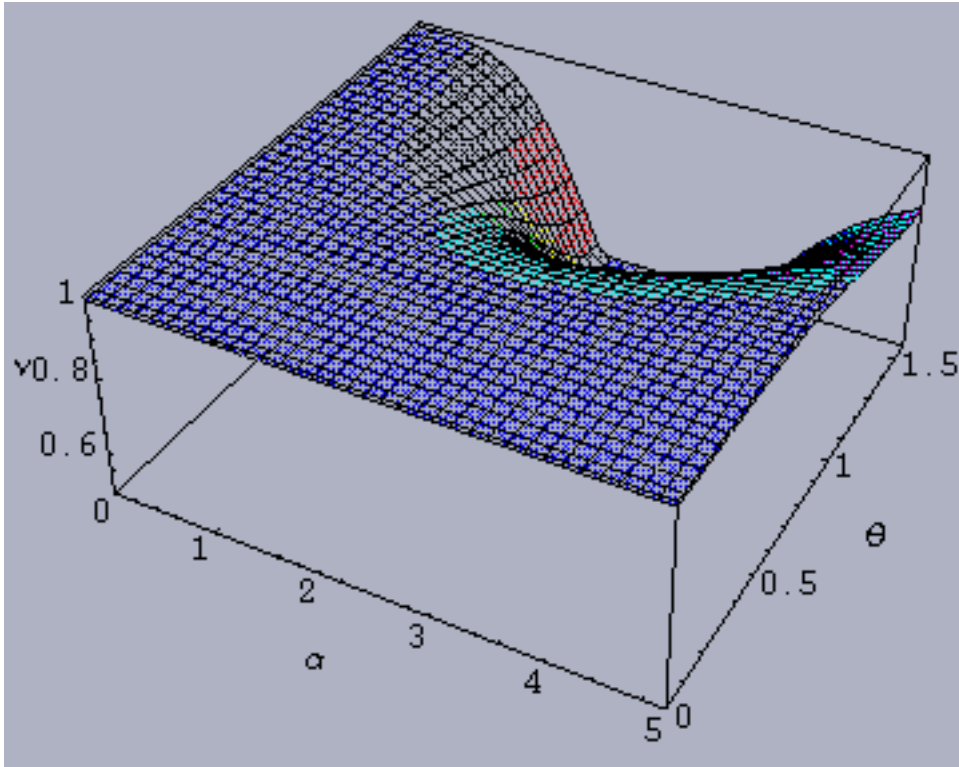


FIG. 11. Uhlmann visibility for Gibbsian spin- $\frac{1}{2}$  systems



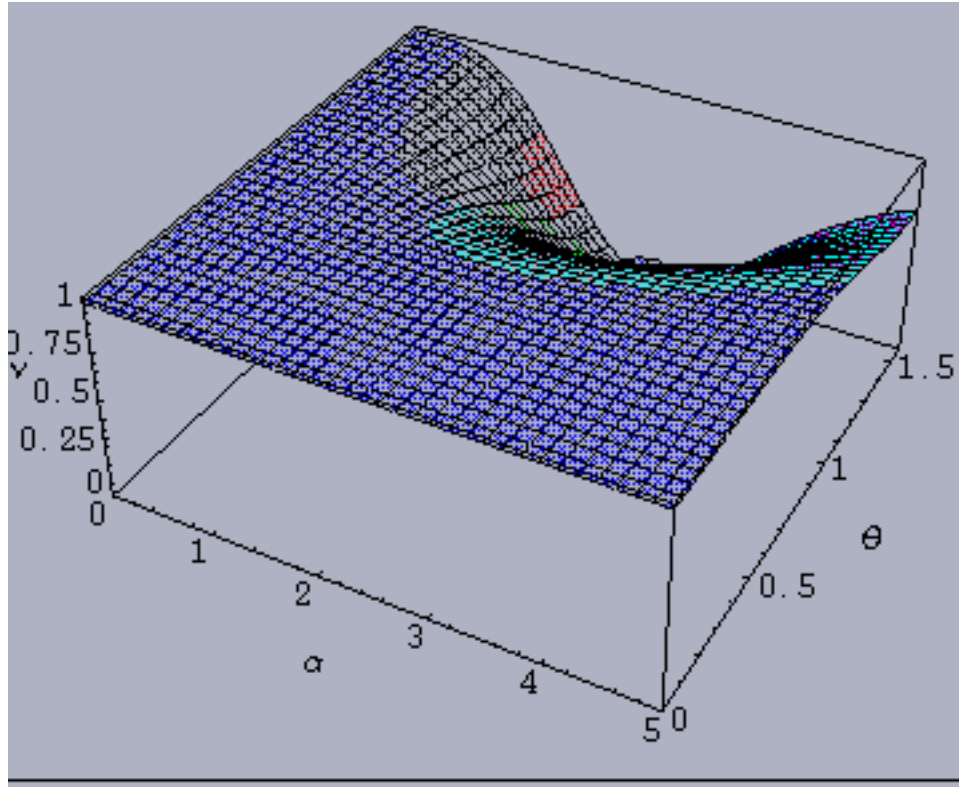


FIG. 12. Uhlmann visibility for Gibbsian spin-1 systems

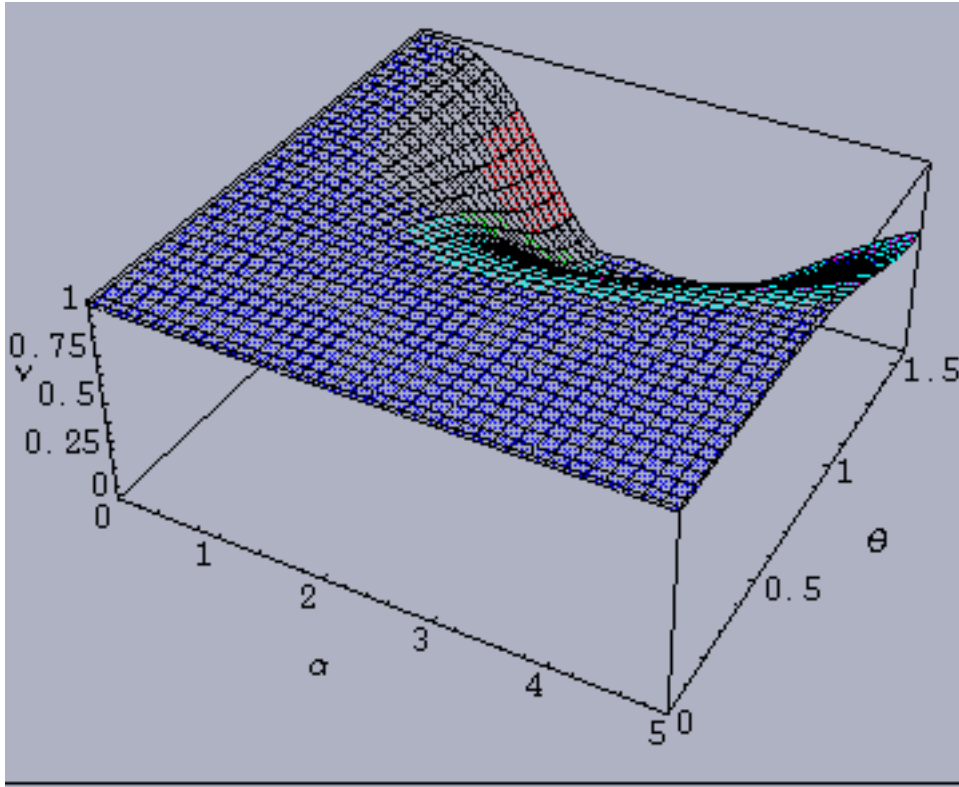


FIG. 13. Uhlmann visibility for Gibbsian spin- $\frac{3}{2}$  systems

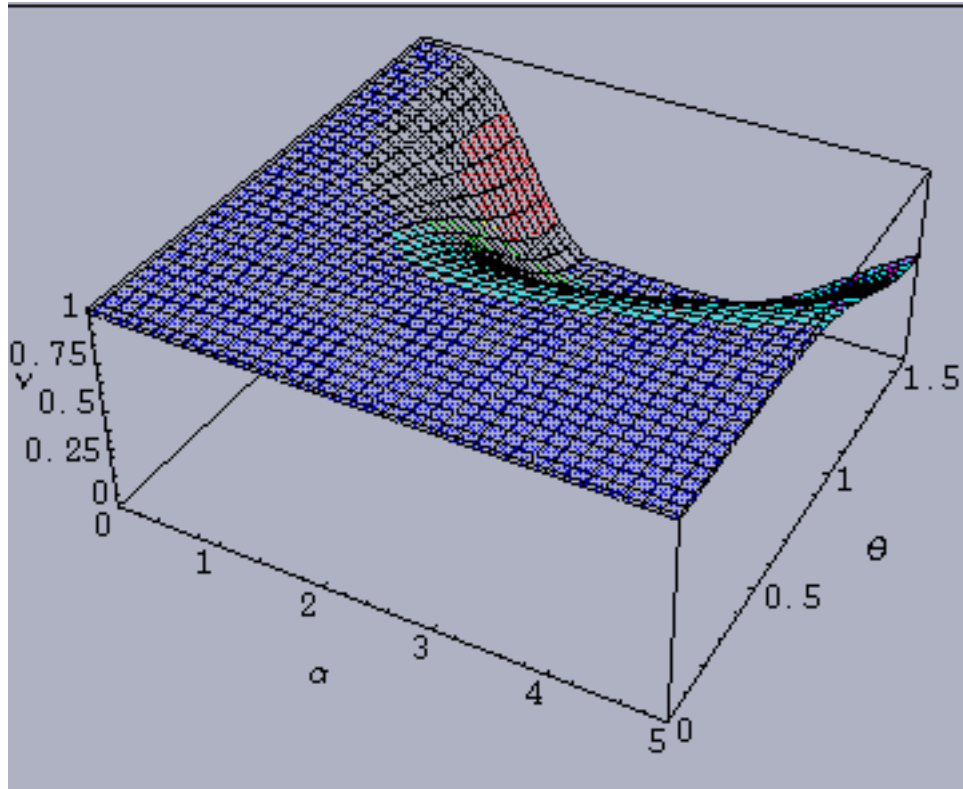


FIG. 14. Uhlmann visibility for Gibbsian spin-2 systems

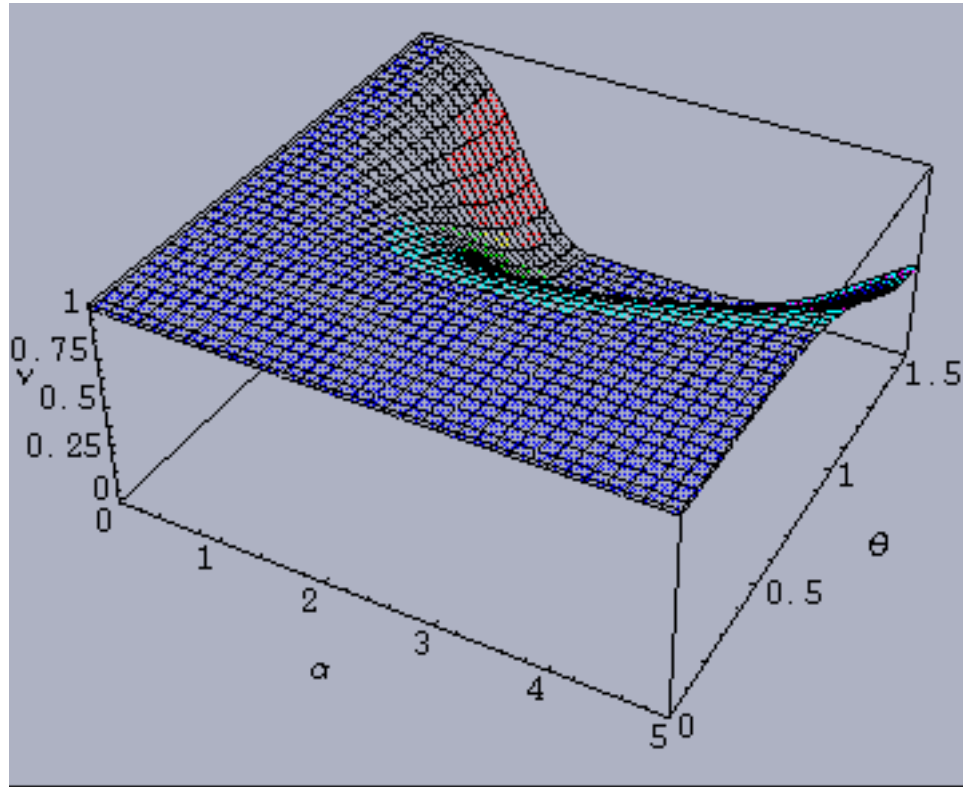


FIG. 15. Uhlmann visibility for Gibbsian spin- $\frac{5}{2}$  systems

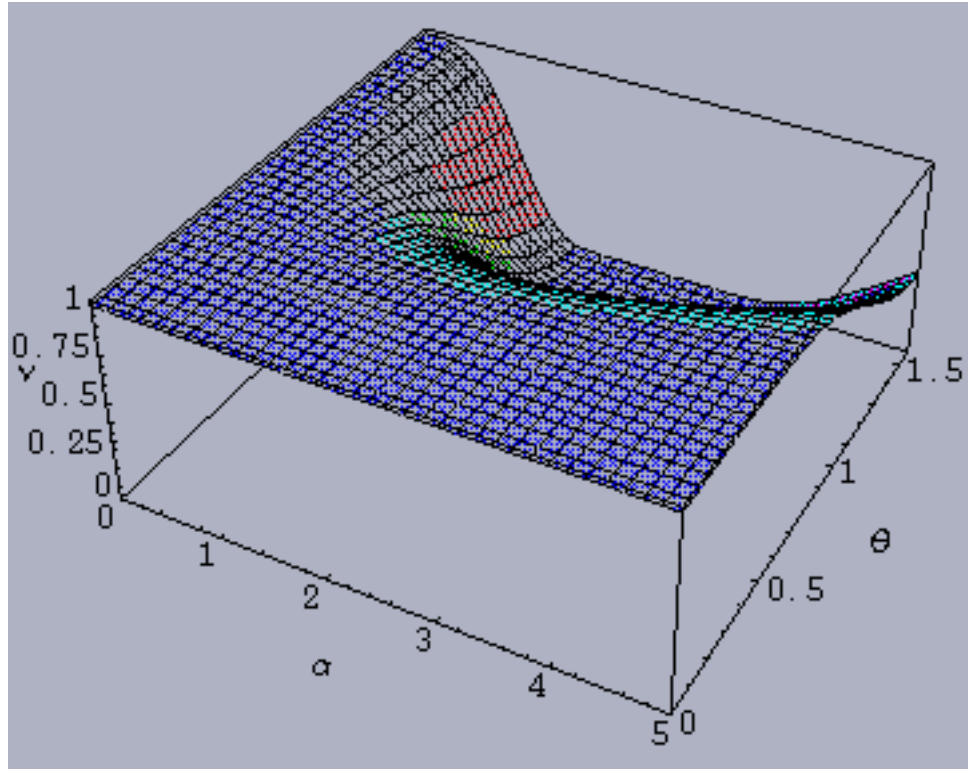


FIG. 16. Uhlmann visibility for Gibbsian spin-3 systems

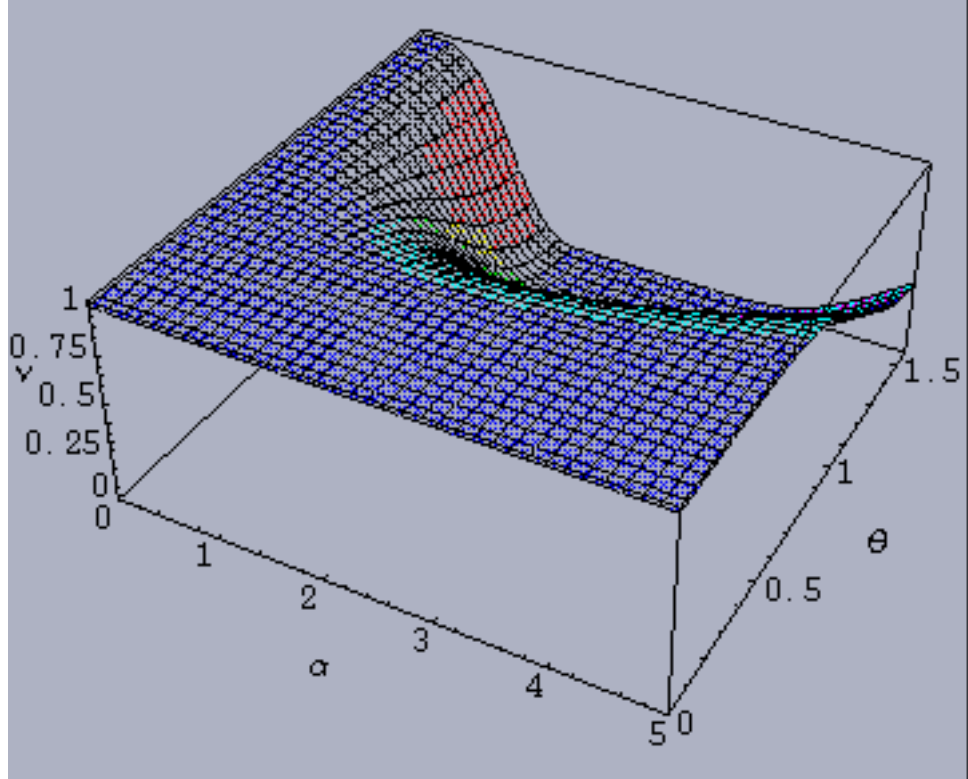


FIG. 17. Uhlmann visibility for Gibbsian spin- $\frac{7}{2}$  systems

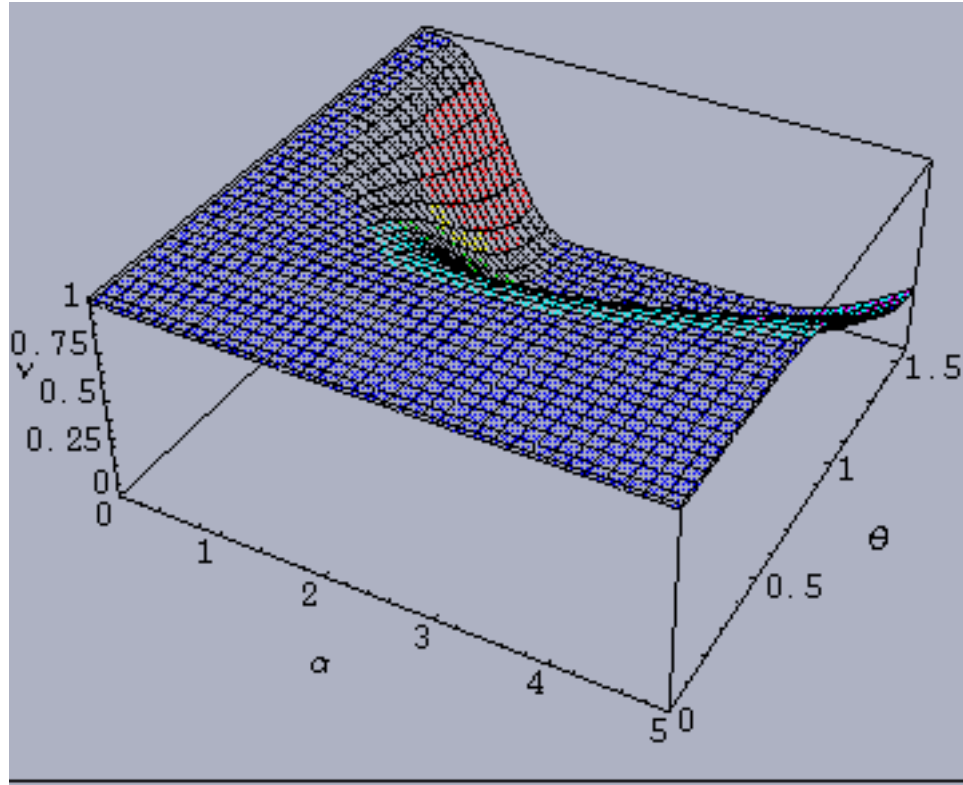


FIG. 18. Uhlmann visibility for Gibbsian spin-4 systems

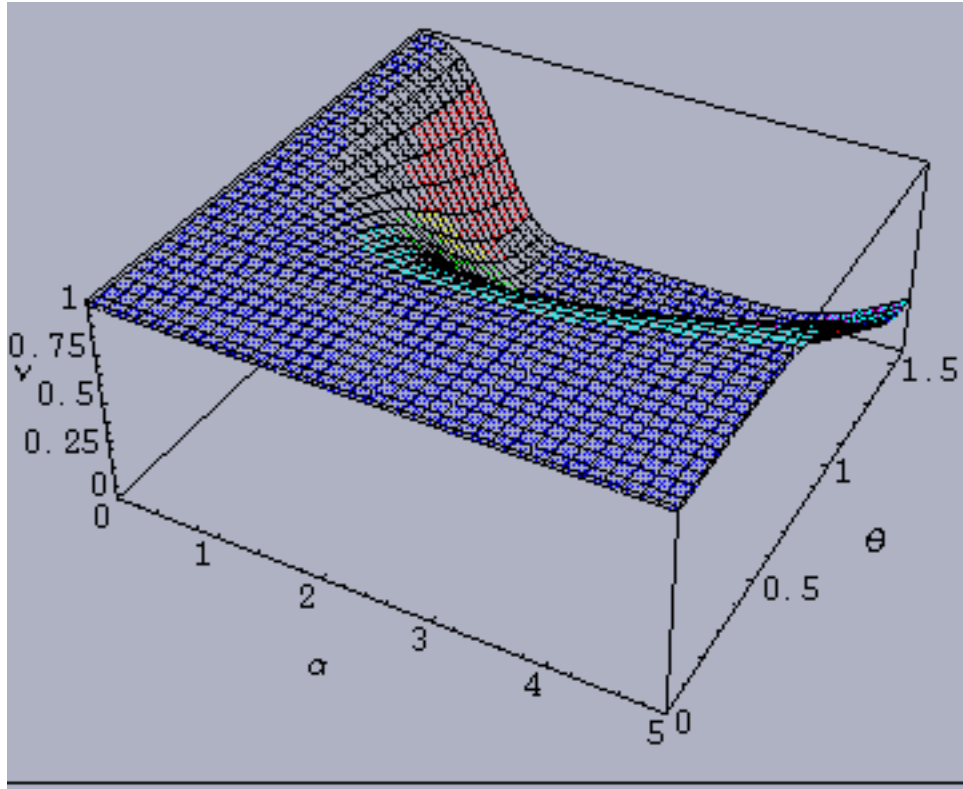


FIG. 19. Uhlmann visibility for Gibbsian spin- $\frac{9}{2}$ -systems



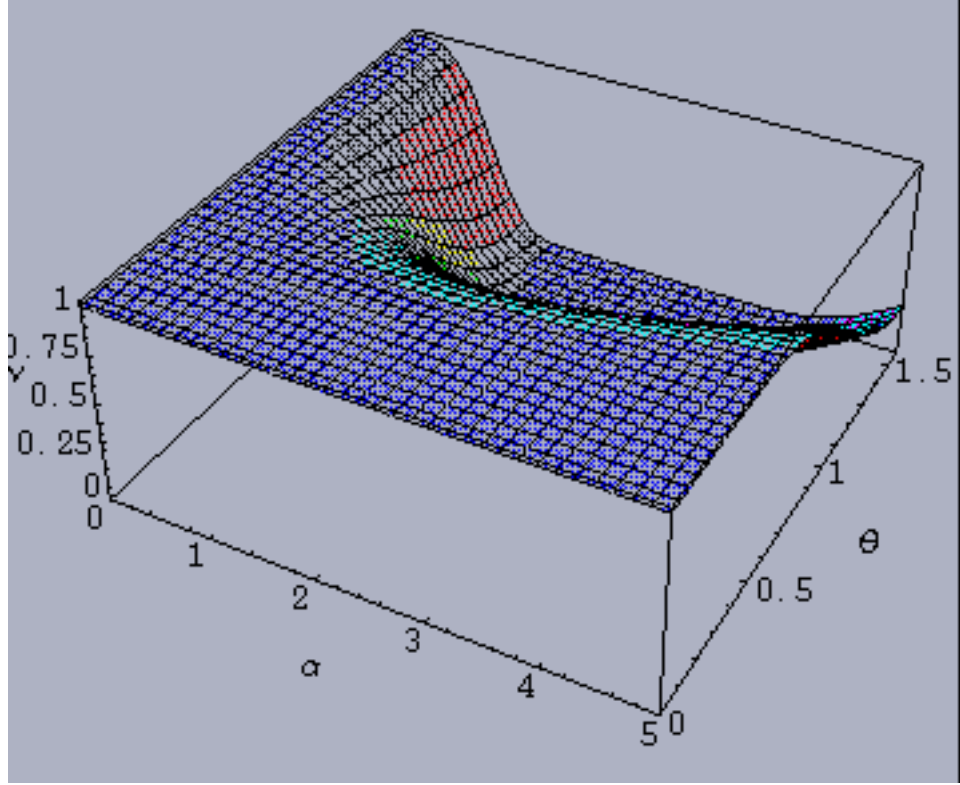


FIG. 20. Uhlmann visibility for Gibbsian spin-5 systems

#### IV. COMPARISONS ACROSS GIBBSIAN $N$ -LEVEL SYSTEMS OF UHLMANN GEOMETRIC PHASES AND VISIBILITIES

In the spin- $\frac{1}{2}$  case (Figs. 1 and 11), we have that the geometric phase  $\gamma_{\frac{1}{2}}$  is the arctangent of  $\frac{y}{x}$ , taking into account which quadrant the point  $(x, y)$  lies in, where

$$x = -\cosh i\pi\kappa, \quad y = -\frac{\cos\theta \sin\pi\kappa \tanh\frac{\alpha}{2}}{\kappa} \quad (8)$$

Also, the visibility in this spin- $\frac{1}{2}$  case is given by

$$\nu_{\frac{1}{2}} = \sqrt{1 + \frac{4 \sinh^2 i\pi\kappa}{\zeta}}, \quad (9)$$

where

$$\zeta = 3 - \cos 2\theta + 2 \cos^2 \theta \cosh \alpha, \quad (10)$$

and  $\kappa$  is as defined in (5). The comparable results in the spin-1 case (Figs. 2 and 12) are similarly based on

$$x = \frac{e^{-2i\pi\kappa} \left( 2(e^\alpha + 2e^{2i\pi\kappa} + e^{\alpha+4i\pi\kappa}) \cos^2 \theta + (2 + 2e^{4i\pi\kappa} + e^\alpha(1 + e^{2i\pi\kappa})^2) \operatorname{sech}^2 \frac{\alpha}{2} \sin^2 \theta \right)}{4\kappa^2(1 + 2 \cosh \alpha)}, \quad (11)$$

and

$$y = \frac{e^\alpha \cos \theta \sin 2\pi\kappa}{\kappa + 2\kappa \cos \alpha}. \quad (12)$$

One feature distinguishing the (strikingly similar) visibility plots (Figs. 11 - 20) from one another is that as  $j$  increases,  $\nu_j$  decreases at the (boundary) point  $\alpha = 5, \theta = \frac{\pi}{2}$ . For instance this value is .871618 in Fig. 11 and .498776 in Fig. 15.

In Fig. 21, we plot  $\gamma_j$  ( $j = \frac{1}{2}, \dots$ ) versus  $\theta$ , holding  $\alpha$  fixed at 1. Curves for lower-dimensional Gibbsian systems here strictly dominate those for higher-dimensional systems. (As  $\alpha$  increases, however, above certain thresholds for  $\theta$ , this simple monotonic behavior vanishes [cf. Fig. 24].)

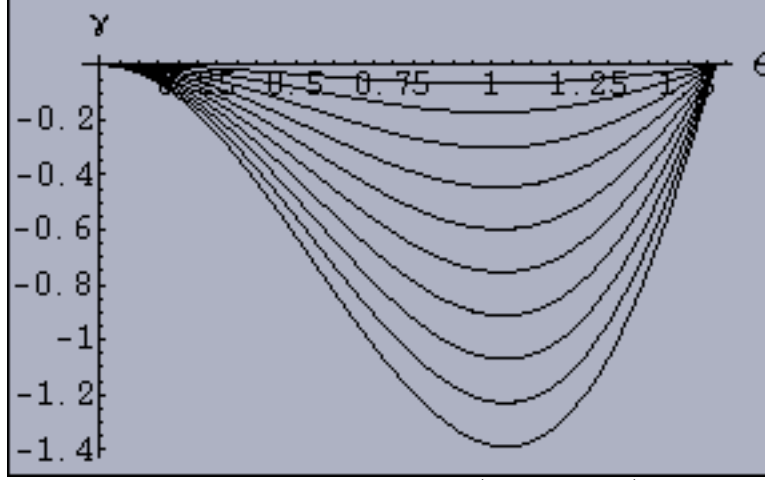


FIG. 21. Uhlmann geometric phases for  $n$ -level Gibbsian systems ( $n = 2, \dots, 11$ ) holding  $\alpha = 1$ . The curve for  $n = 2$  dominates that for  $n = 3$ , which dominates that for  $n = 4, \dots$

In Fig. 22, we “reverse” this scenario, now holding  $\theta$  fixed at  $\frac{\pi}{10}$  and letting  $\alpha$  vary over  $[0, 5]$ . The monotonicity of the ten curves is completely analogous to that in Fig. 21, with curves for lower  $j$  dominating those for higher  $j$ .

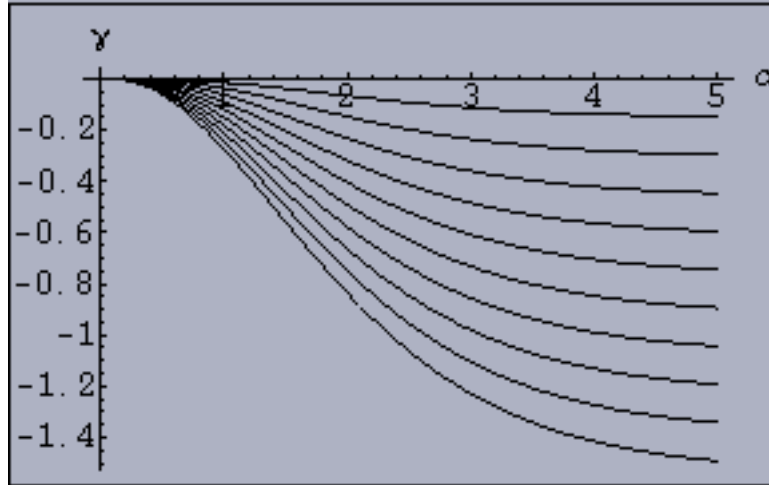


FIG. 22. Uhlmann geometric phases for  $n$ -level Gibbsian systems ( $n = 2, \dots, 11$ ) holding  $\theta$  fixed at  $\frac{\pi}{10}$ . The curve for  $n = 2$  dominates that for  $n = 3$ , which dominates that for  $n = 4, \dots$

In Fig. 23, we hold  $\alpha$  at 2 and plot the *visibilities* for the ten spin scenarios. Again, as in Figs. 21 and 22, curves for lower values of  $j$  dominate those for higher values.

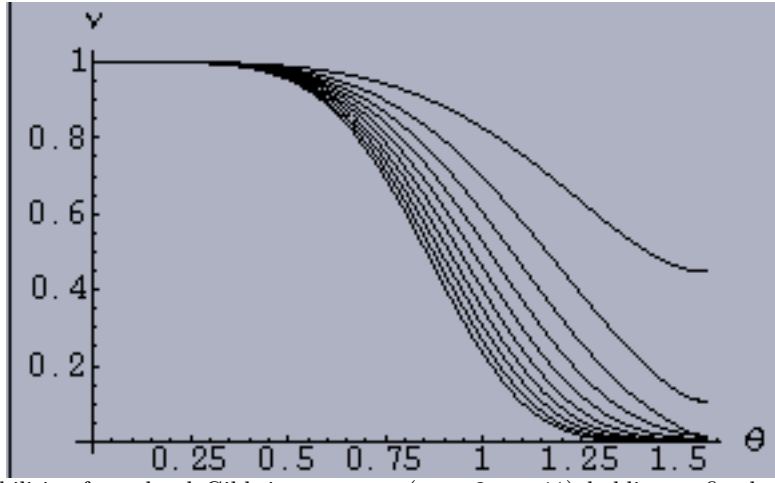


FIG. 23. Uhlmann visibilities for  $n$ -level Gibbsian systems ( $n = 2, \dots, 11$ ) holding  $\alpha$  fixed at 2. The curve for  $n = 2$  dominates that for  $n = 3$ , which dominates that for  $n = 4, \dots$

While in Fig. 21 the inverse temperature parameter  $\alpha$  was fixed at 1, in Fig. 24, it is held at 2. Now the same simple monotonicity with  $j$  observed in the preceding three figures, holds below  $\theta \approx .65$ . However, it is lost at higher values of  $\theta$ , with the curves for the higher spin states oscillating from  $-\frac{\pi}{2}$  to  $\frac{\pi}{2}$  at lower values of  $\theta$  than do the curves for some of the lower spin states.

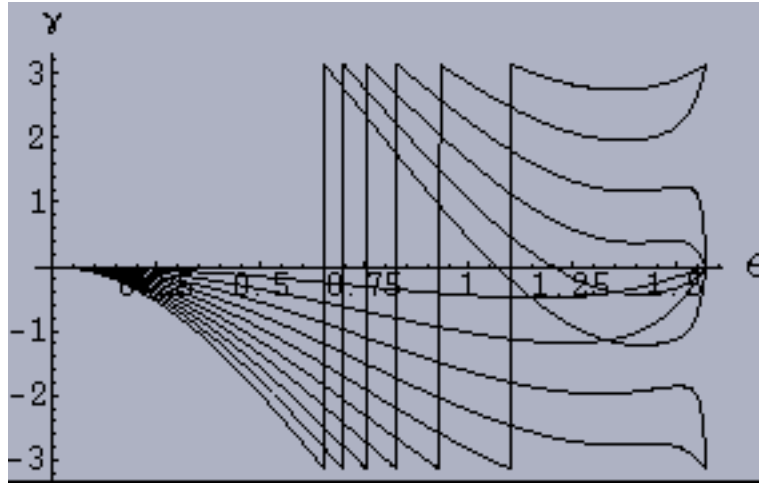


FIG. 24. Uhlmann geometric phases for  $n$ -level Gibbsian systems ( $n = 2, \dots, 11$ ) holding  $\alpha = 2$ . Only below  $\theta \approx .65$  does the curve for  $n = 2$  dominate that for  $n = 3$ , which dominates that for  $n = 4, \dots$

In Fig. 25, in which  $\theta$  is fixed at  $\frac{\pi}{5}$ , similar behavior to that observed in Fig. 24 takes place. Below  $\alpha \approx 1.43$ , the simple monotonicity with  $j$  holds, then the curves begin to jump from  $-\frac{\pi}{2}$  to  $\frac{\pi}{2}$  with the curves for higher  $j$  jumping first.

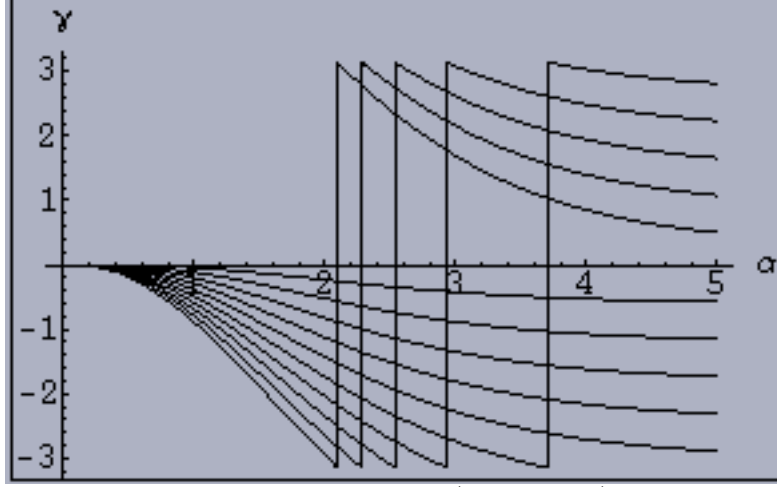


FIG. 25. Uhlmann geometric phases for  $n$ -level Gibbsian systems ( $n = 2, \dots, 11$ ) holding  $\theta = \frac{\pi}{5}$ . Only below  $\alpha \approx 2$  does the curve for  $n = 2$  dominate that for  $n = 3$ , which dominates that for  $n = 4, \dots$

In Fig. 26, holding  $\theta = \frac{\pi}{2}$ , we plot the various visibilities over the range  $\alpha \in [1, 4]$ . At  $\alpha = 2.2$ , the values of  $\nu_j$  monotonically decline from  $j = \frac{1}{2}$  to  $\frac{9}{2}$ .

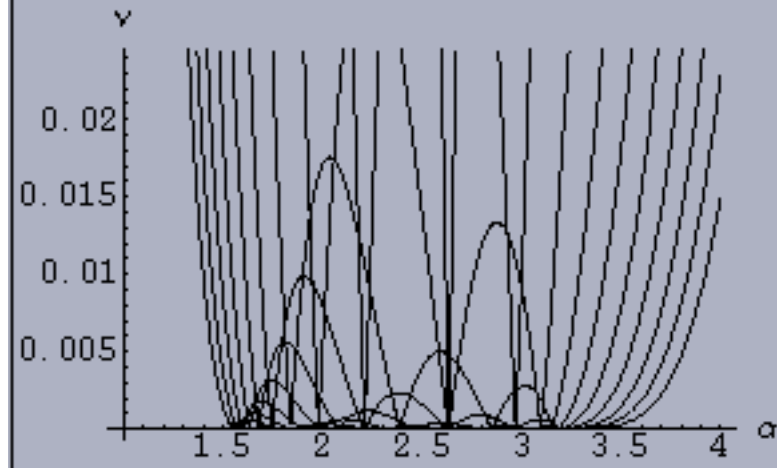


FIG. 26. Uhlmann visibilities for  $n$ -level Gibbsian systems ( $n = 2, \dots, 11$ ) fixing  $\theta = \frac{\pi}{2}$ . At  $\alpha = 2.1$ , the values of  $\nu$  monotonically decline as  $n$  increases. The highest peak belongs to  $n = 2$ .

## V. HIGHER-ORDER UHLMANN HOLONOMY INVARIANTS

### A. Traces of powers of Uhlmann holonomy invariants

All the analyses above have been conducted on the basis of the trace of the holonomy invariant (7). In addition, however, the traces of the higher powers of (7) are also invariants [5, eq. (102)] (all reducing, however, for pure states, to simple powers of the “Berry phase” [5, eq. (112.5)] (cf. [6])). In Fig. 27, we show the argument of the *second* power of the holonomy invariant for the spin- $\frac{1}{2}$  case ( $n = 2$ ), which we express in the form of the arctangent of  $\frac{y}{x}$ , taking into account which quadrant the point  $(x, y)$  lies in, where

$$x = \frac{1}{2\zeta} \left( \zeta(-1 + (1 + \cosh \alpha) \cosh 2i\pi\kappa) \operatorname{sech}^2 \frac{\alpha}{2} - 8 \sinh^2 i\pi\kappa \right), \quad y = -\frac{2i\kappa \cos \theta \sinh \alpha \sinh 2i\pi\kappa}{\zeta}. \quad (13)$$

The corresponding absolute value (Fig. 28) is the square root of

$$x^2 + y^2 = 1 - \frac{2 \cosh 2i\pi\kappa}{1 + \cosh \alpha} + \frac{1}{4} \operatorname{sech}^4 \frac{\alpha}{2} + \frac{4(2 + \cosh \alpha) \operatorname{sech}^2 \frac{\alpha}{2} \sinh^2 i\pi\kappa}{\zeta} + \frac{16 \sinh^4 i\pi\kappa}{\zeta^2}. \quad (14)$$



(In some of the later [computationally-intensive] figures in this section, it proved essentially necessary to omit the [otherwise obvious] axes labels, due to some quite distinct peculiarities of the graphics facilities for the local installation of MATHEMATICA on the more powerful workstations.)

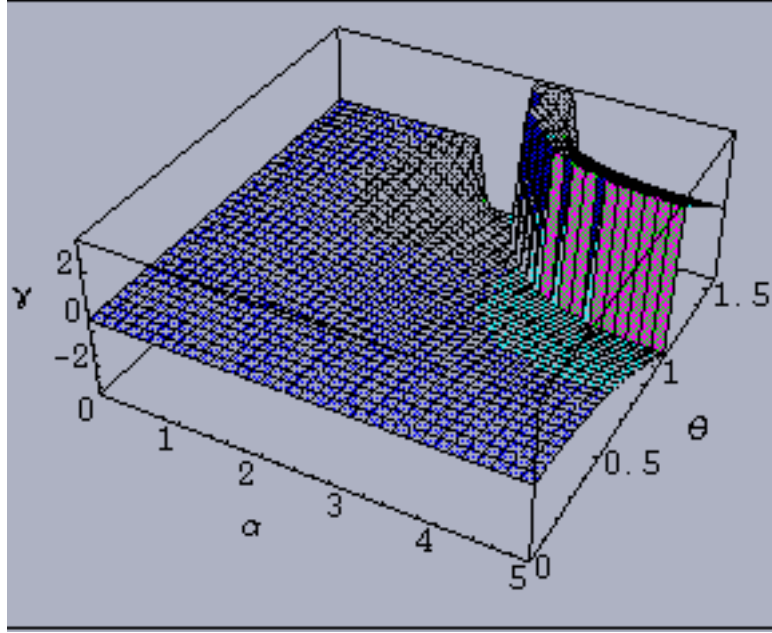


FIG. 27. Argument of the trace of the *second* power of the holonomy invariant (7) for the two-level Gibbsian systems ( $n=2$ )

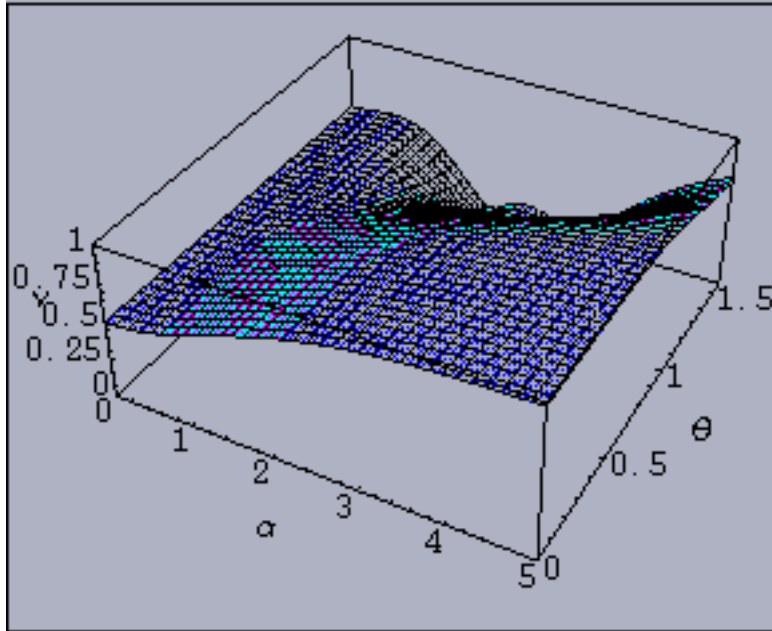


FIG. 28. Absolute value of the trace of the *second* power of the holonomy invariant (7) for the *two*-level Gibbsian systems ( $n=2$ )

In Figs. 29 and 30 are shown the analogous quantities for Gibbsian spin-1 systems.

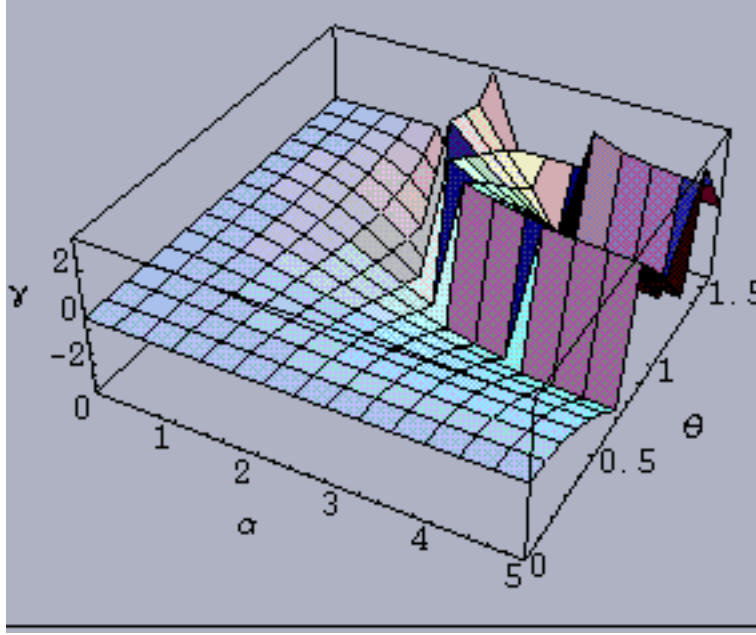


FIG. 29. Argument of the trace of the *second* power of the holonomy invariant (7) for the *three*-level Gibbsian systems ( $n = 3$ )

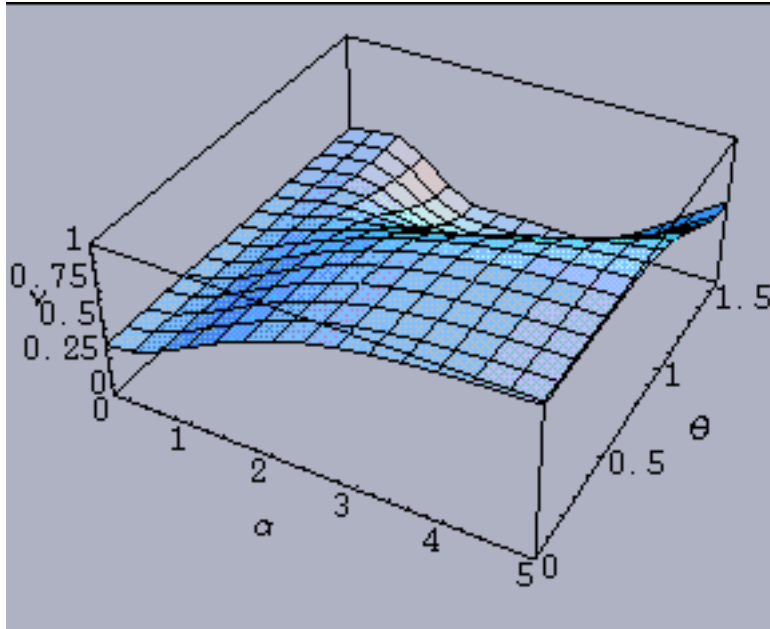


FIG. 30. Absolute value of the trace of the *second* power of the holonomy invariant (7) for the *three*-level Gibbsian systems ( $n = 3$ )

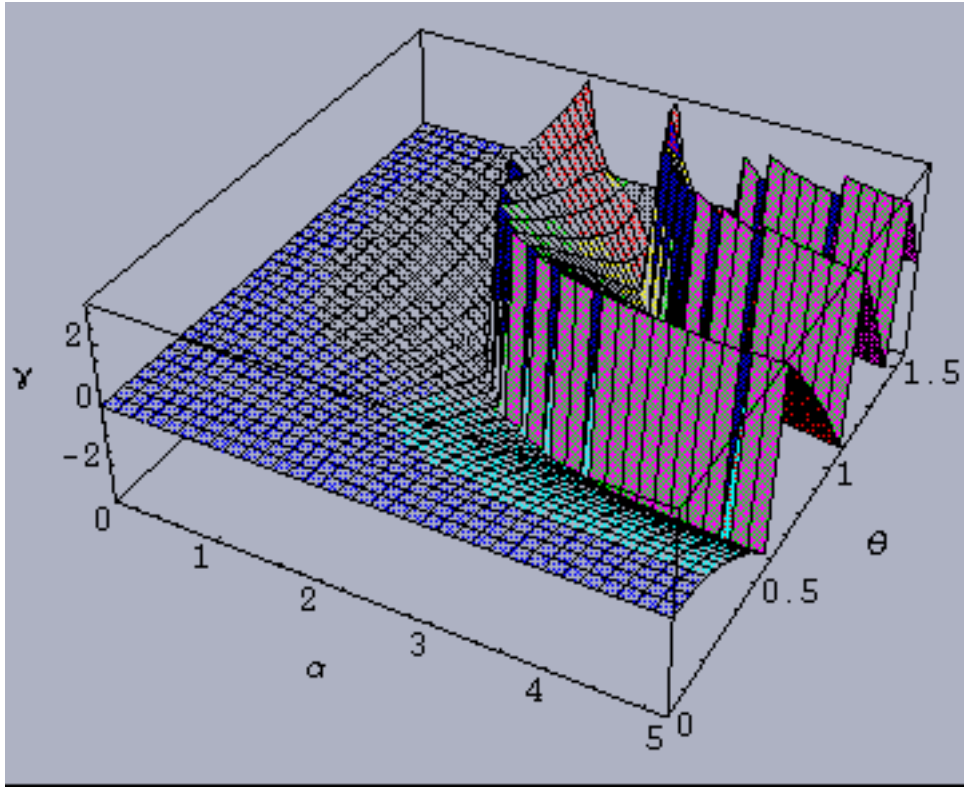


FIG. 31. Argument of the trace of the *third* power of the holonomy invariant (7) for the *three*-level Gibbsian systems ( $n = 3$ )

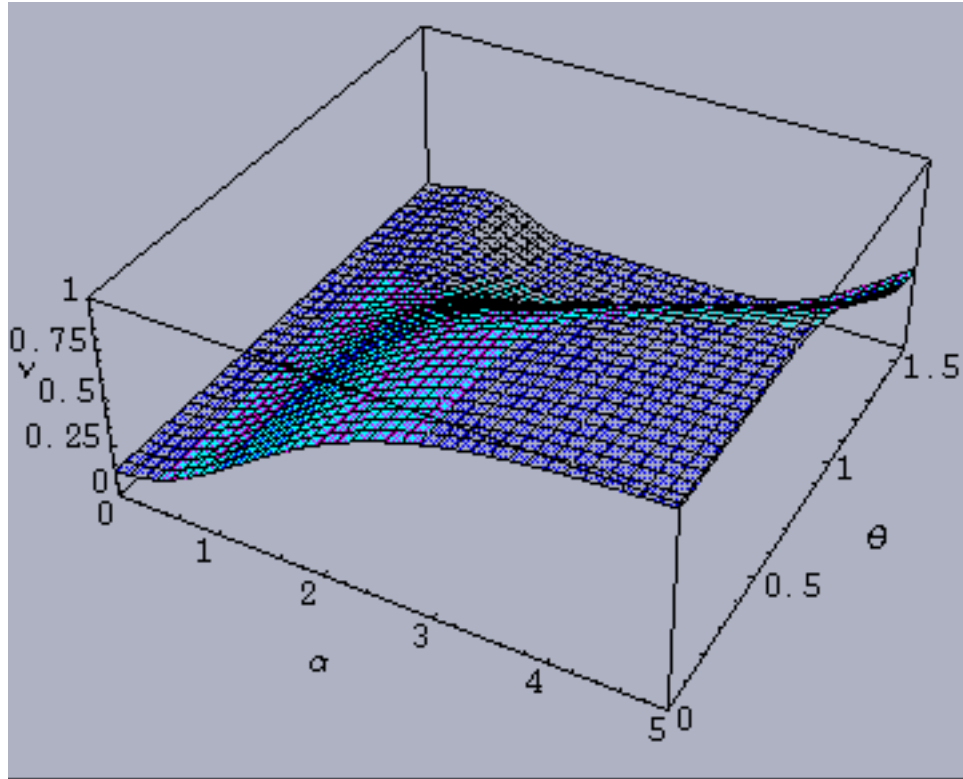


FIG. 32. Absolute value of the trace of the *third* power of the holonomy invariant (7) for the *three*-level Gibbsian systems ( $n = 3$ )

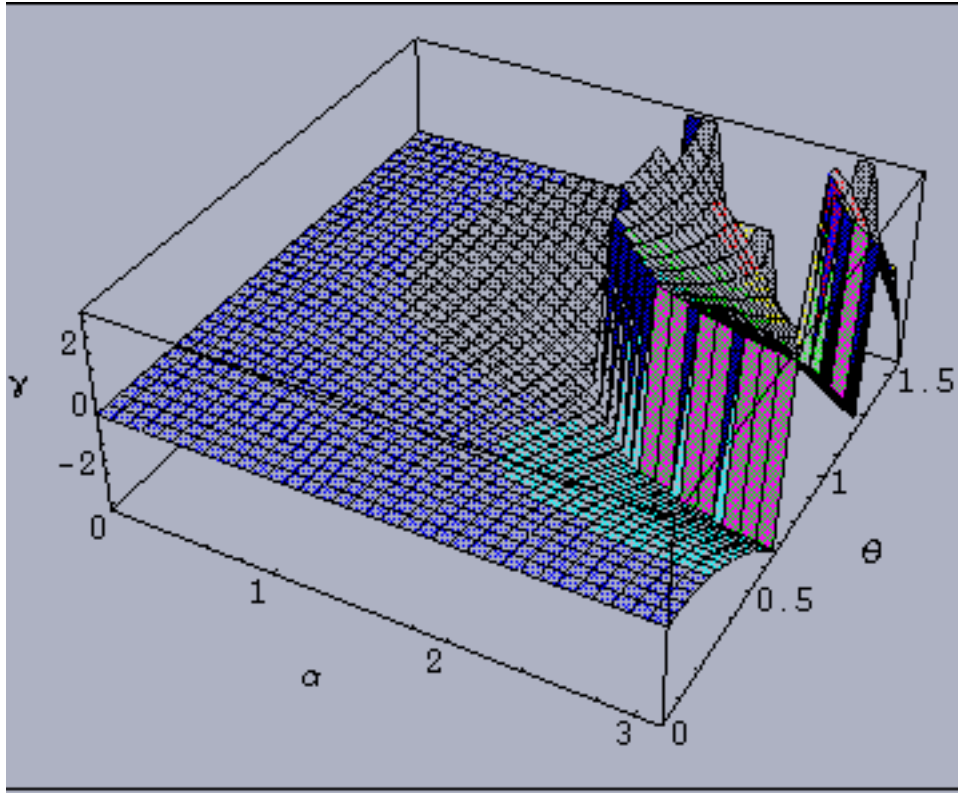


FIG. 33. Argument of the trace of the *second* power of the holonomy invariant (7) for the *four*-level Gibbsian systems ( $n = 4$ )

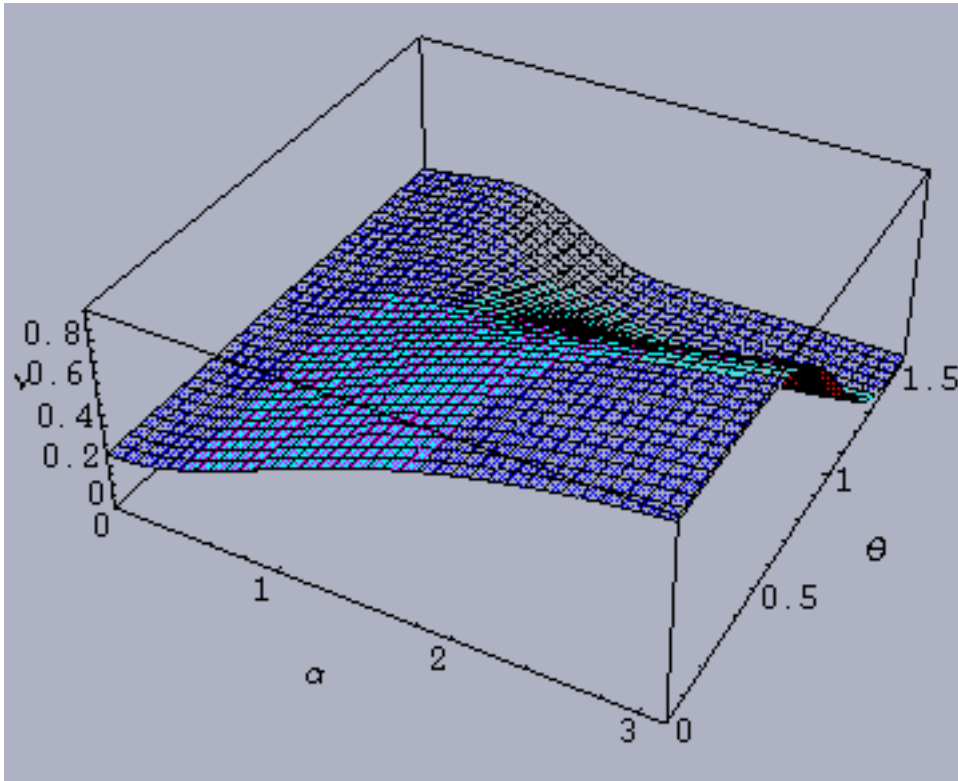


FIG. 34. Absolute value of the trace of the *second* power of the holonomy invariant (7) for the *four*-level Gibbsian systems ( $n = 4$ )



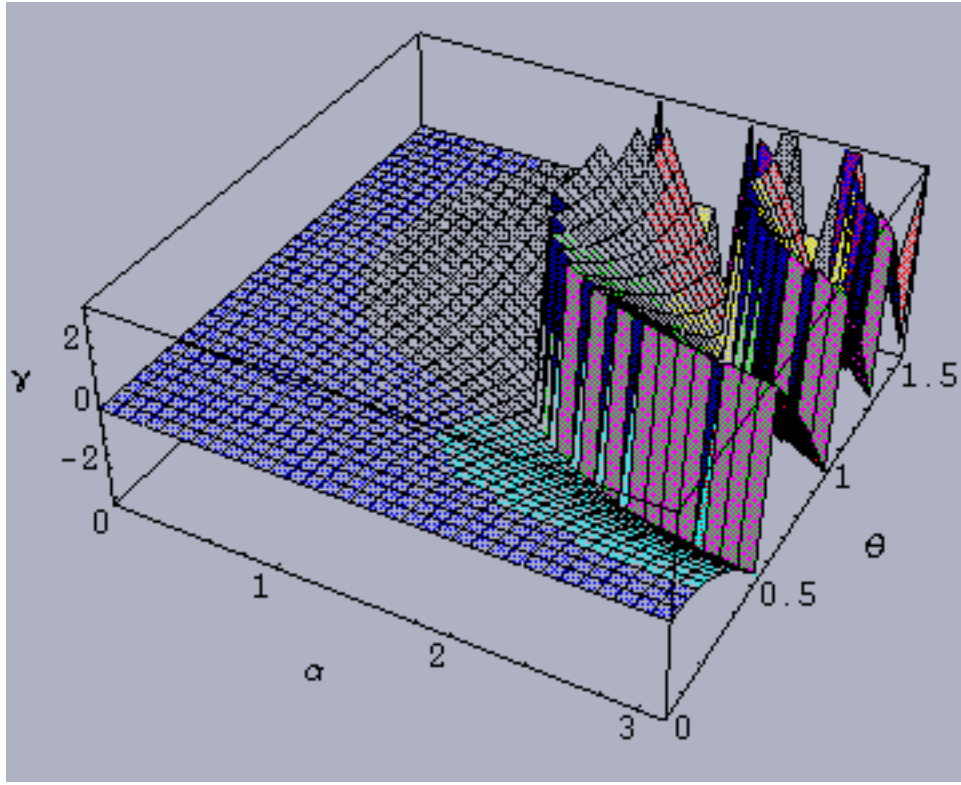


FIG. 35. Argument of the trace of the *third* power of the holonomy invariant (7) for the *four*-level Gibbsian systems ( $n = 4$ )

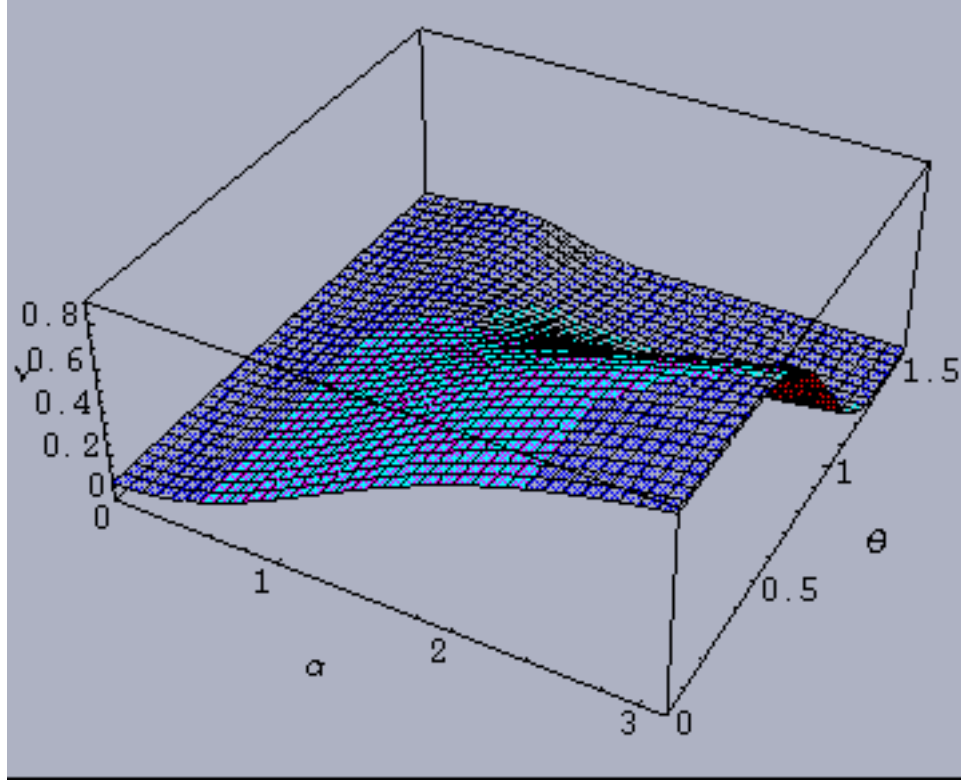


FIG. 36. Absolute value of the trace of the *third* power of the holonomy invariant (7) for the *four*-level Gibbsian systems ( $n = 4$ )

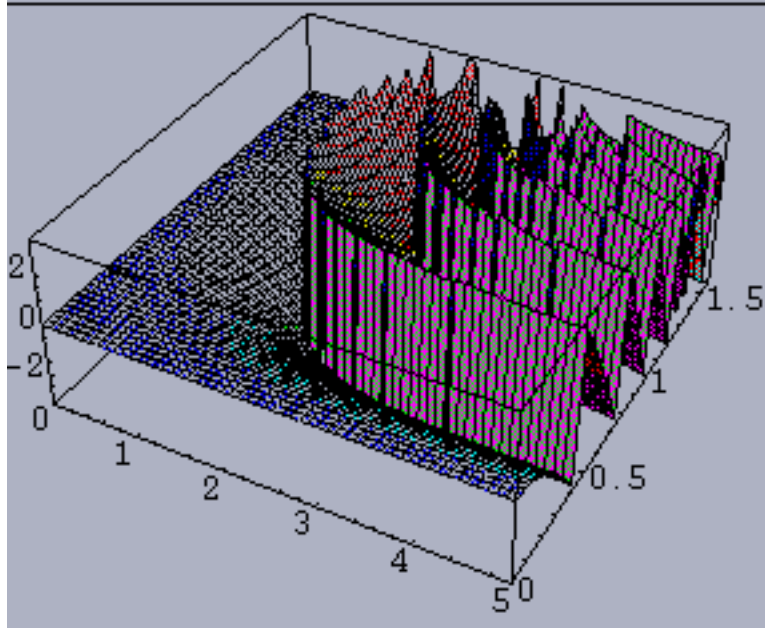


FIG. 37. Argument of the trace of the *fourth* power of the holonomy invariant (7) for the *four*-level Gibbsian systems ( $n = 4$ )

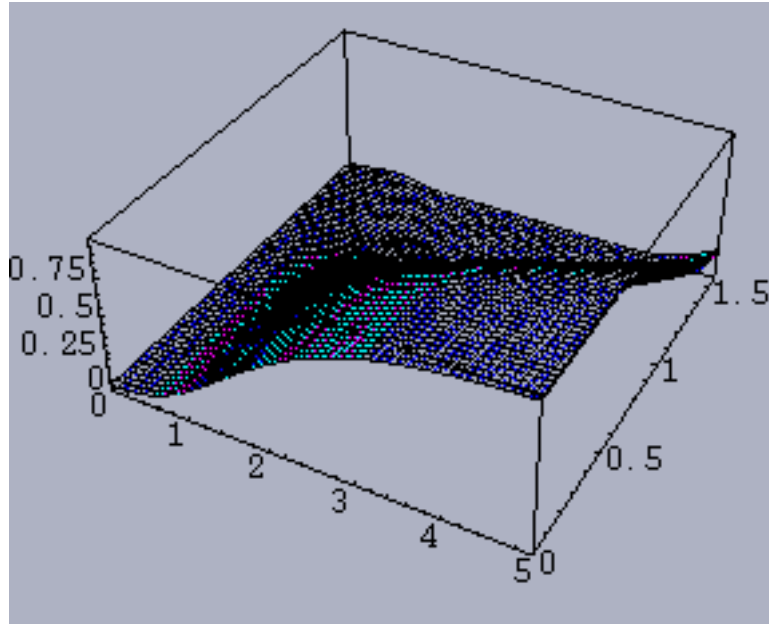


FIG. 38. Absolute value of the trace of the *fourth* power of the holonomy invariant (7) for the *four*-level Gibbsian systems ( $n = 4$ )

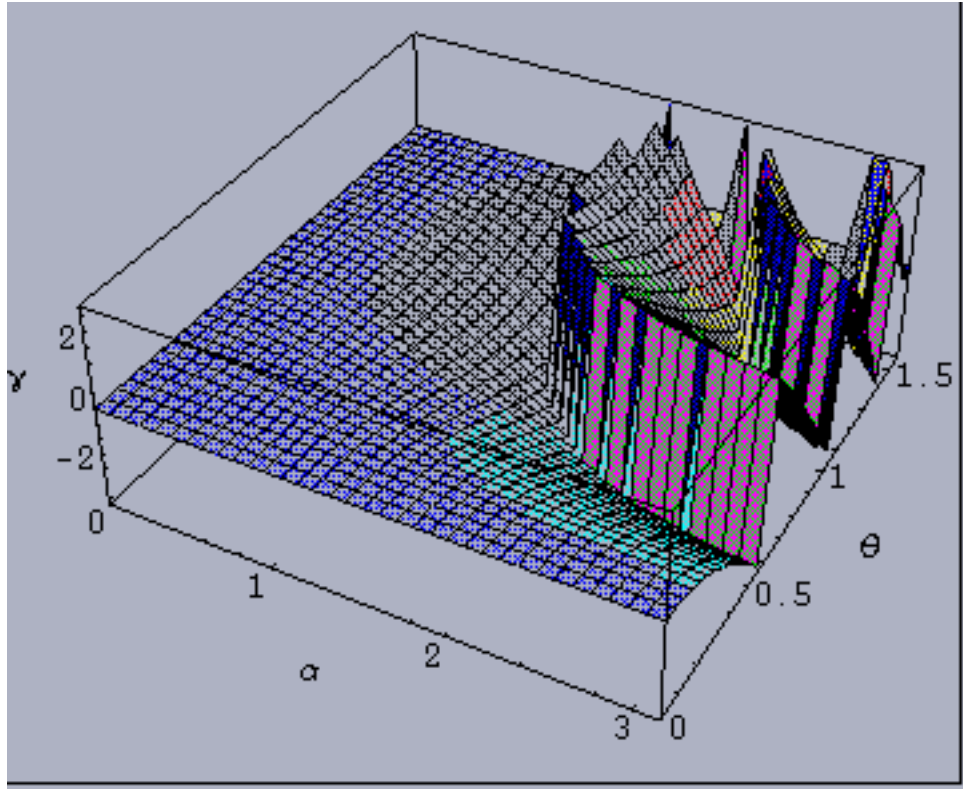


FIG. 39. Argument of the trace of the *second* power of the holonomy invariant (7) for the *five*-level Gibbsian systems ( $n = 5$ )

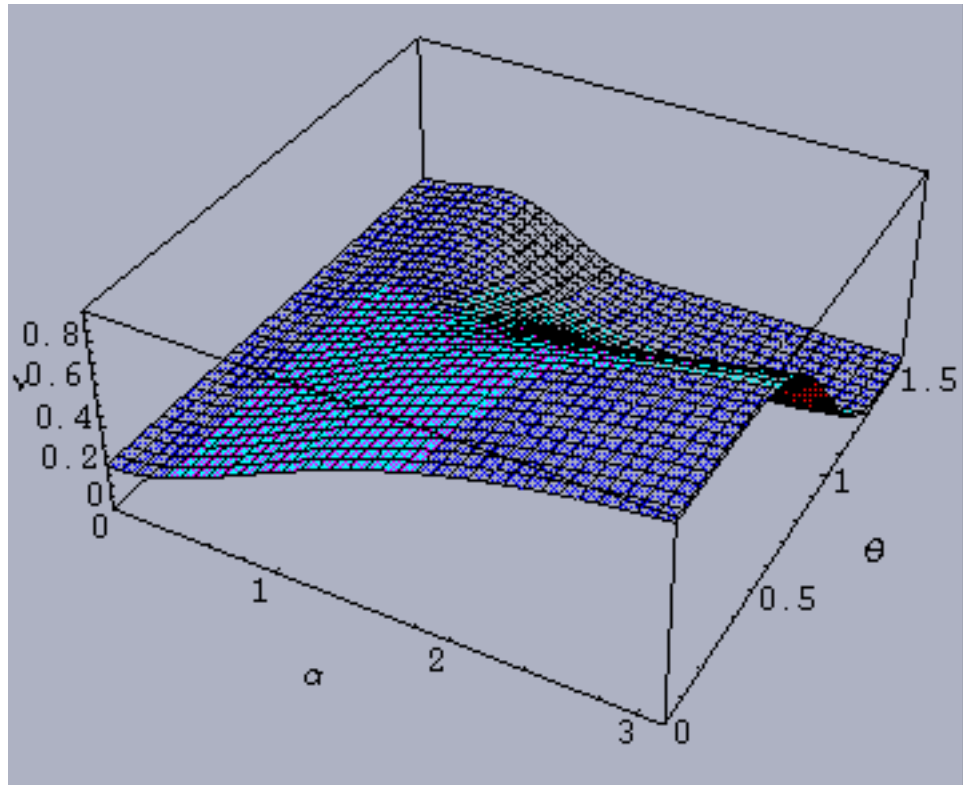


FIG. 40. Absolute value of the trace of the *second* power of the holonomy invariant (7) for the *five*-level Gibbsian systems ( $n = 5$ )

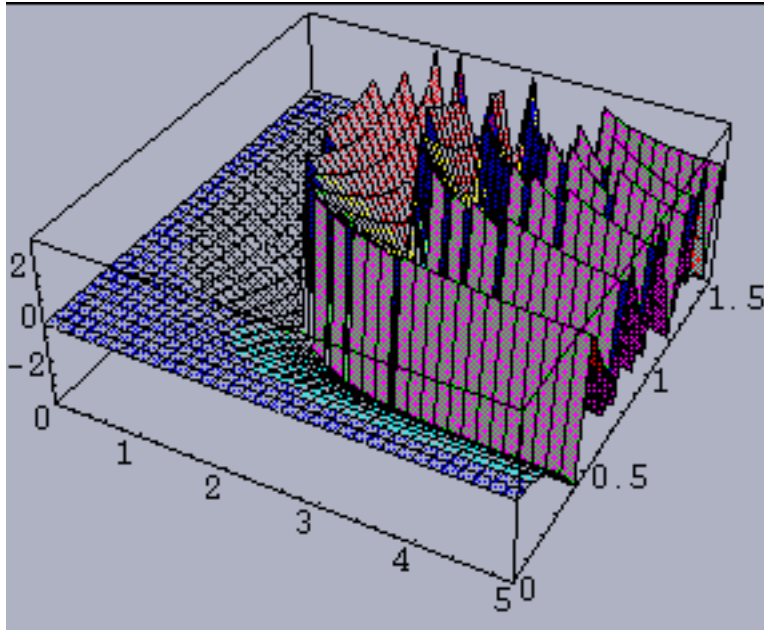


FIG. 41. Argument of the trace of the *third* power of the holonomy invariant (7) for the *five*-level Gibbsian systems ( $n = 5$ )

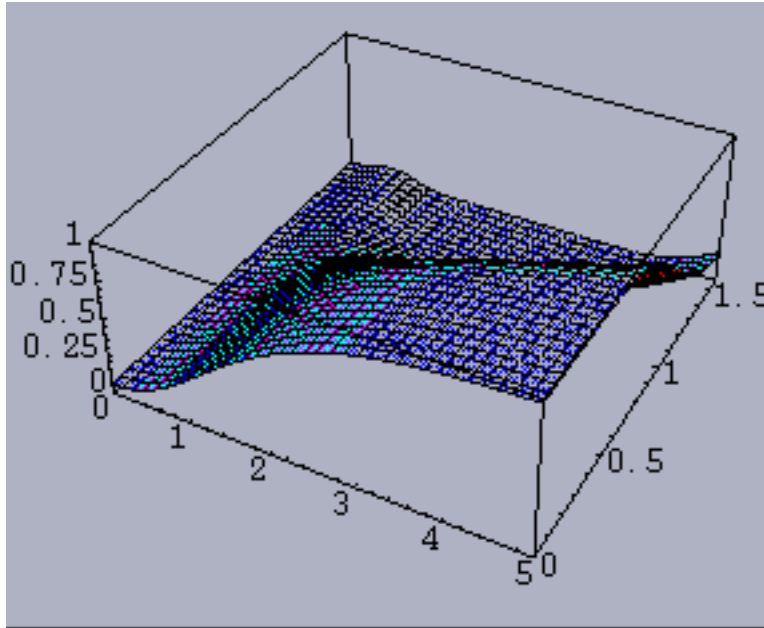


FIG. 42. Absolute value of the trace of the *third* power of the holonomy invariant (7) for the *five*-level Gibbsian systems ( $n = 5$ )



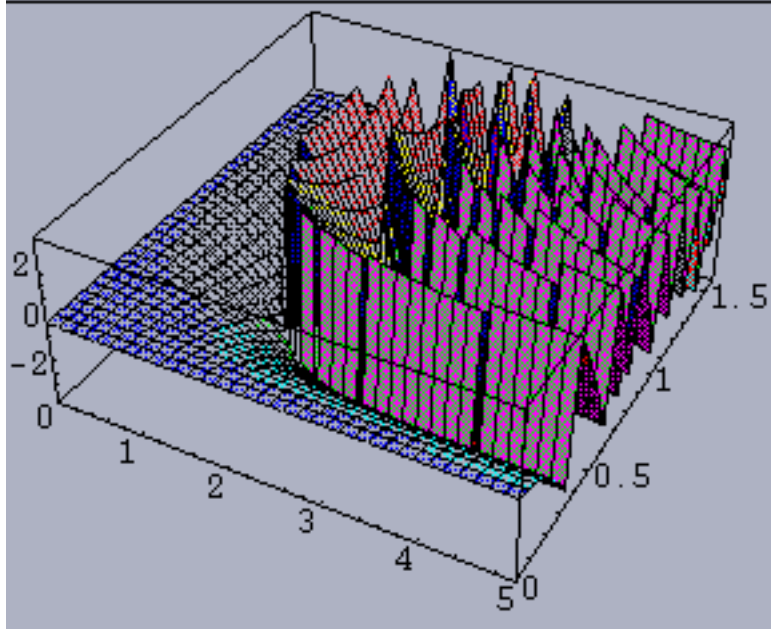


FIG. 43. Argument of the trace of the *fourth* power of the holonomy invariant (7) for the *five*-level Gibbsian systems ( $n = 5$ )

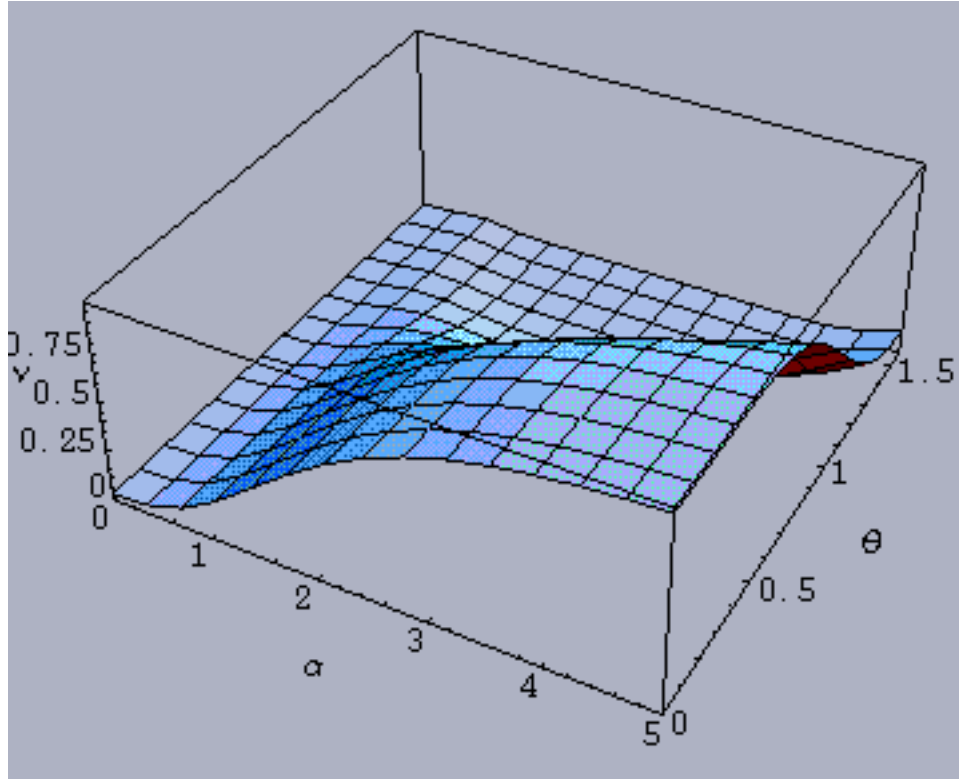


FIG. 44. Absolute value of the trace of the *fourth* power of the holonomy invariant (7) for the *five*-level Gibbsian systems ( $n = 5$ )

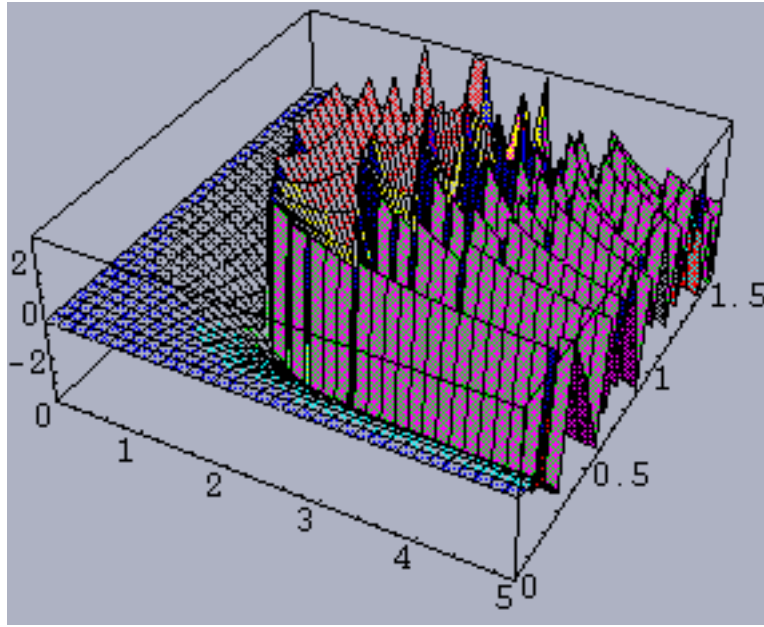


FIG. 45. Argument of the trace of the *fifth* power of the holonomy invariant (7) for the *five*-level Gibbsian systems ( $n = 5$ )

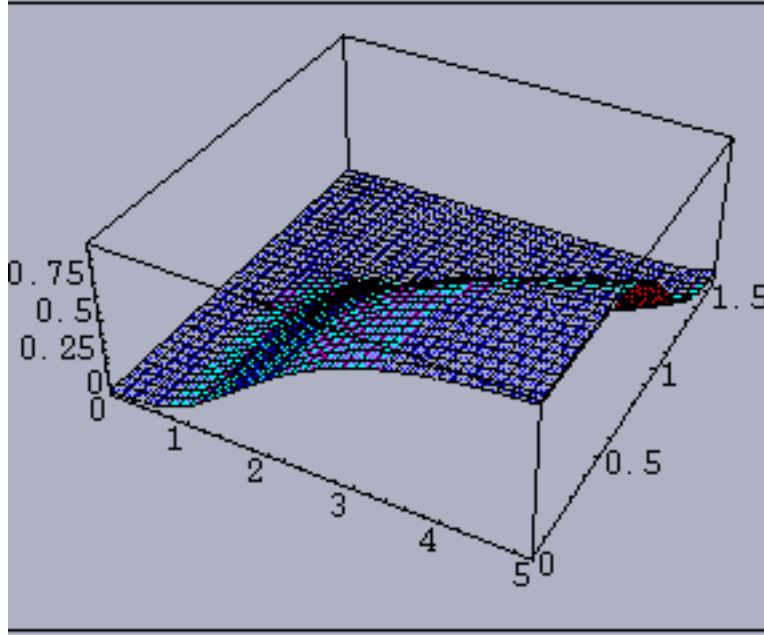


FIG. 46. Absolute value of the trace of the *fifth* power of the holonomy invariant (7) for the *five*-level Gibbsian systems ( $n = 5$ )

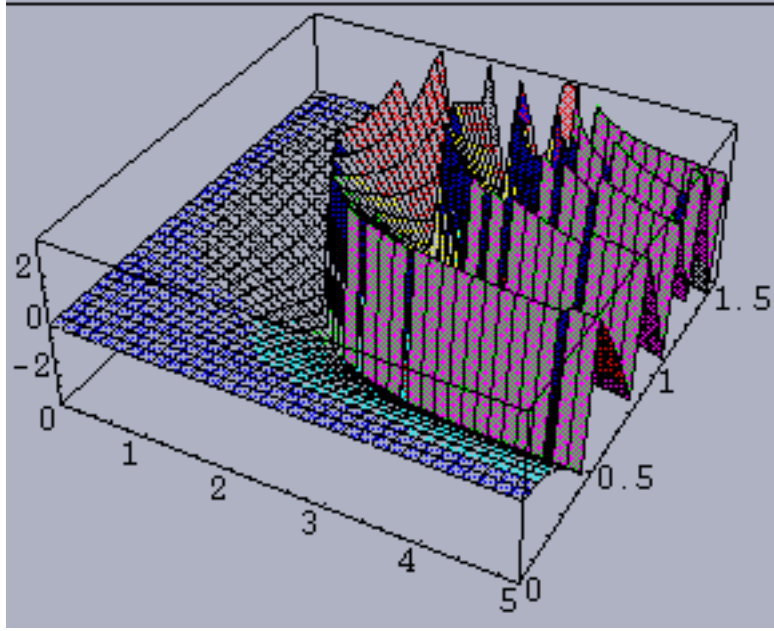


FIG. 47. Argument of the trace of the *second* power of the holonomy invariant (7) for the *six*-level Gaussian systems ( $n = 6$ )

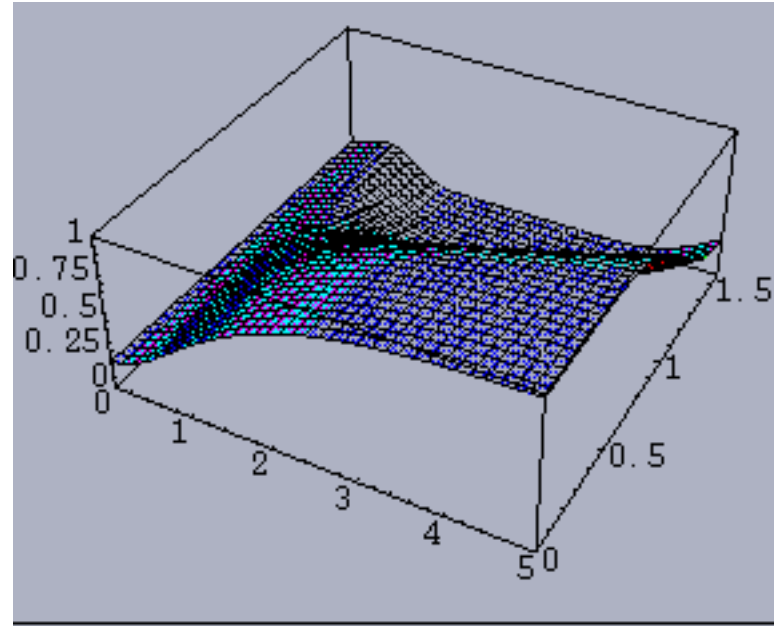


FIG. 48. Absolute value of the trace of the *second* power of the holonomy invariant (7) for the *six*-level Gaussian systems ( $n = 6$ )

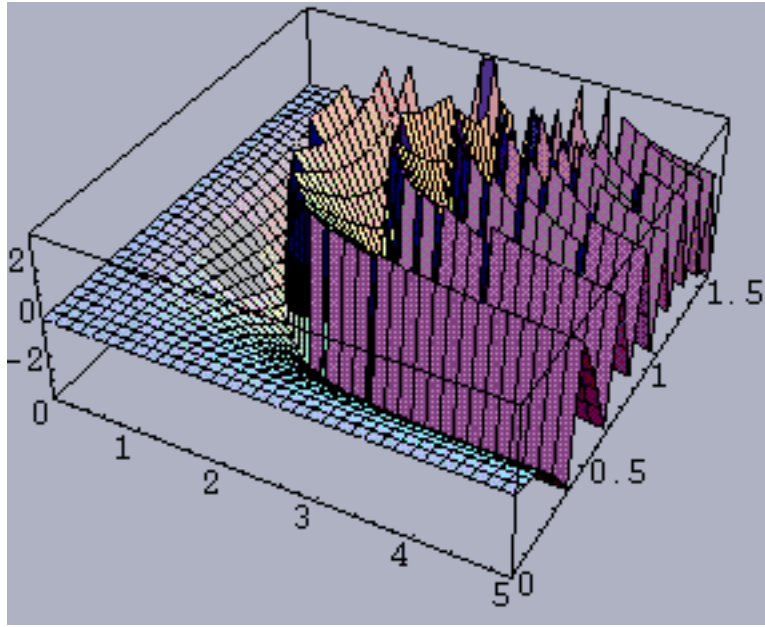


FIG. 49. Argument of the trace of the *third* power of the holonomy invariant (7) for the *six*-level Gibbsian systems ( $n = 6$ )

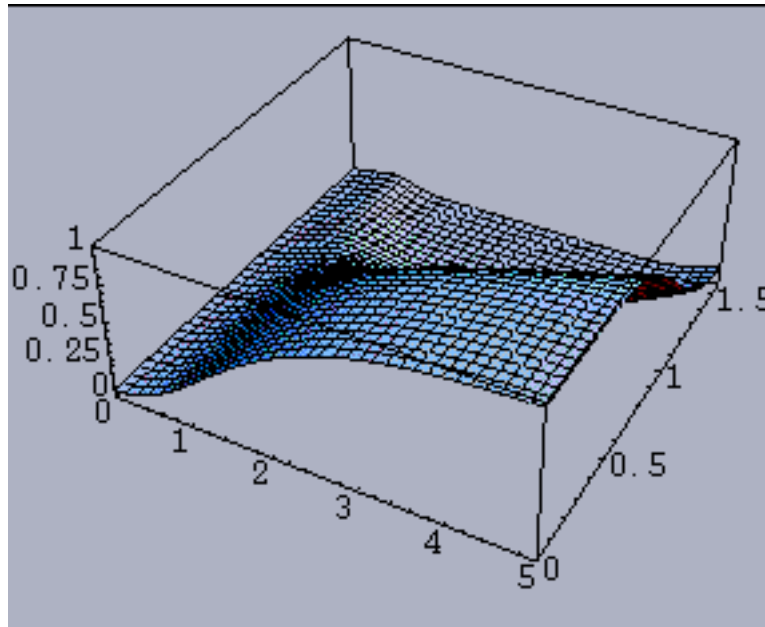


FIG. 50. Absolute value of the trace of the *third* power of the holonomy invariant (7) for the *six*-level Gibbsian systems ( $n = 6$ )

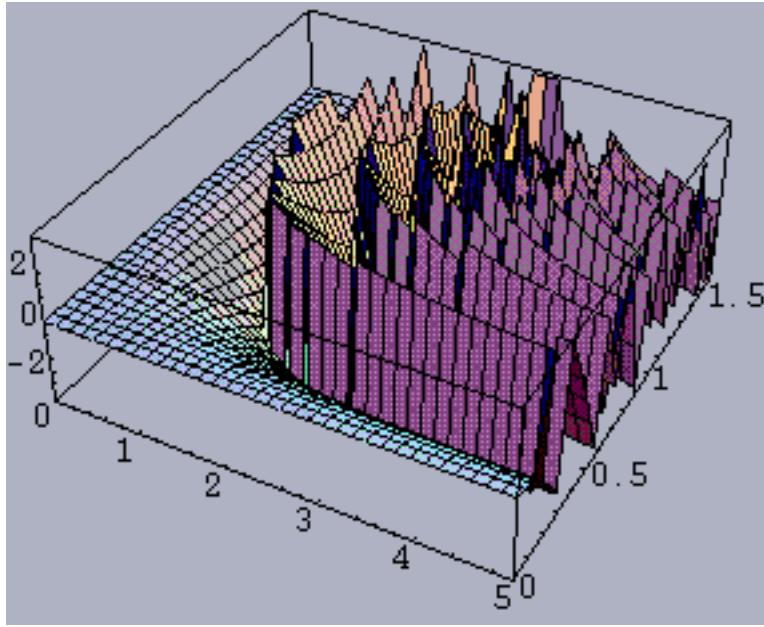


FIG. 51. Argument of the trace of the *fourth* power of the holonomy invariant (7) for the *six*-level Gibbsian systems ( $n = 6$ )

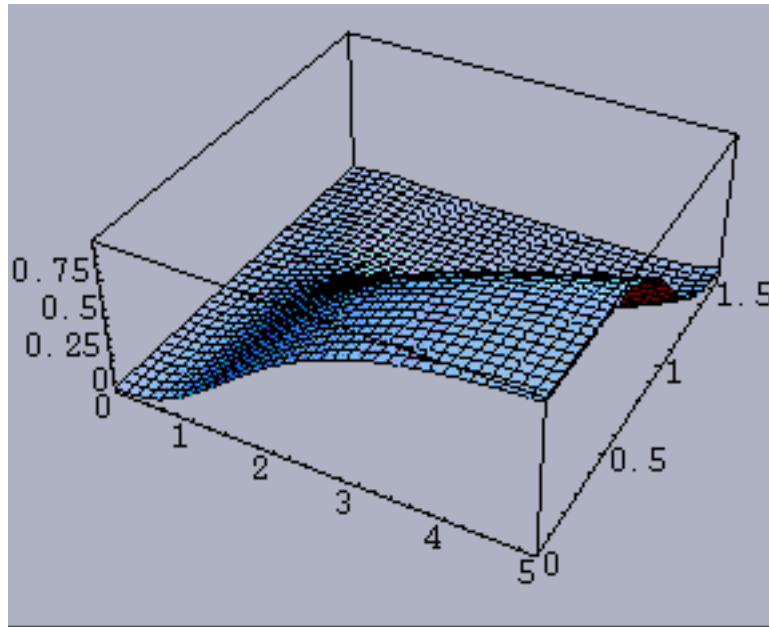


FIG. 52. Absolute value of the trace of the *fourth* power of the holonomy invariant (7) for the *six*-level Gibbsian systems ( $n = 6$ )



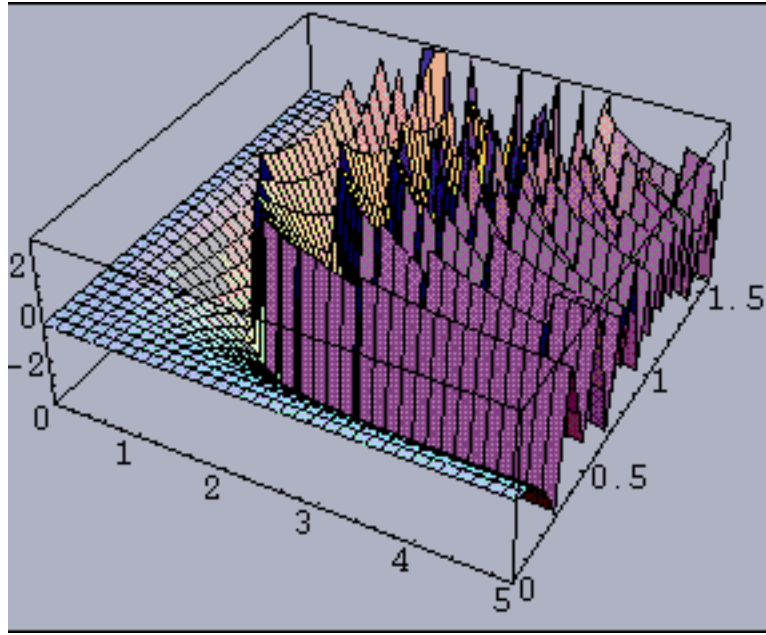


FIG. 53. Argument of the trace of the *fifth* power of the holonomy invariant (7) for the *six*-level Gaussian systems ( $n = 6$ )

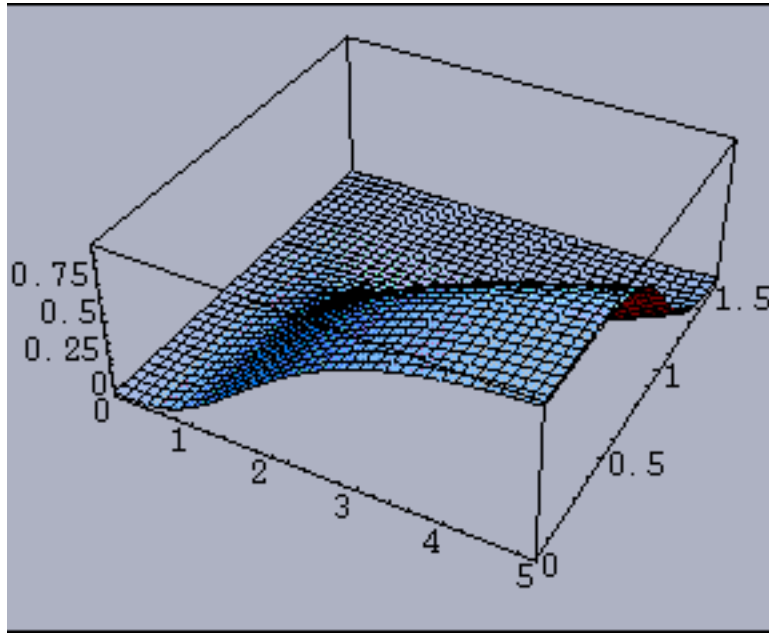


FIG. 54. Absolute value of the trace of the *fifth* power of the holonomy invariant (7) for the *six*-level Gaussian systems ( $n = 6$ )

## B. Cross-comparisons of Uhlmann holonomy invariants

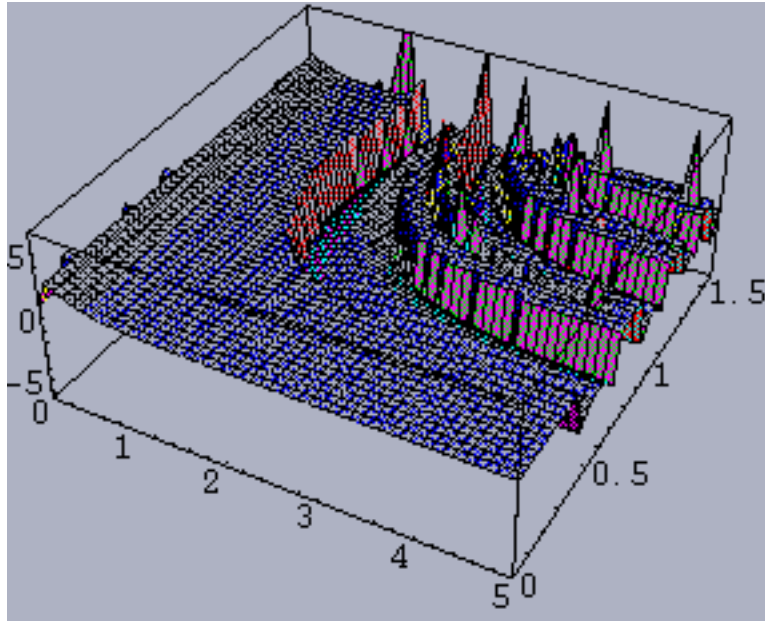


FIG. 55. Ratio of the argument of the trace of the second power of the holonomy invariant (7) to the argument of the trace of the first power for the *eight*-level Gibbsian systems

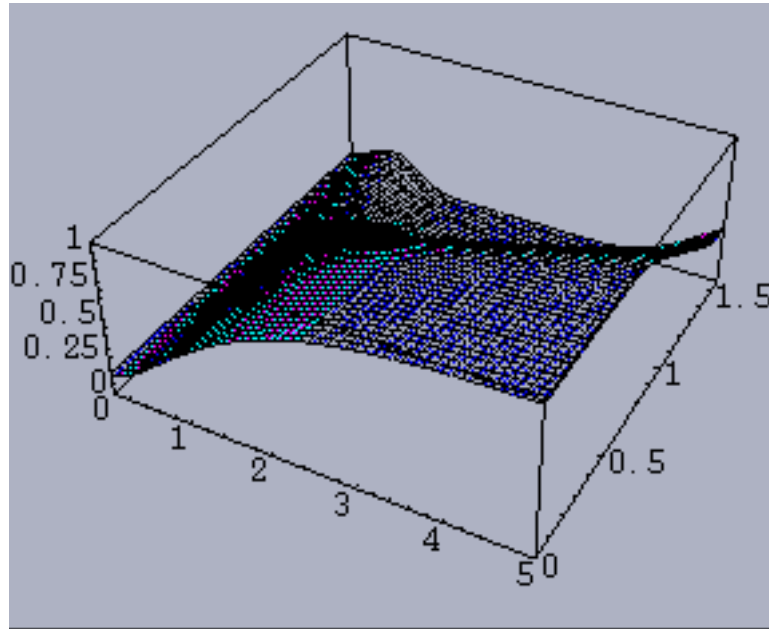


FIG. 56. Ratio of the absolute value of the trace of the second power of the holonomy invariant (7) to the absolute value of the trace of the first power for the *eight*-level Gibbsian systems

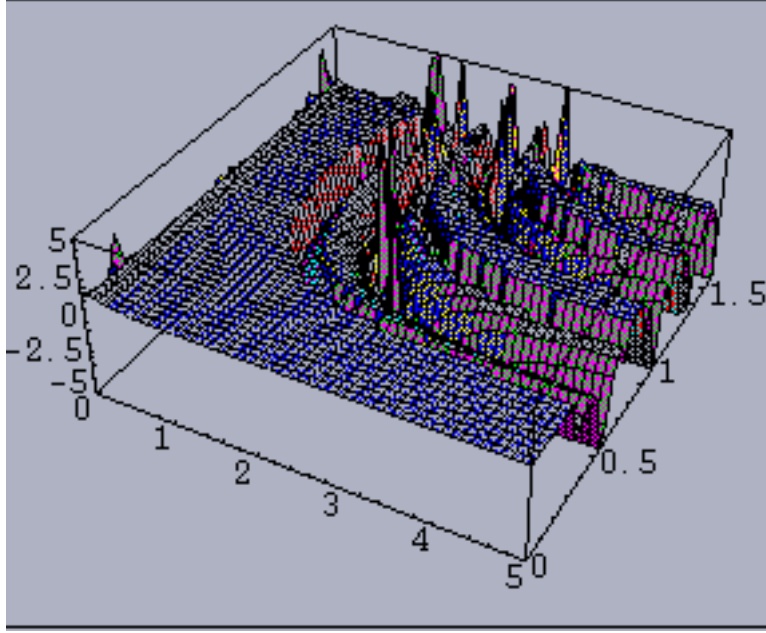


FIG. 57. Ratio of the argument of the trace of the third power of the holonomy invariant (7) to the argument of the trace of the second power for the *eight*-level Gibbsian systems

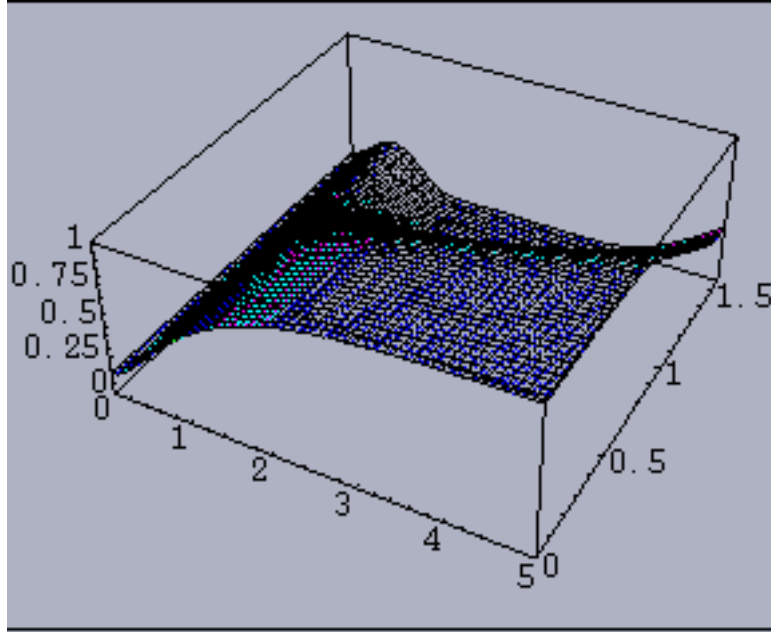


FIG. 58. Ratio of the absolute value of the trace of the third power of the holonomy invariant (7) to the absolute value of the trace of the second power for the *eight*-level Gibbsian systems

### C. Eigenvalues of Uhlmann holonomy invariant for $n = 2, 3, 5$

To supplement our consideration above of the *traces* of various powers of the Uhlmann holonomy invariant (7), here we examine the eigenvalues themselves. (Both these traces and eigenvalues are themselves invariants, of course.) In Figs. 59 and 60 are shown the arguments of the dominant and subordinate eigenvalues of the holonomy invariant (7) for the case  $n = 2$ , and in Figs. 61 and 62, the corresponding absolute values.

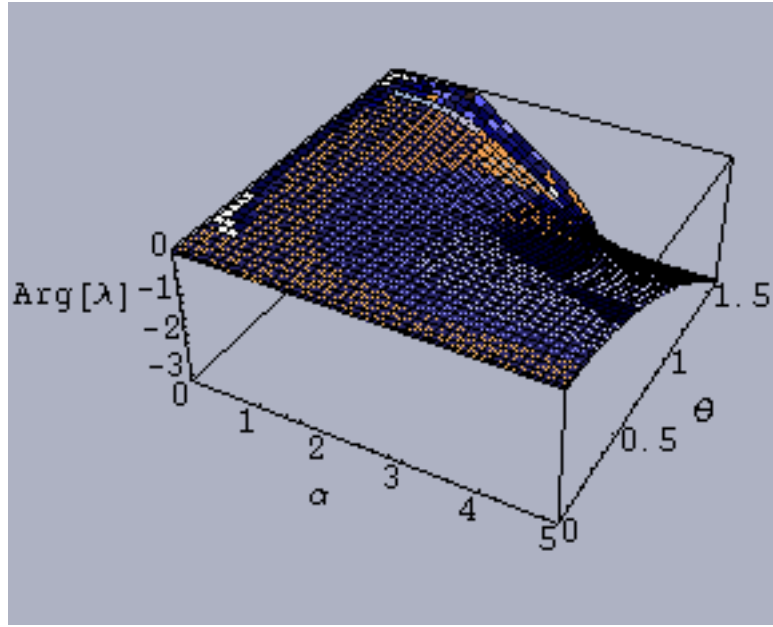


FIG. 59. Argument of the dominant eigenvalue of the Uhlmann holonomy invariant (7) for the *two*-level Gibbsian density matrices

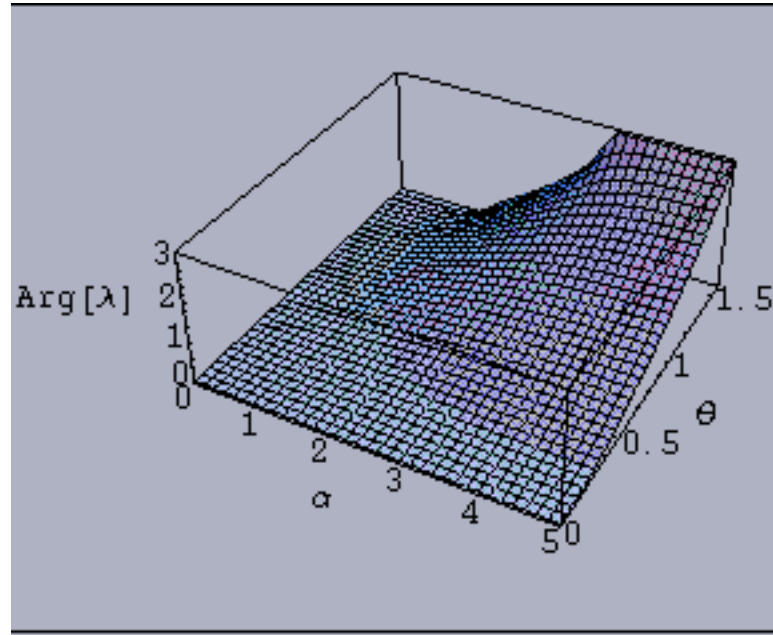


FIG. 60. Argument of the subordinate eigenvalue of the Uhlmann holonomy invariant (7) for the *two*-level Gibbsian density matrices

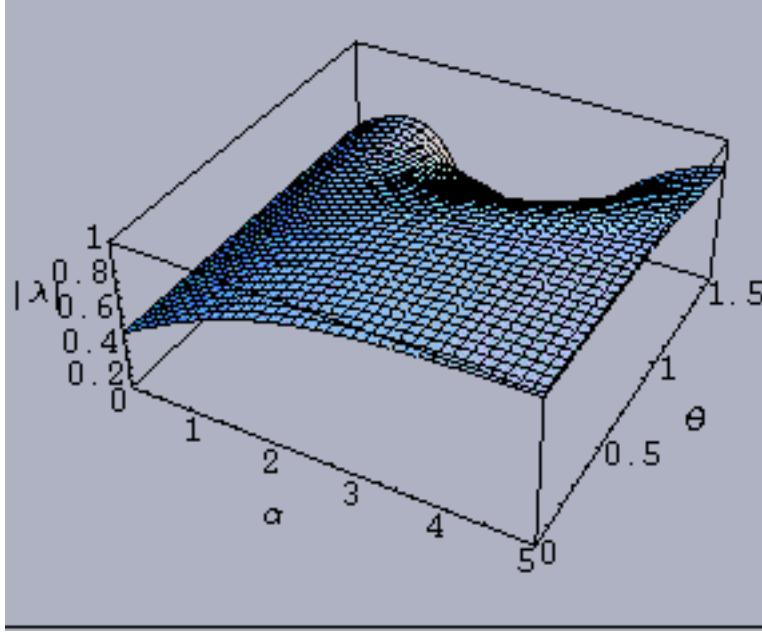


FIG. 61. Absolute value of the dominant eigenvalue of the Uhlmann holonomy invariant (7) for the *two*-level Gibbsian density matrices

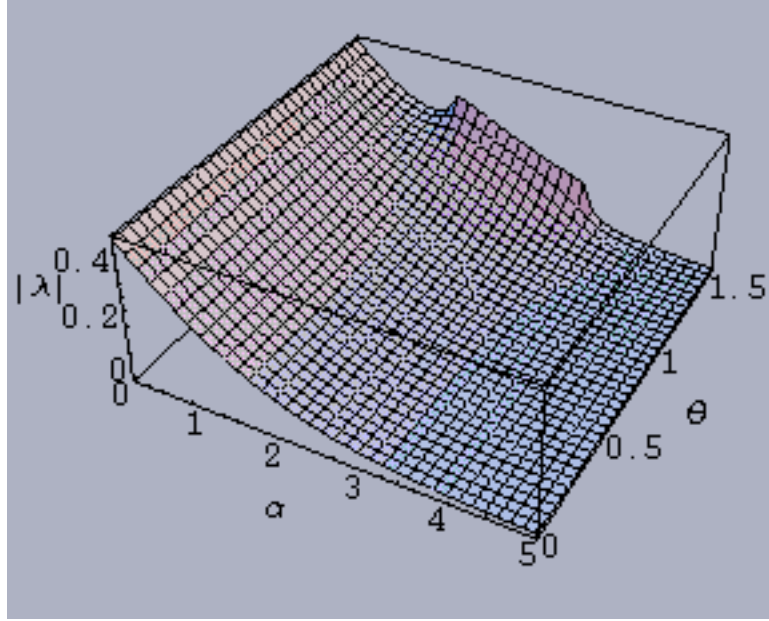


FIG. 62. Absolute value of the subordinate eigenvalue of the Uhlmann holonomy invariant (7) for the *two*-level Gibbsian density matrices

In Figs. 63 and 64, we plot the arguments of the dominant and subordinate eigenvalues of the holonomy invariant (7) for the case  $n = 3$  and in Figs. 65 and 67, the absolute values of the two corresponding eigenvalues. The argument of the intermediate (in absolute value) one of the three eigenvalues appears to always be identically zero, that is, this intermediate eigenvalue is real (Fig. 66). It also appears numerically, on the basis of further analyses we have conducted, that this result is generalizable to the proposition that for odd  $n$ , the central/most intermediate one (that is, the  $\lceil \frac{n}{2} \rceil$ -th) of the  $n$  eigenvalues is real. (Also, the centrally located diagonal entry of the holonomy invariant for odd  $n$  appears to be real, in general.)



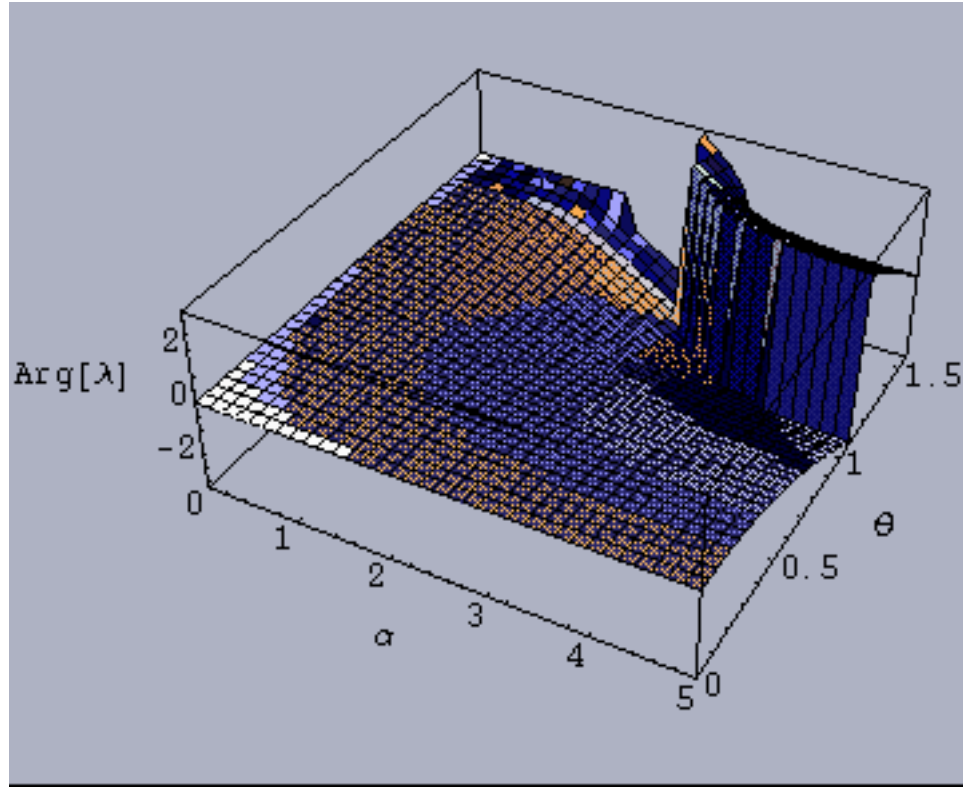


FIG. 63. Argument of the dominant eigenvalue of the Uhlmann holonomy invariant (7) for the *three*-level Gibbsian density matrices

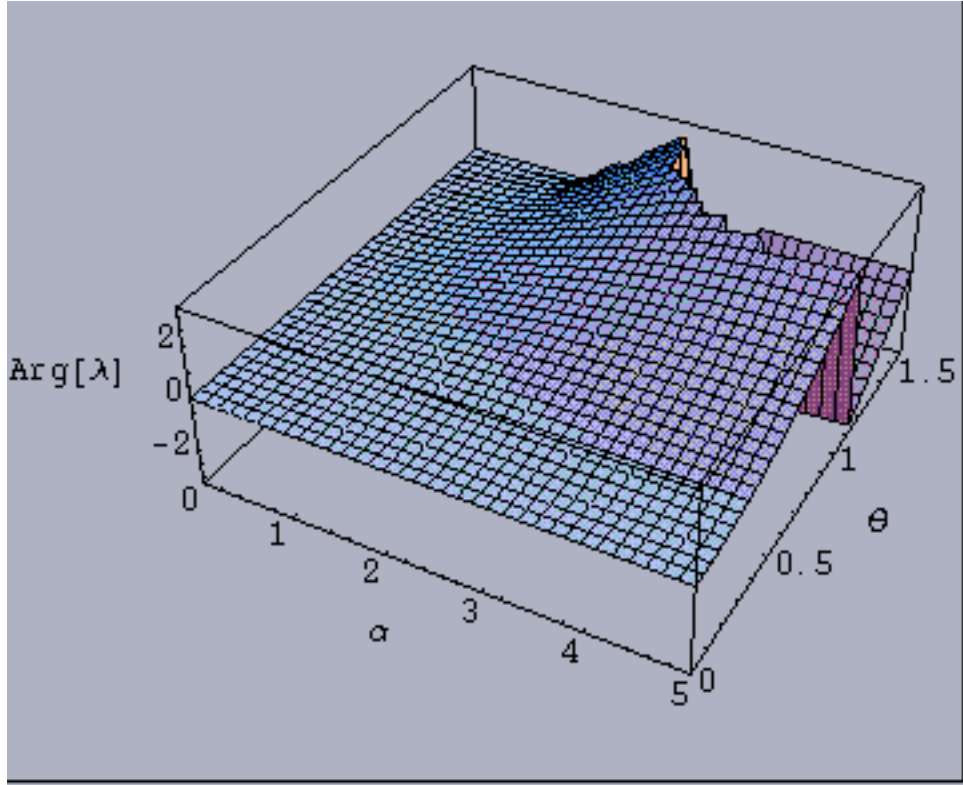


FIG. 64. Argument of the subordinate eigenvalue of the Uhlmann holonomy invariant (7) for the *three*-level Gibbsian density matrices

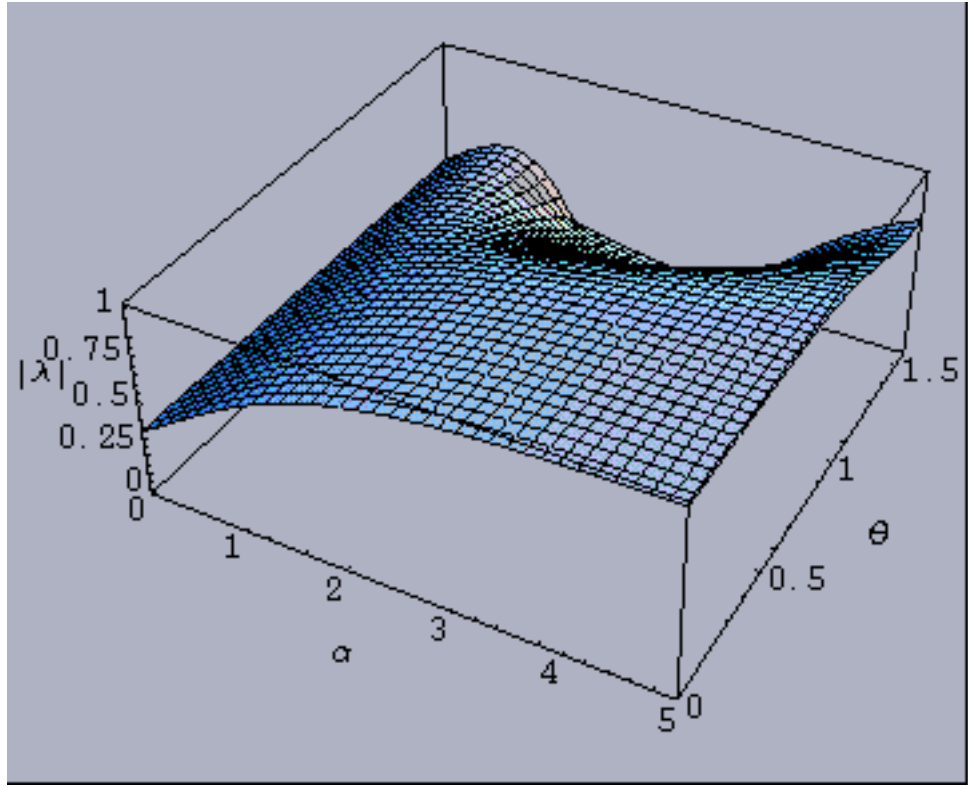


FIG. 65. Absolute value of the dominant eigenvalue of the Uhlmann holonomy invariant (7) for the *three*-level Gibbsian density matrices

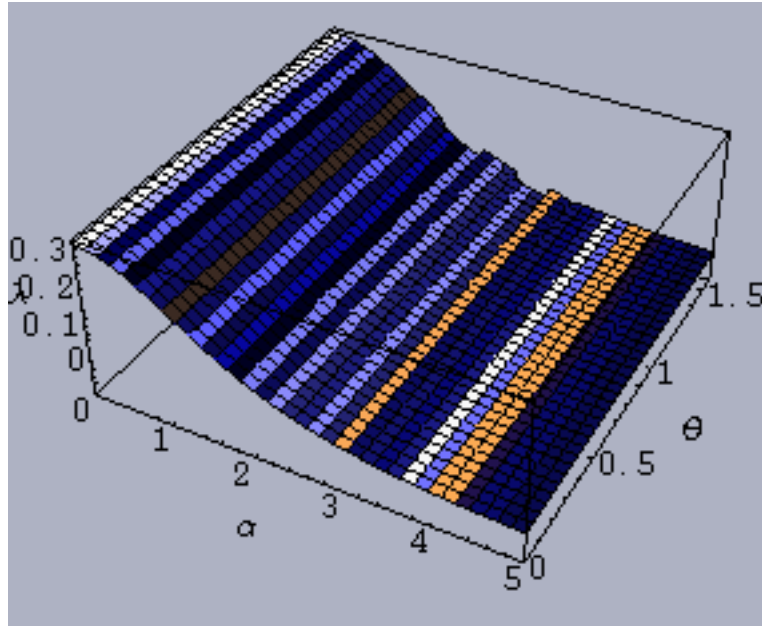


FIG. 66. Intermediate eigenvalue of the Uhlmann holonomy invariant (7) for the *three*-level Gibbsian density matrices

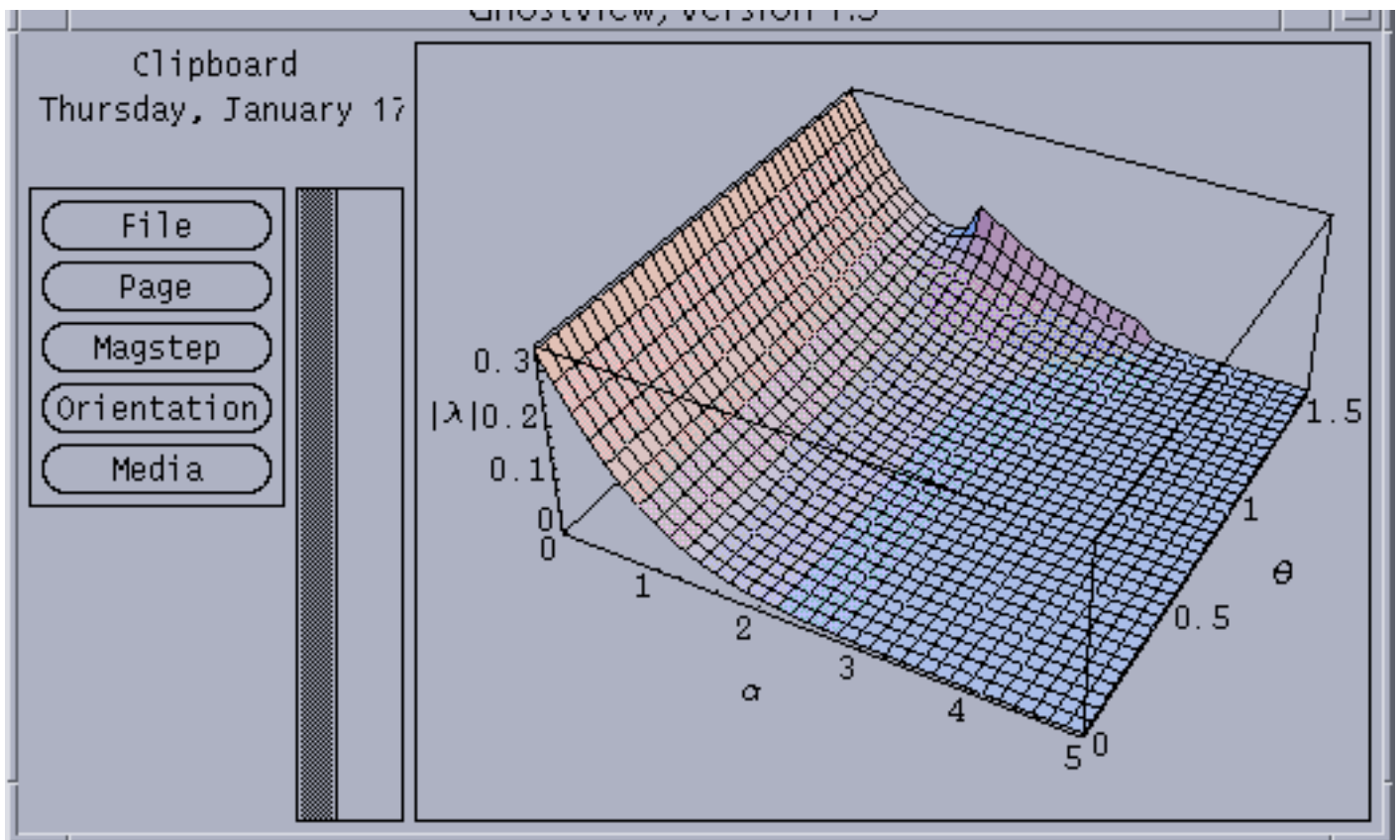


FIG. 67. Absolute value of the subordinate eigenvalue of the Uhlmann holonomy invariant (7) for the *three*-level Gibbsian density matrices

In Figs. 68-71, we show the arguments of the eigenvalues of the Uhlmann holonomy invariant (7) in the case  $n = 5$ . (The case  $n = 4$  proved more intractable in nature.) The third eigenvalue is simply real. In Figs. 72, 73, 75, 76 are shown the corresponding absolute values. In Fig. 74 is shown the value of the (real) intermediate eigenvalue.

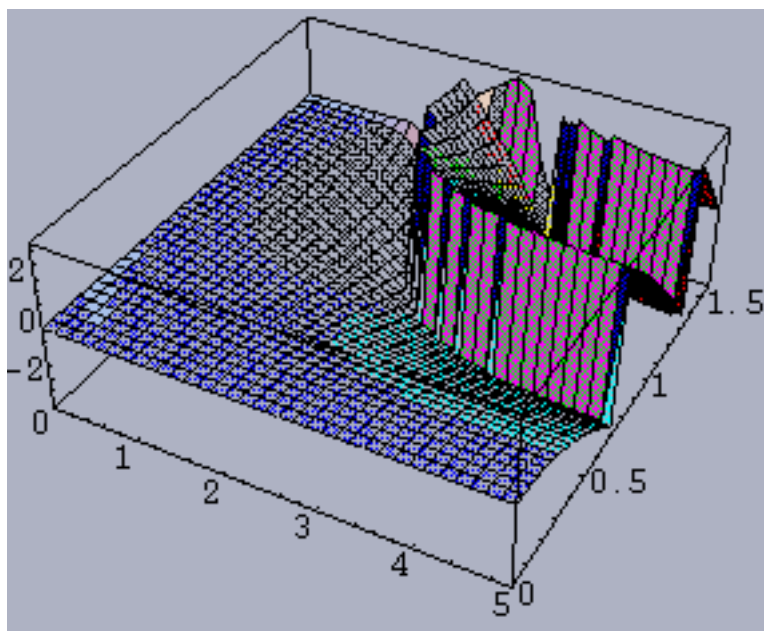


FIG. 68. Argument of the leading eigenvalue of the Uhlmann holonomy invariant (7) for the *five*-level Gibbsian density matrices

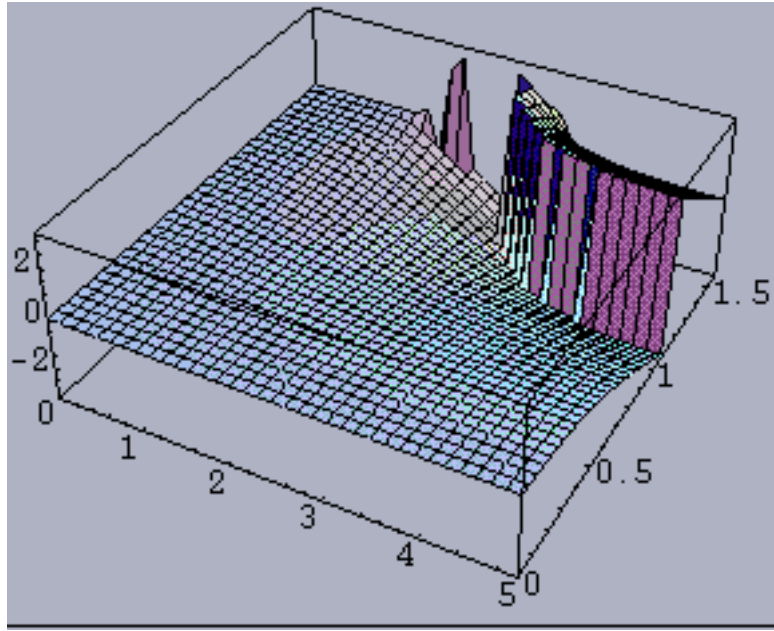


FIG. 69. Argument of the second leading eigenvalue of the Uhlmann holonomy invariant (7) for the *five*-level Gibbsian density matrices

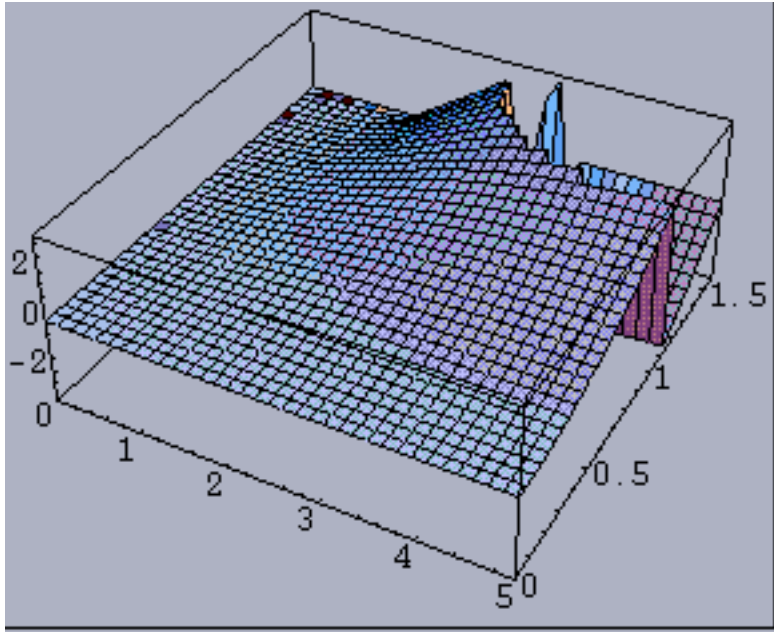


FIG. 70. Argument of the second smallest eigenvalue of the Uhlmann holonomy invariant (7) for the *five*-level Gibbsian density matrices



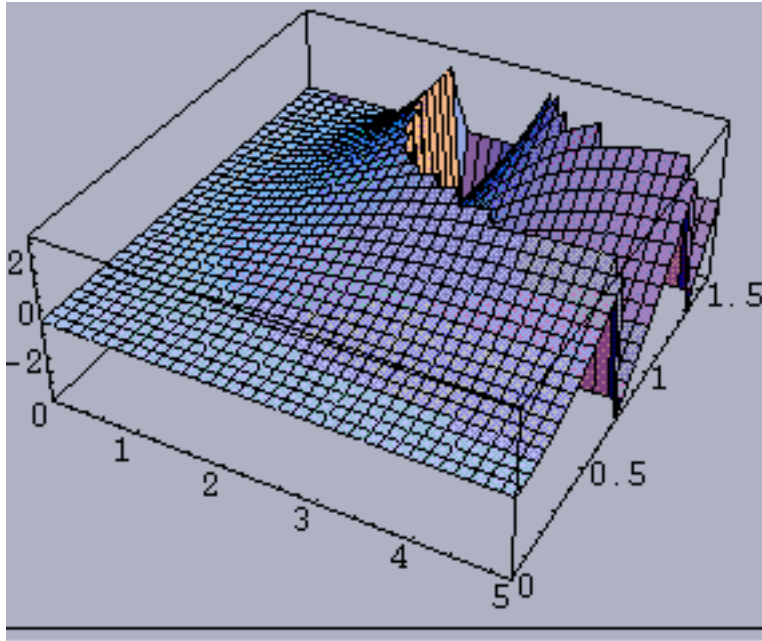


FIG. 71. Argument of the last eigenvalue of the Uhlmann holonomy invariant (7) for the *five*-level Gibbsian density matrices

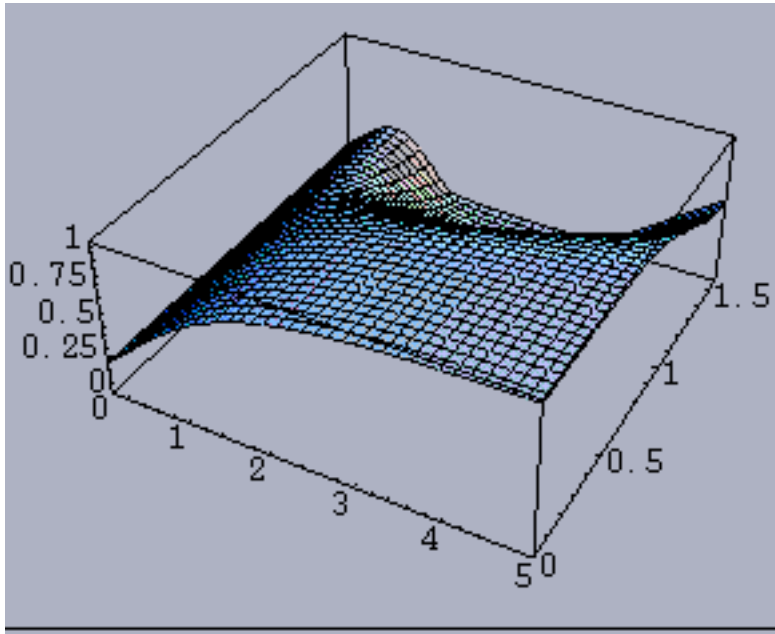


FIG. 72. Absolute value of the leading eigenvalue of the Uhlmann holonomy invariant (7) for the *five*-level Gibbsian density matrices



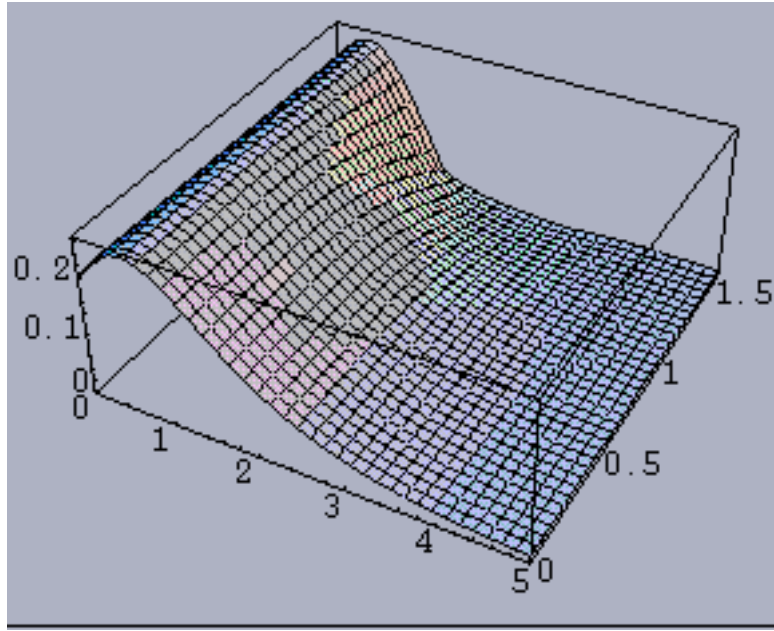


FIG. 73. Absolute value of the second leading eigenvalue of the Uhlmann holonomy invariant (7) for the *five*-level Gibbsian density matrices

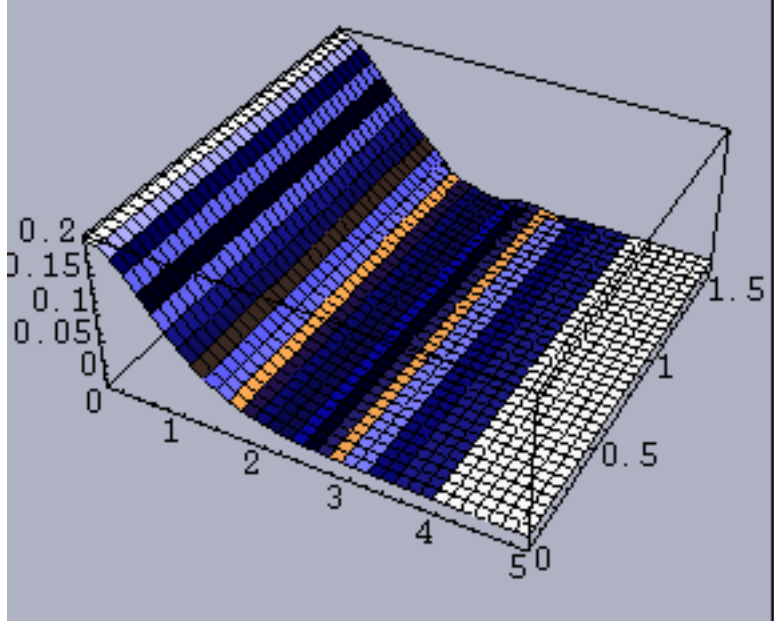


FIG. 74. Central eigenvalue of the Uhlmann holonomy invariant (7) for the *five*-level Gibbsian density matrices

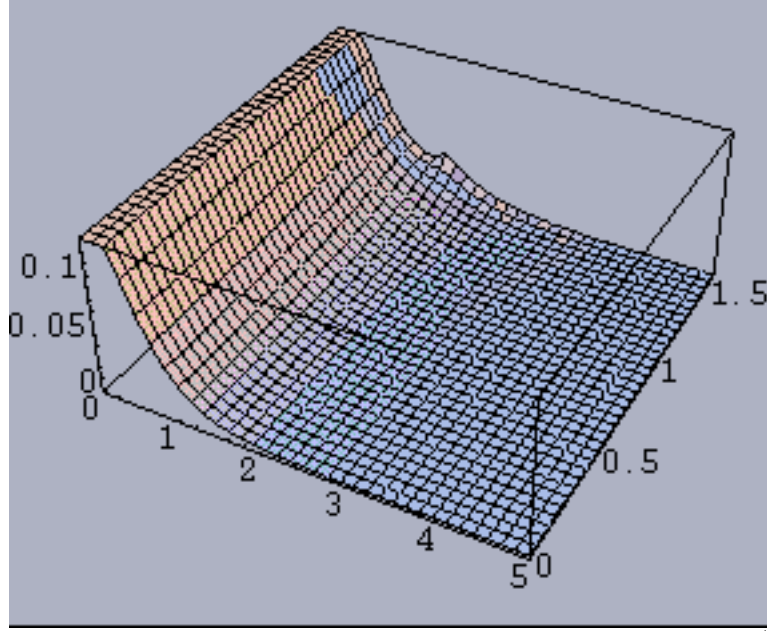


FIG. 75. Absolute value of the second smallest eigenvalue of the Uhlmann holonomy invariant (7) for the *five*-level Gibbsian density matrices

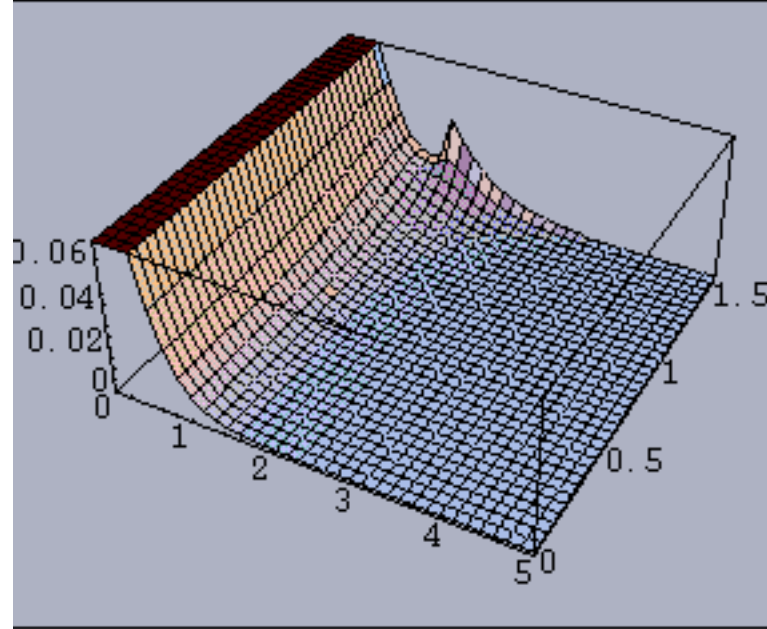


FIG. 76. Absolute value of the last eigenvalue of the Uhlmann holonomy invariant (7) for the *five*-level Gibbsian density matrices

## VI. SJÖQVIST *ET AL* GEOMETRIC PHASES FOR GIBBSIAN $N$ -LEVEL SYSTEMS ( $N = 2, \dots, 11$ )

In the approach of Sjöqvist *et al* [1] every pure state that diagonalizes the initial density matrix is parallel transported separately. By weighting the associated holonomy of each such pure state by the corresponding eigenvalues, we obtain the measure proposed in [1] “in the experimental context of quantum interferometry”. Since it is essentially trivial to obtain the pure states that diagonalize the *initial* (diagonal)  $n$ -level Gibbsian density matrix and the associated eigenvalues, and since Uhlmann has presented the holonomy invariant (the trace of which is the Berry phase)

$$W_{2\pi} W_0^* = (-1)^{2j} \rho_0^{1/2} e^{2\pi i \cos \theta J_z} \rho_0^{1/2} = e^{-2\pi i m(1-\cos \theta)} |m\rangle\langle m|, \quad (15)$$

for the circular evolution of pure states, we can directly compute the Sjöqvist *et al* geometric phase ( $\gamma$ ) and visibility ( $\nu$ ) for the  $n$ -level Gibbsian density matrices. These are presented in Figs 77 to 86 and Figs. 87 to 96. The trace of the weighted (by the eigenvalues) sum of the holonomy invariants (15) for  $n = 2$  is

$$\cos(\pi \cos \theta) + i \sin(\pi \cos \theta) \tanh \frac{\alpha}{2}, \quad (16)$$

while for  $n = 3$ , it is

$$\frac{1 + 2 \cos(2\pi \cos \theta) \cosh \alpha + 2i \sin(2\pi \cos \theta) \sinh \alpha}{1 + 2 \cosh \alpha}, \quad (17)$$

for  $n = 4$ ,

$$\frac{e^{-3i\pi \cos \theta} (1 + e^{\alpha + 2i\pi \cos \theta}) (1 + e^{2\alpha + 4i\pi \cos \theta})}{(1 + e^{\alpha})(1 + e^{2\alpha})}. \quad (18)$$

and for  $n = 5$ ,

$$\frac{1 + 2 \cos(2\pi \cos \theta) \cosh \alpha + 2 \cos(4\pi \cos \theta) \cosh 2\alpha + 2i \sin(2\pi \cos \theta) \sinh \alpha + 2i \sin(4\pi \cos \theta) \sinh 2\alpha}{1 + 2 \cosh \alpha + 2 \cosh 2\alpha}. \quad (19)$$

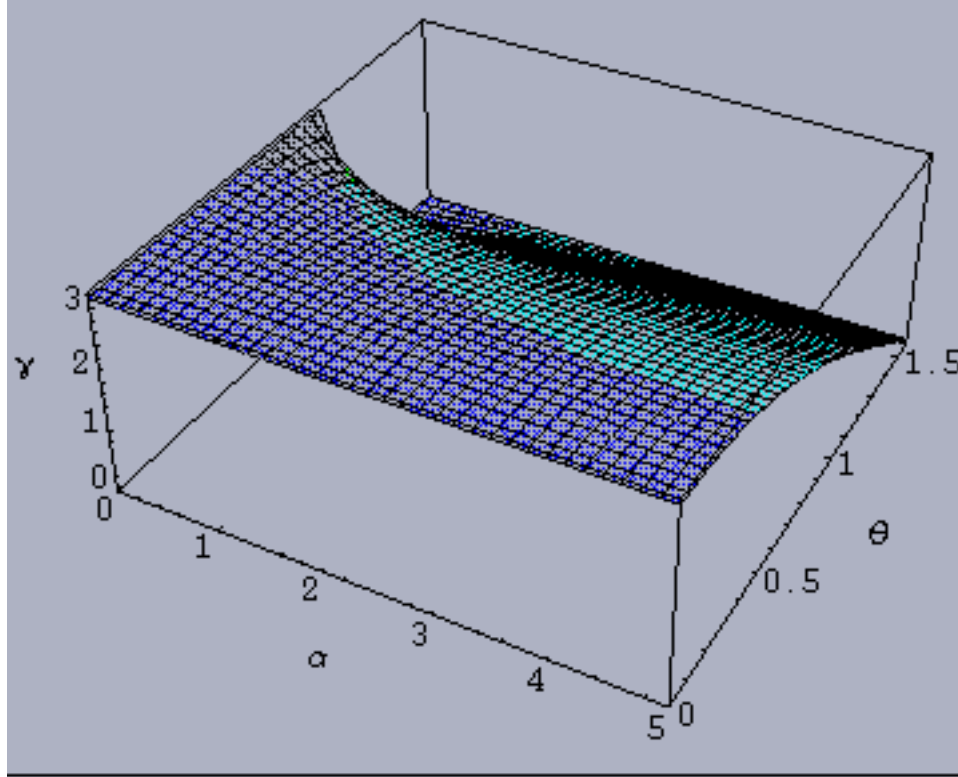


FIG. 77. Sjöqvist *et al* geometric phase for Gibbsian spin- $\frac{1}{2}$  systems

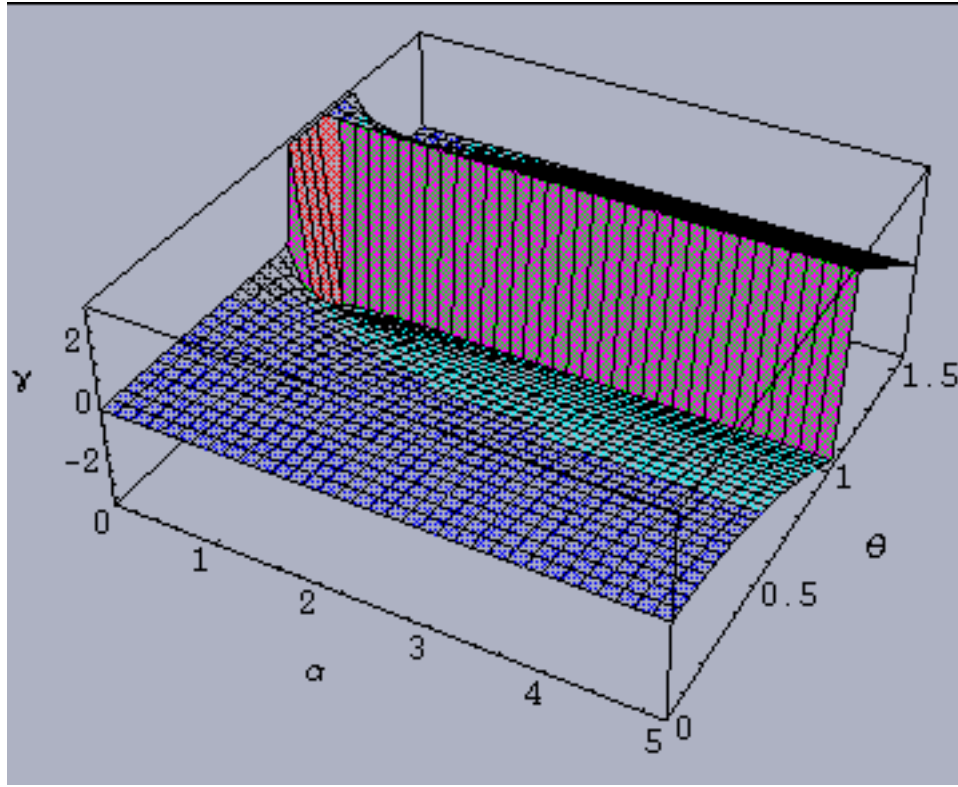


FIG. 78. Sjöqvist *et al* geometric phase for Gibbsian spin-1 systems

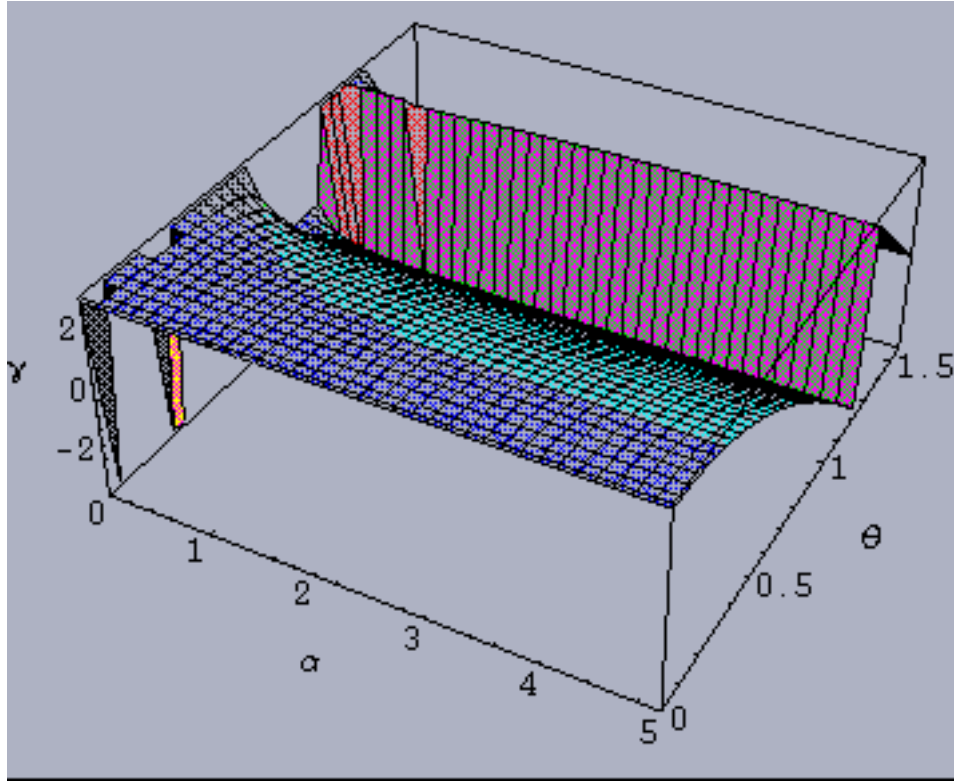


FIG. 79. Sjöqvist *et al* geometric phase for Gibbsian spin- $\frac{3}{2}$  systems



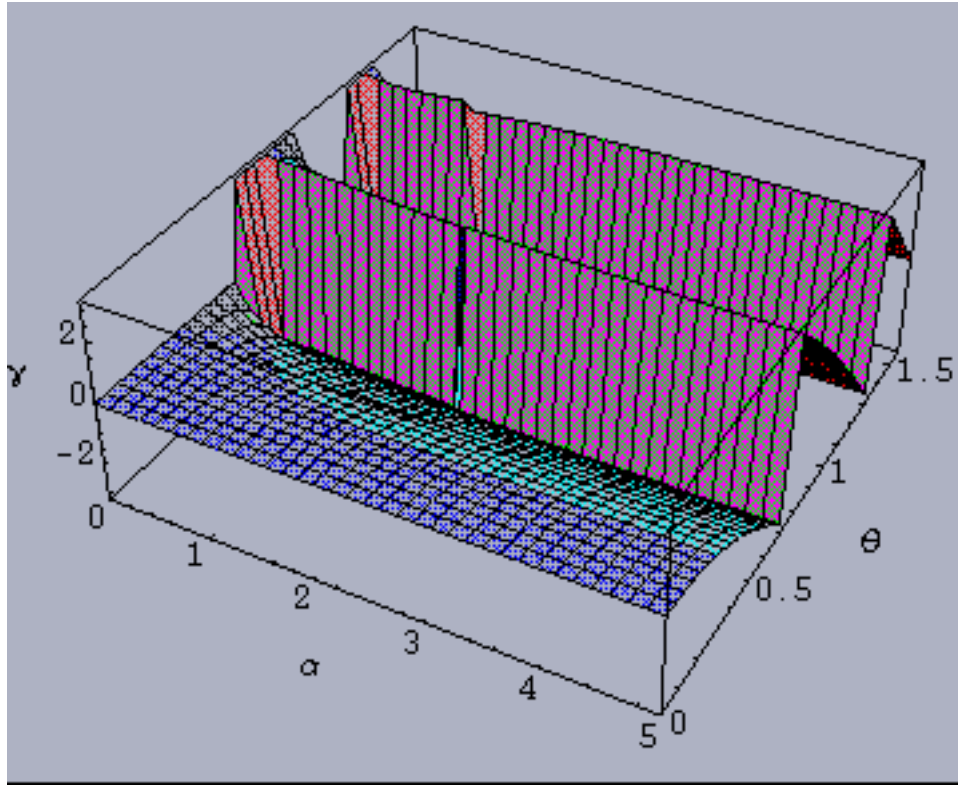


FIG. 80. Sjöqvist *et al* geometric phase for Gibbsian spin-2 systems

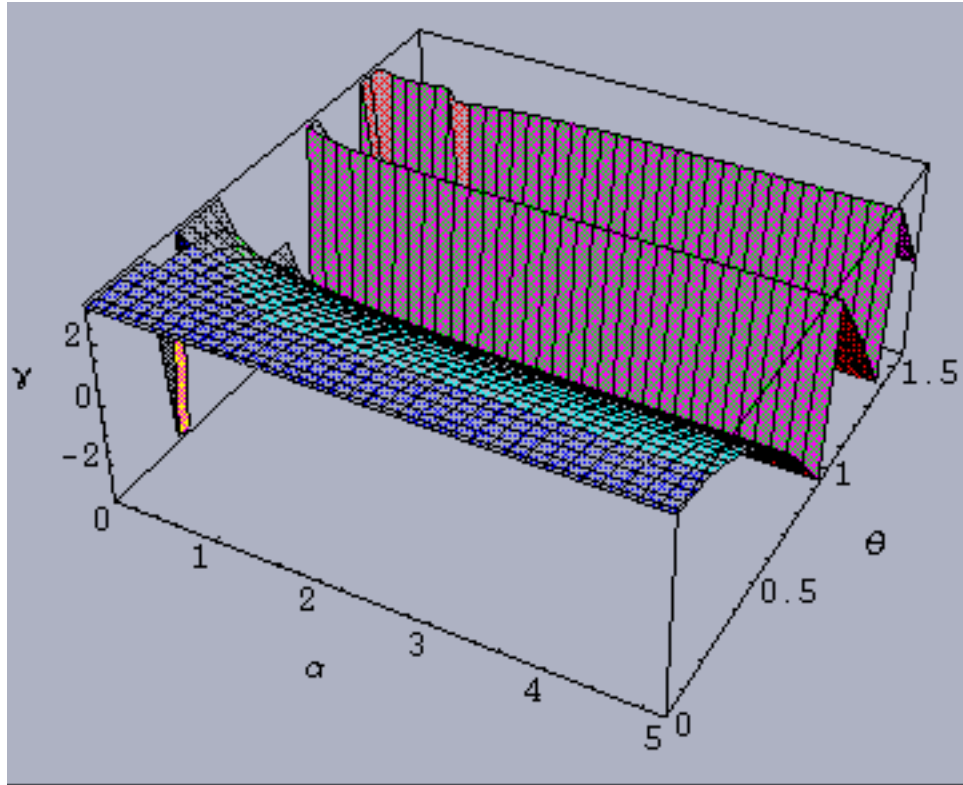


FIG. 81. Sjöqvist *et al* geometric phase for Gibbsian spin- $\frac{5}{2}$  systems



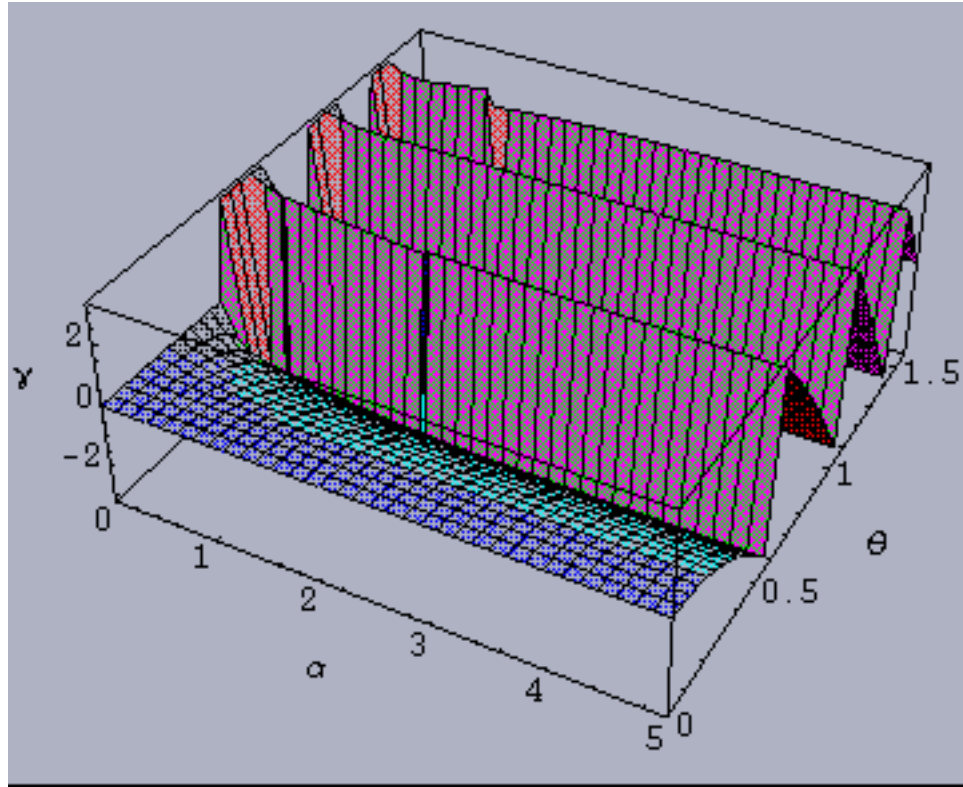


FIG. 82. Sjöqvist *et al* geometric phase for Gibbsian spin-3 systems

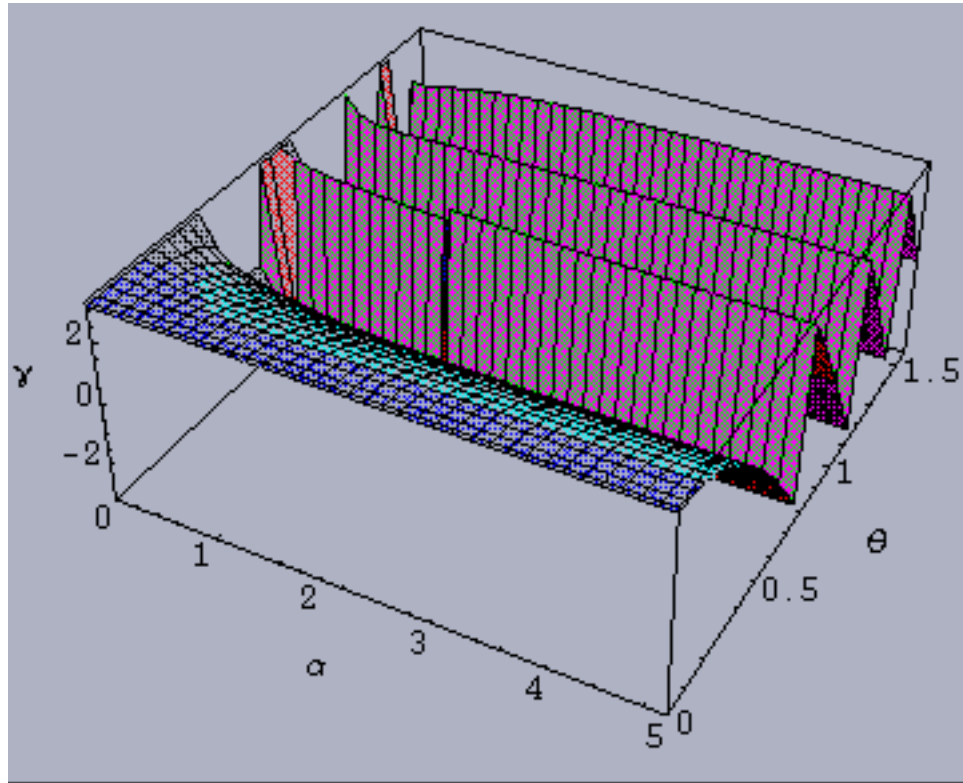


FIG. 83. Sjöqvist *et al* geometric phase for Gibbsian spin- $\frac{7}{2}$  systems

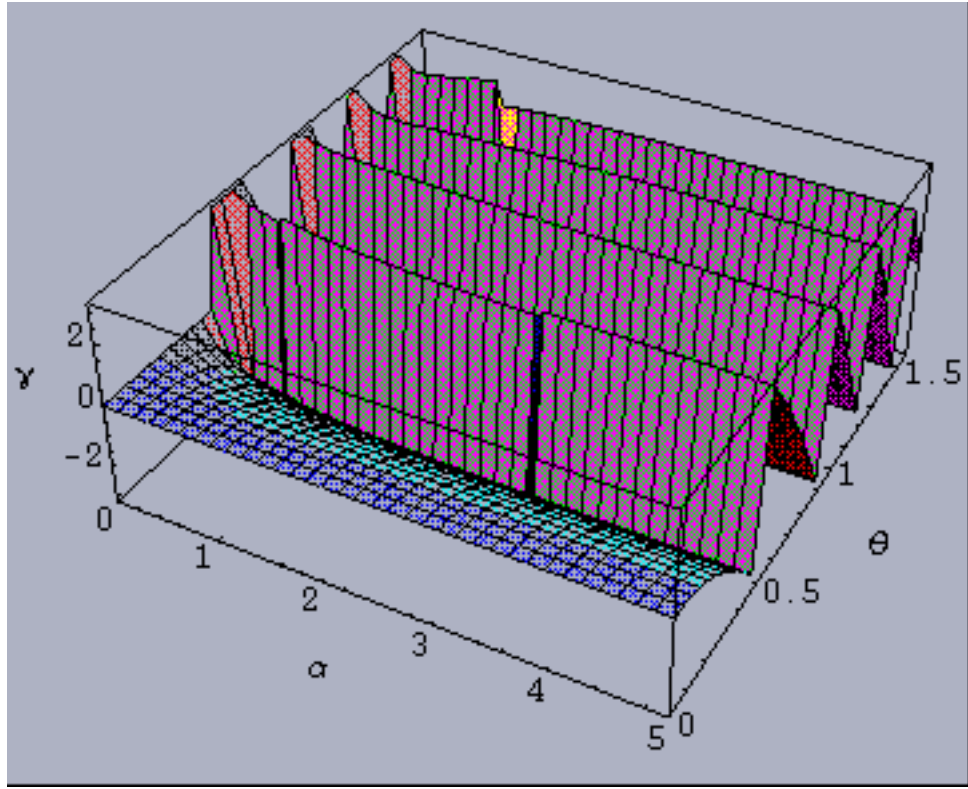


FIG. 84. Sjöqvist *et al* geometric phase for Gibbsian spin-4 systems

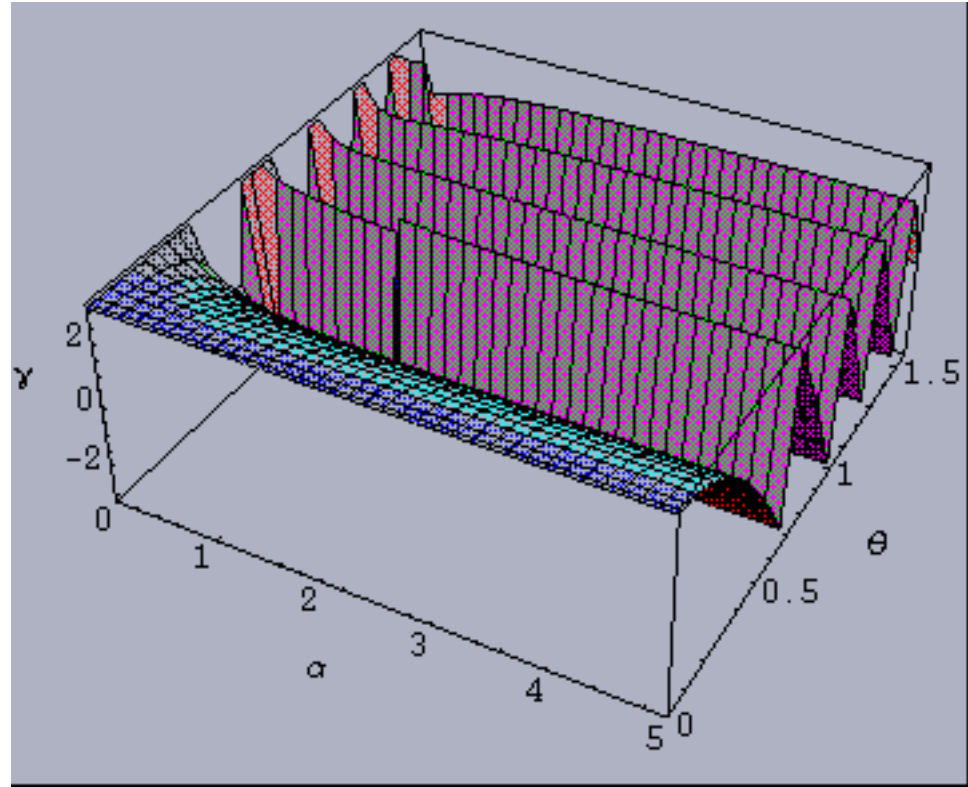


FIG. 85. Sjöqvist *et al* geometric phase for Gibbsian spin- $\frac{9}{2}$  systems

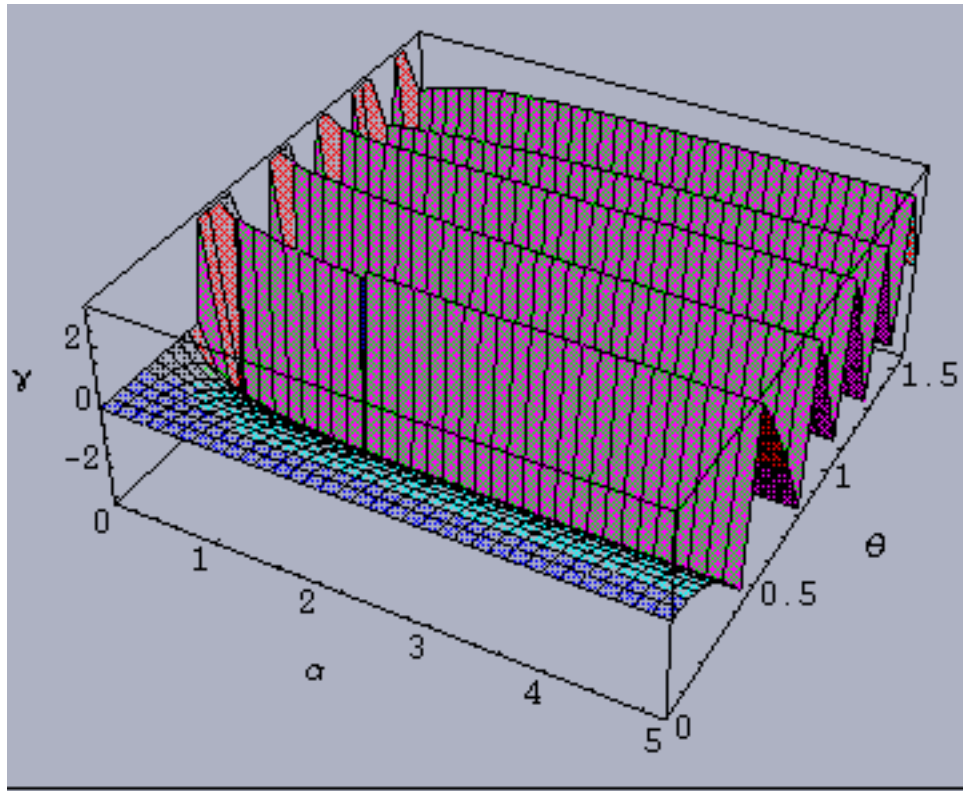


FIG. 86. Sjöqvist *et al* geometric phase for Gibbsian spin-5 systems

VII. SJÖQVIST *ET AL* VISIBILITIES FOR GIBBSIAN  $N$ -LEVEL SYSTEMS ( $N = 2, \dots, 11$ )

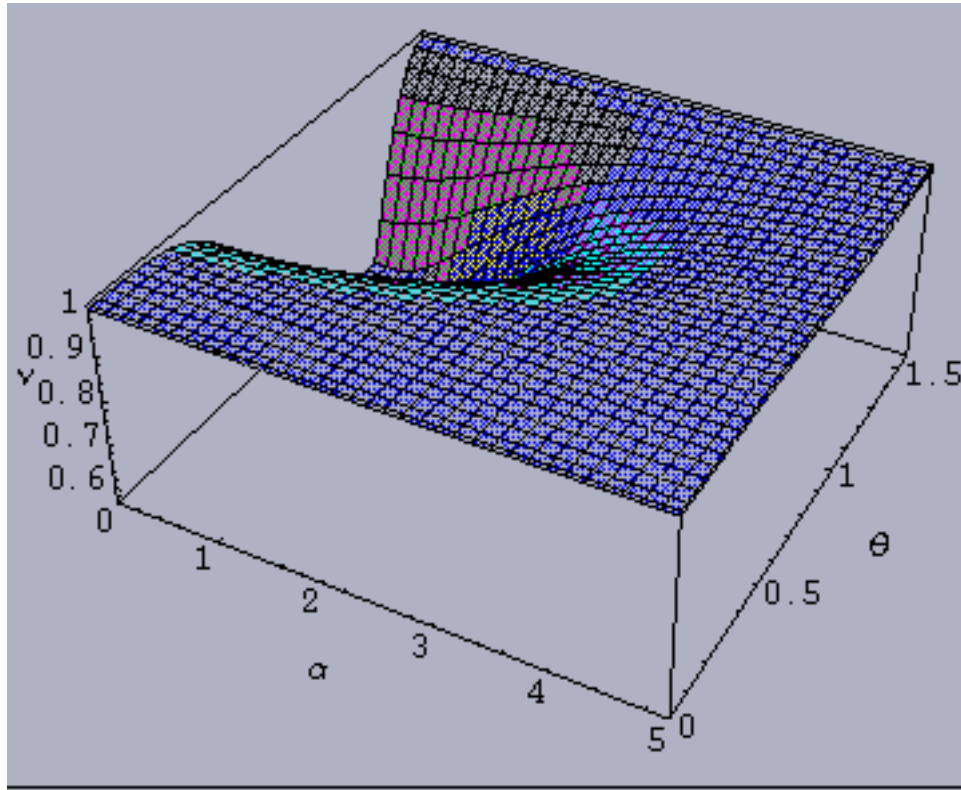


FIG. 87. Sjöqvist *et al* visibility for Gibbsian spin- $\frac{1}{2}$  systems



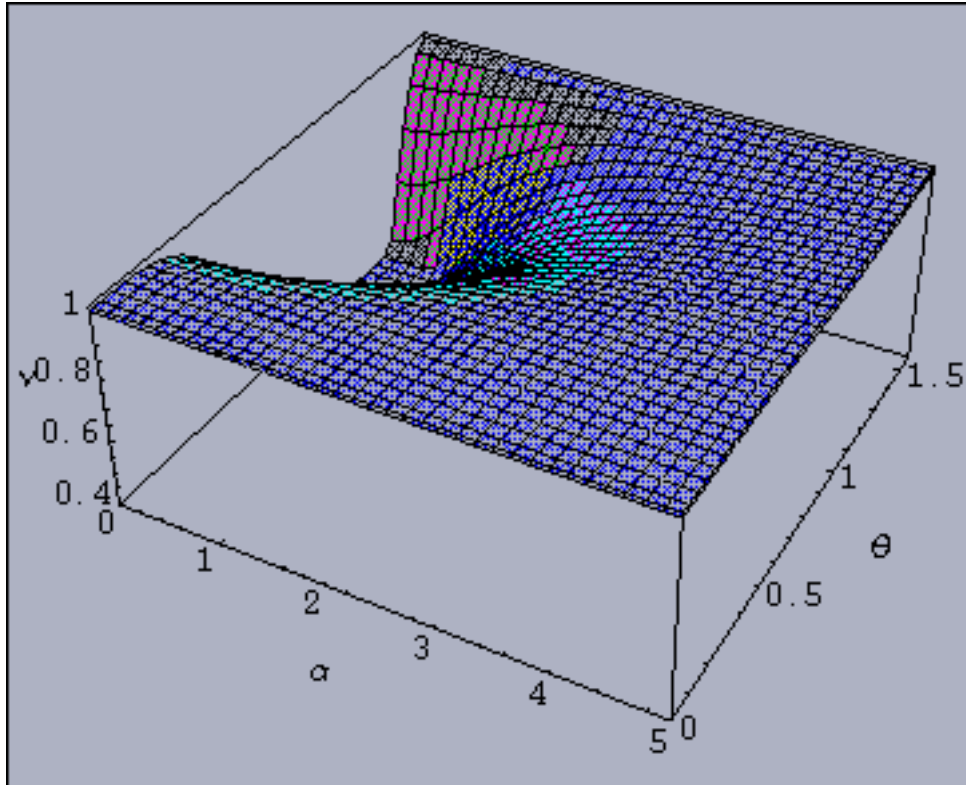


FIG. 88. Sjöqvist *et al* visibility for Gibbsian spin-1 systems

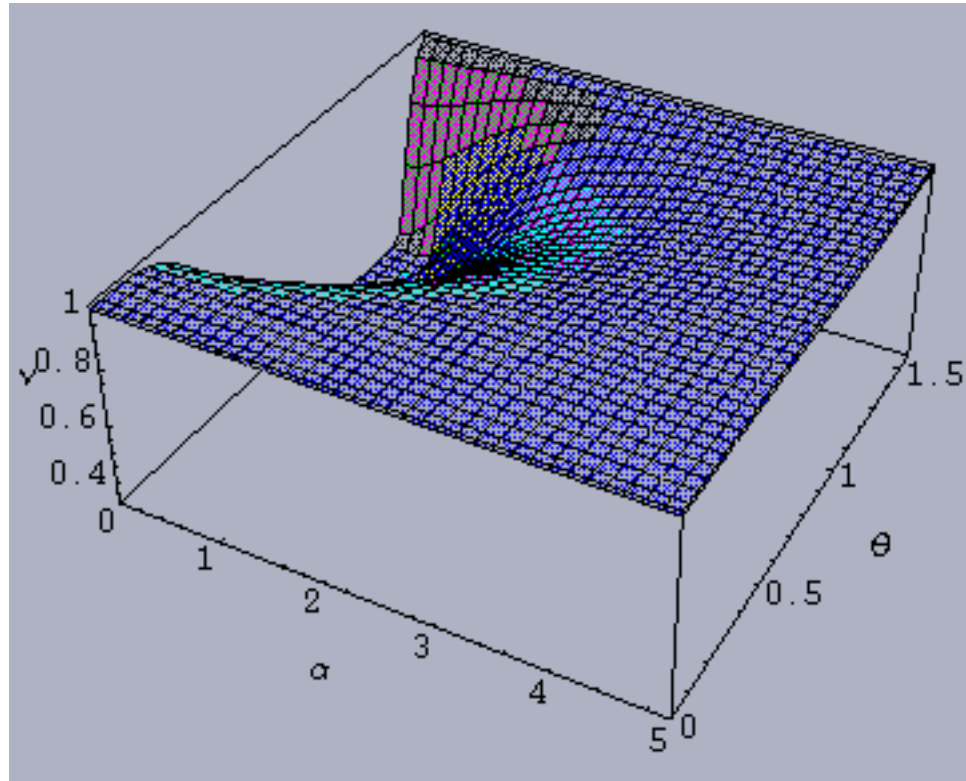


FIG. 89. Sjöqvist *et al* visibility for Gibbsian spin- $\frac{3}{2}$  systems



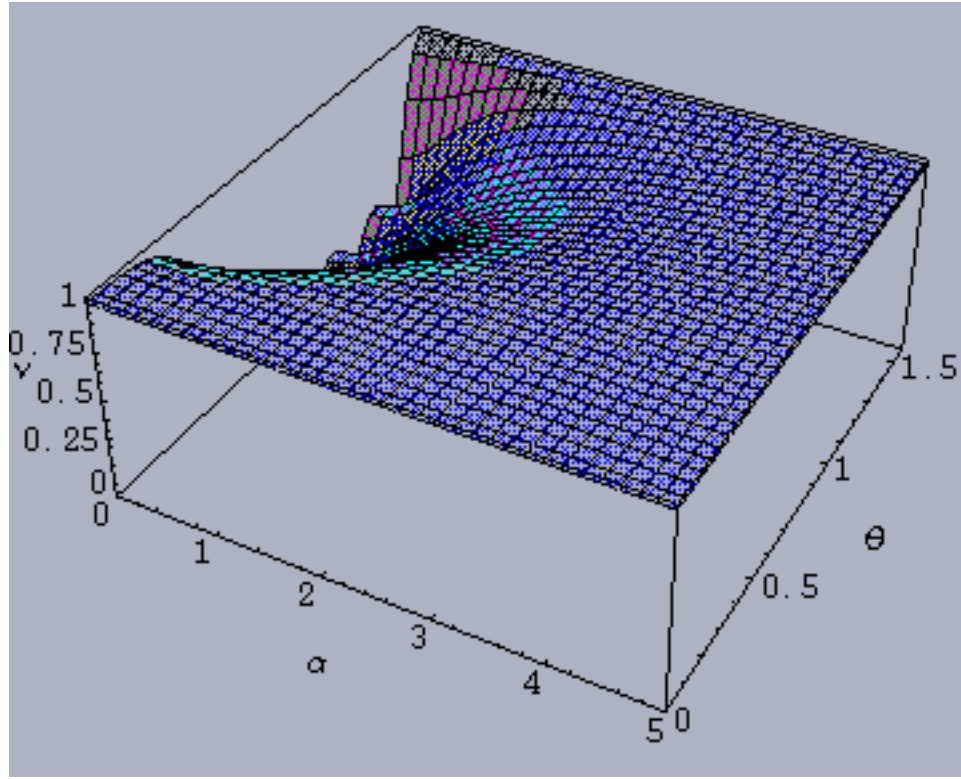


FIG. 90. Sjöqvist *et al* visibility for Gibbsian spin-2 systems

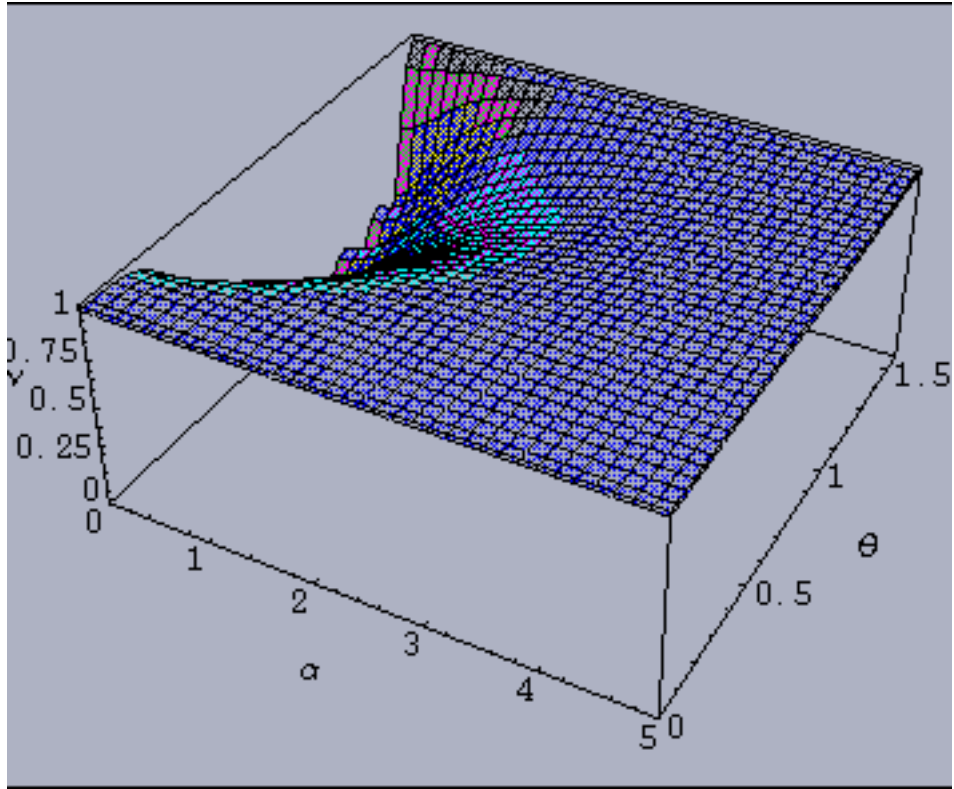


FIG. 91. Sjöqvist *et al* visibility for Gibbsian spin- $\frac{5}{2}$  systems

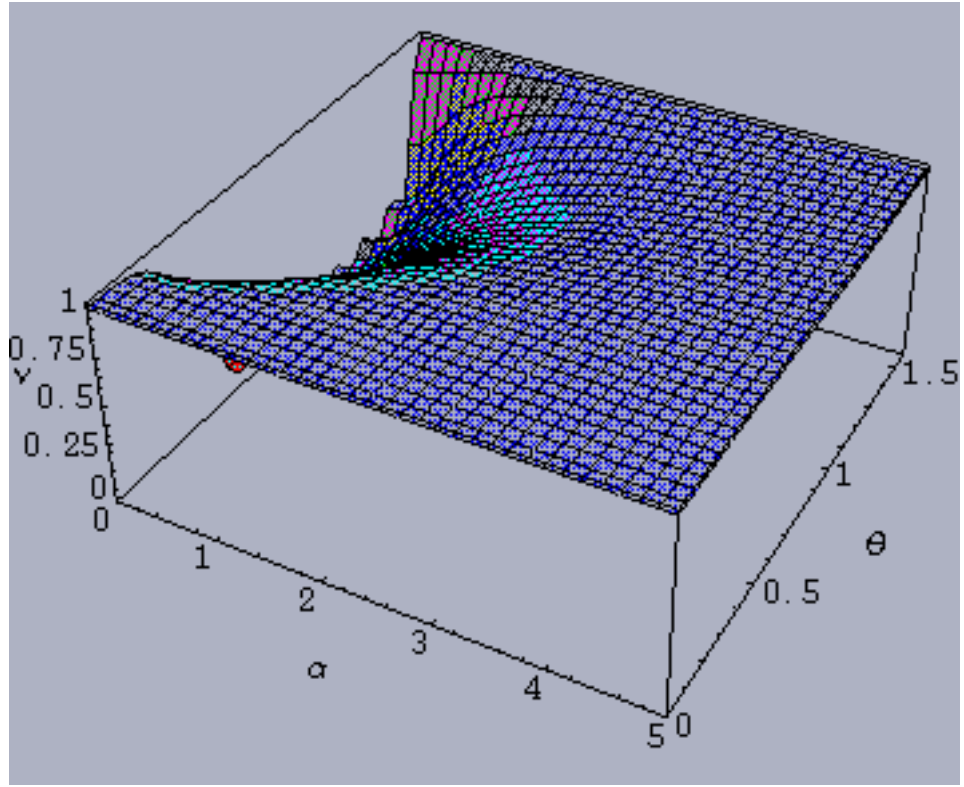


FIG. 92. Sjöqvist *et al* visibility for Gibbsian spin-3 systems

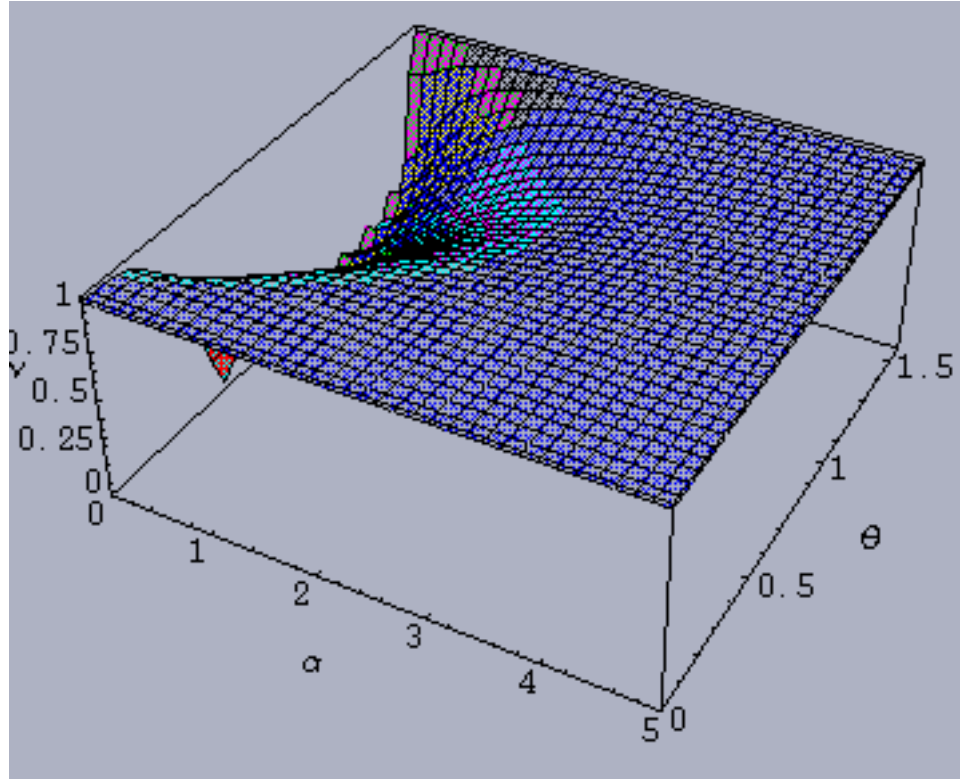


FIG. 93. Sjöqvist *et al* visibility for Gibbsian spin- $\frac{7}{2}$  systems

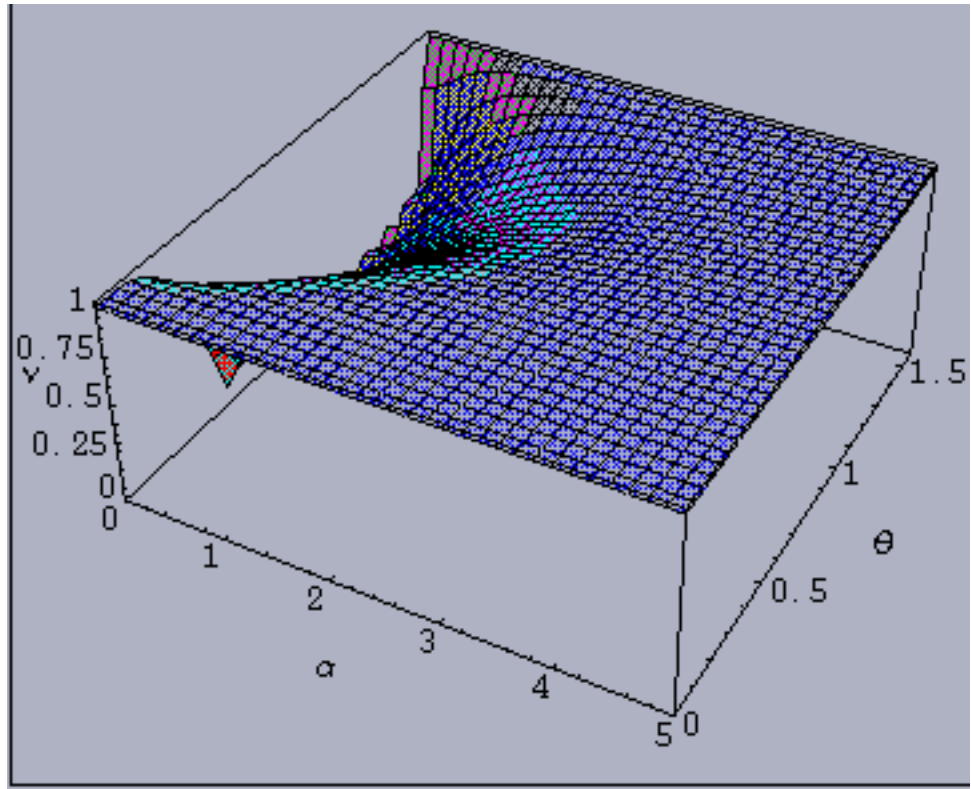


FIG. 94. Sjöqvist *et al* visibility for Gibbsian spin-4 systems

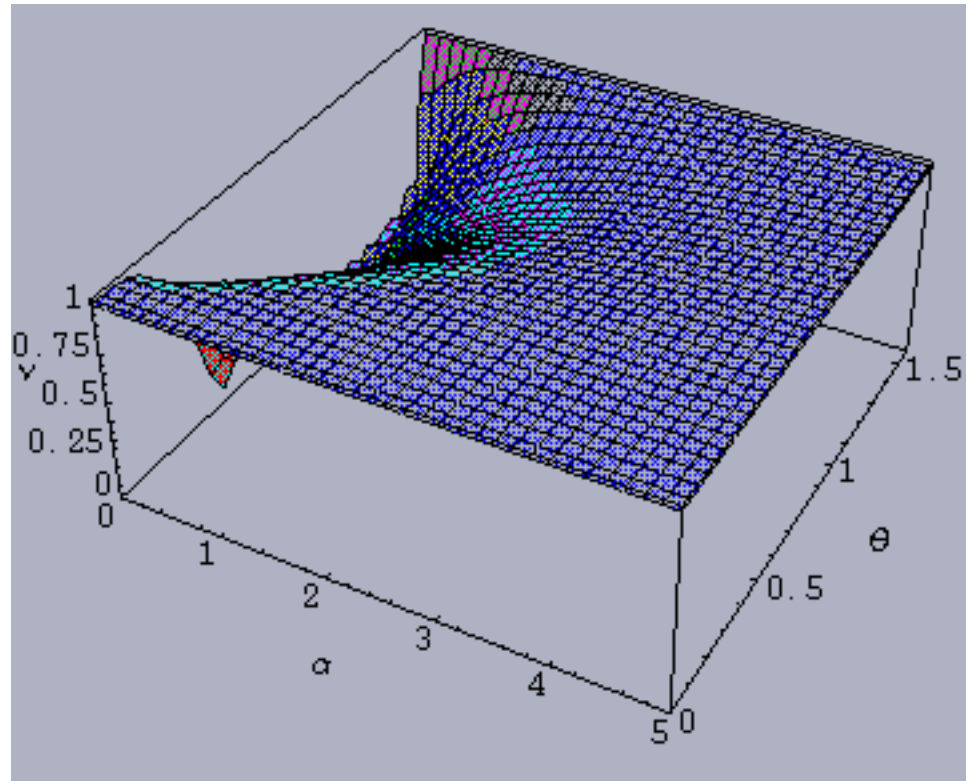


FIG. 95. Sjöqvist *et al* visibility for Gibbsian spin- $\frac{9}{2}$  systems

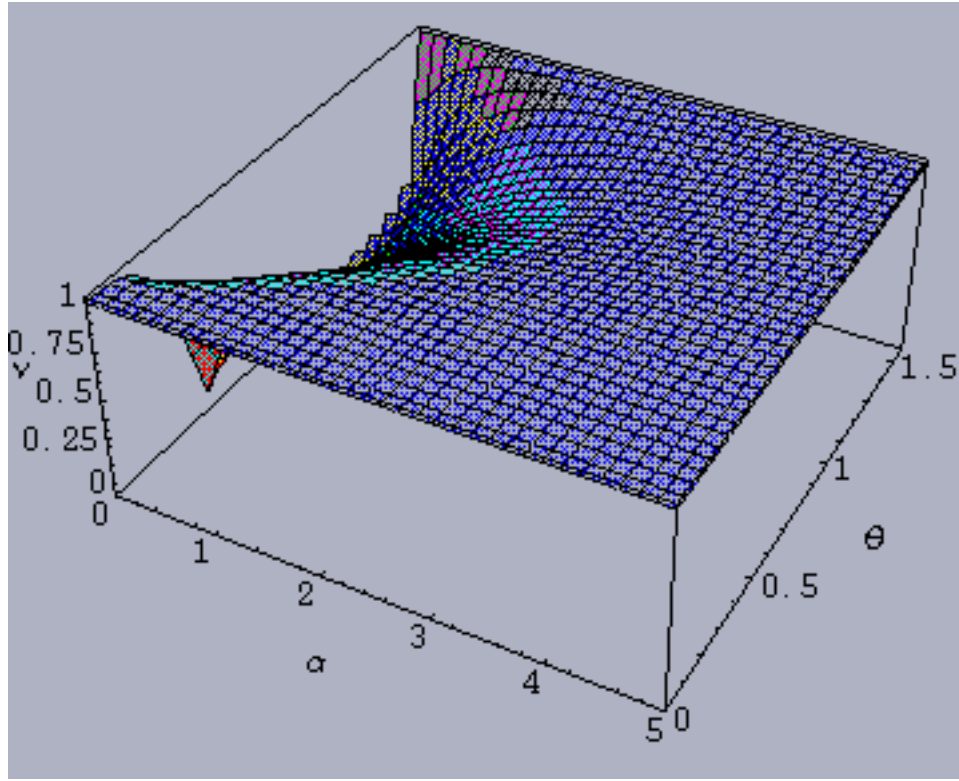


FIG. 96. Sjöqvist *et al* visibility for Gibbsian spin-5 systems

### VIII. COMPARISONS ACROSS GIBBSIAN $N$ -LEVEL SYSTEMS OF SJÖQVIST *ET AL* GEOMETRIC PHASES AND VISIBILITIES

In Figs. 97-101, we display the direct counterparts of Figs. 21-25, but now based on the methodology [1] of Sjöqvist *et al* rather than Uhlmann. (We omit the counterpart of Fig. 26 because it appears to consist of essentially noise.)

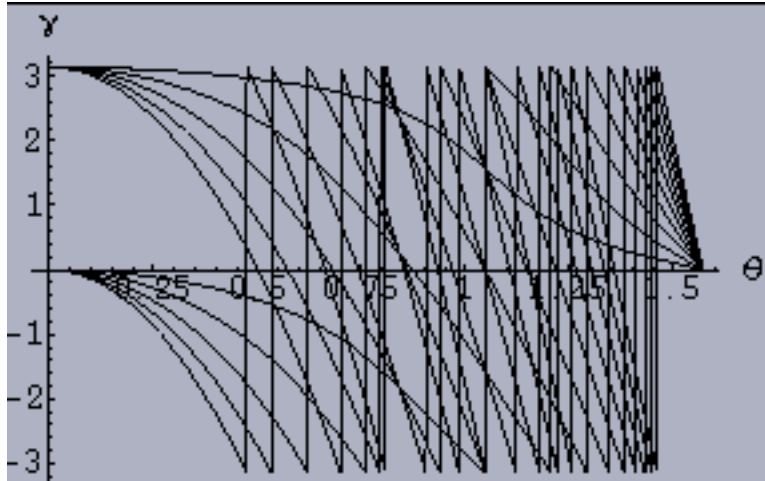


FIG. 97. Sjöqvist *et al* geometric phases for  $n$ -level Gibbsian systems ( $n = 2, \dots, 11$ ) holding  $\alpha = 1$ . At  $\theta = .25$ , the curve for  $n = 2$  is dominant, followed in order by those for  $n = 4, 6, 8, 10$ , (all having *positive* values at  $\theta = .25$ ) and  $n = 3, 5, 7, 9, 11$  (all having *negative* values at  $\theta = .25$ ), cf. Fig. 21



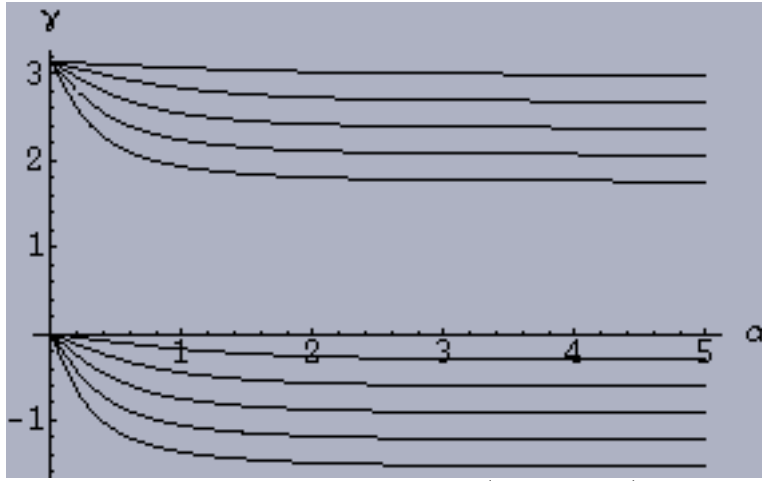


FIG. 98. Sjöqvist *et al* geometric phases for  $n$ -level Gibbsian systems ( $n = 2, \dots, 11$ ) holding  $\theta$  fixed at  $\frac{\pi}{10}$ . In monotonically decreasing order are the curves for (the even)  $n = 2, 4, 6, 8, 10$ , followed by those for (the odd)  $n = 3, 5, 7, 9, 11$ , cf. Fig. 22

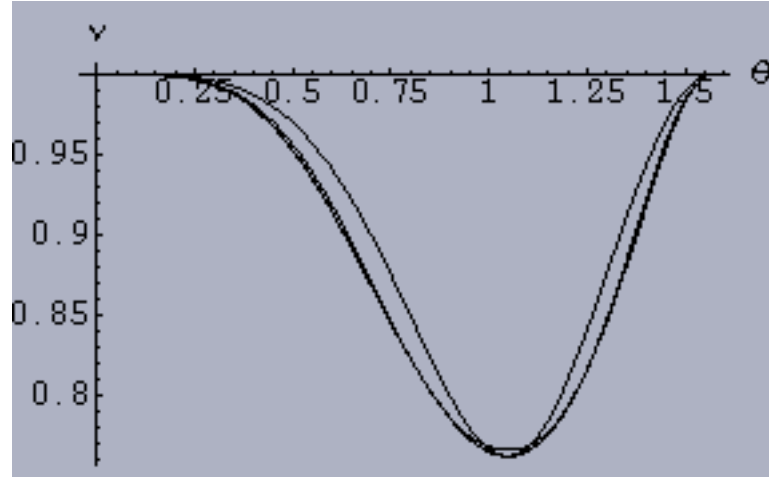


FIG. 99. Sjöqvist *et al* visibilities for  $n$ -level Gibbsian systems ( $n = 2, \dots, 11$ ) holding  $\alpha$  fixed at 2. The curve for  $n = 2$  stands out from the other nine, cf. Fig. 23

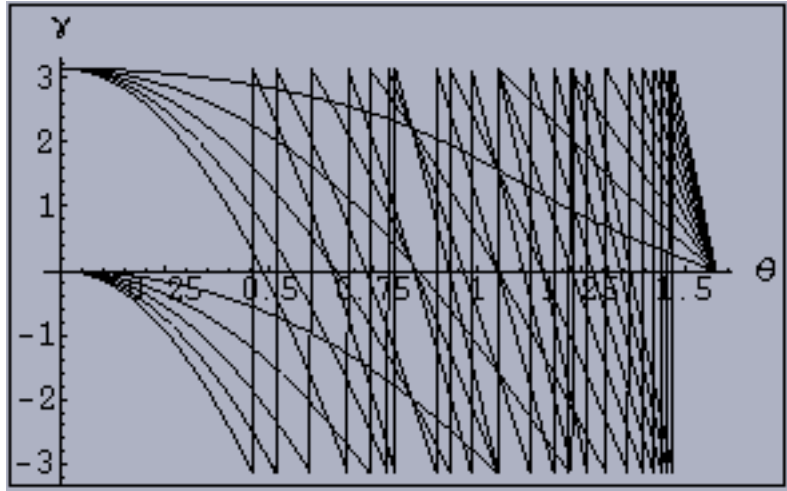


FIG. 100. Sjöqvist *et al* geometric phases for  $n$ -level Gibbsian systems ( $n = 2, \dots, 11$ ) holding  $\alpha = 2$ . In order of decreasing dominance at  $\theta = .25$  are the curves for (the even)  $n = 2, 4, 6, 8, 10$ , followed by those for (the odd)  $n = 3, 5, 7, 9, 11$ , cf. Fig. 24



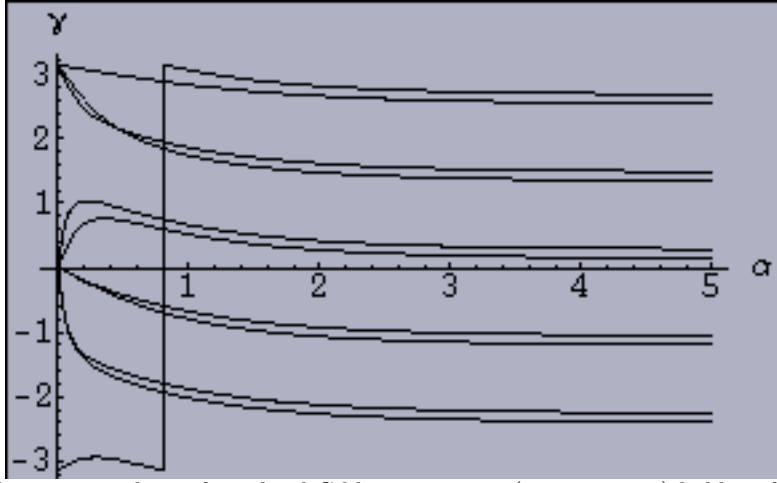


FIG. 101. Sjöqvist *et al* geometric phases for  $n$ -level Gibbsian systems ( $n = 2, \dots, 11$ ) holding  $\theta = \frac{\pi}{5}$ . At  $\alpha = 2$ , in order of decreasing dominance are the curves for  $n = 7, 2, 9, 4, 11, 6, 8, 3, 10, 5$ , cf. Fig. 25

### IX. DIRECT COMPARISONS OF UHLMANN AND SJÖQVIST *ET AL* RESULTS

In Fig. 102, we plot for  $n = 6$  the ratio of the Sjöqvist *et al* geometric phase (Fig. 81) to the Uhlmann geometric phase (Fig. 5), and in Fig. 103, the corresponding ratio for  $n = 11$ . In the next two figures (Figs. 104 and 105), we show the ratios of the associated visibilities.

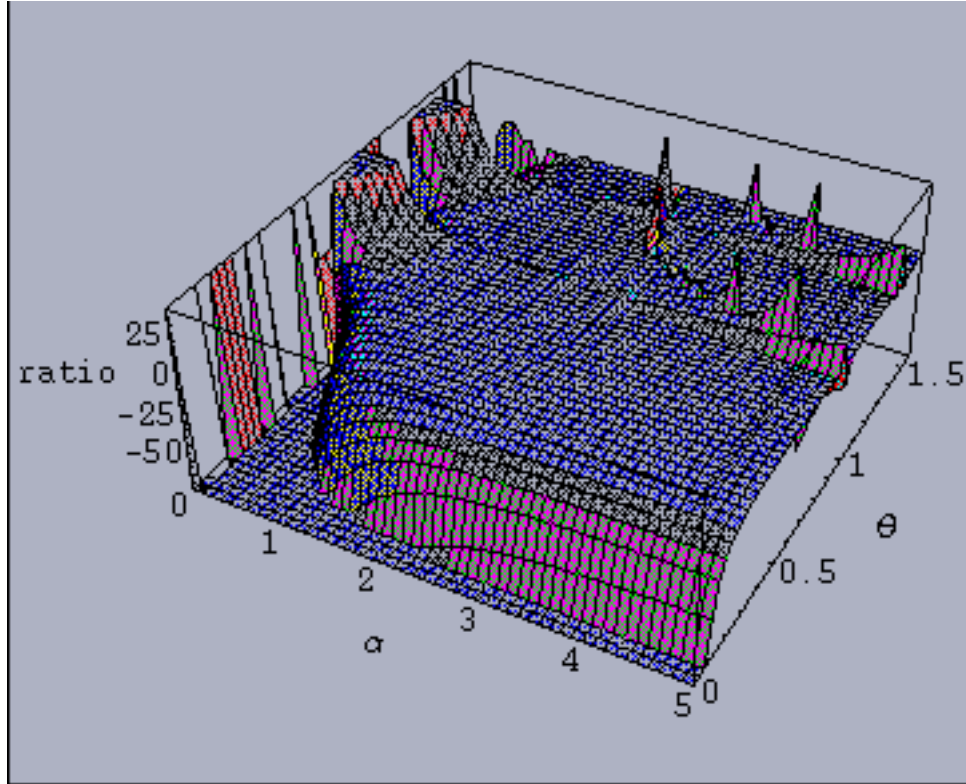


FIG. 102. Ratio of the Sjöqvist *et al* geometric phase (Fig. 81) to the Uhlmann geometric phase (Fig. 5) for *six*-level Gibbsian systems

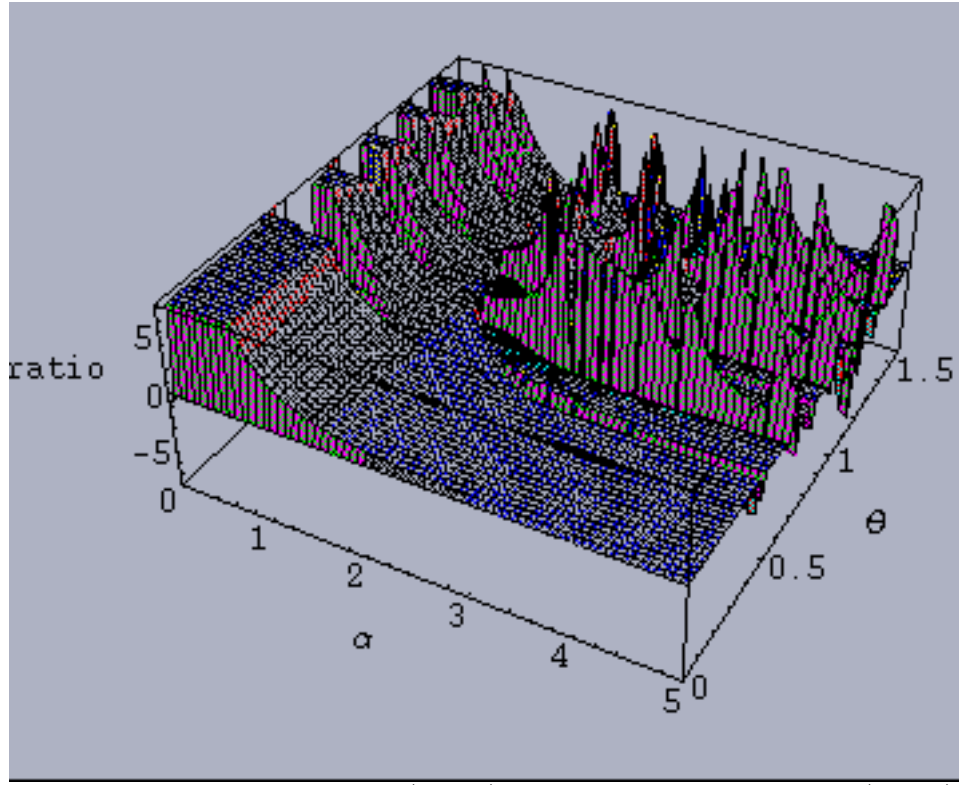


FIG. 103. Ratio of the Sjöqvist *et al* geometric phase (Fig. 86) to the Uhlmann geometric phase (Fig. 10) for the *eleven*-level Gibbsian systems

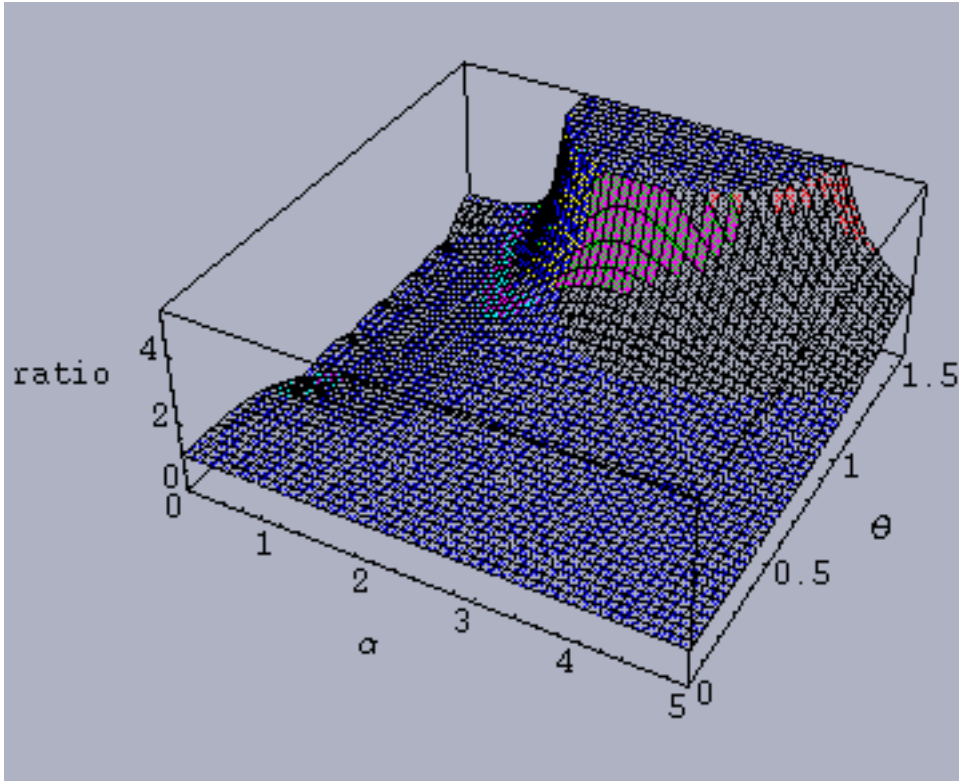


FIG. 104. Ratio of the Sjöqvist *et al* visibility (Fig. 91) to the Uhlmann visibility (Fig. 15) for the *six*-level Gibbsian systems

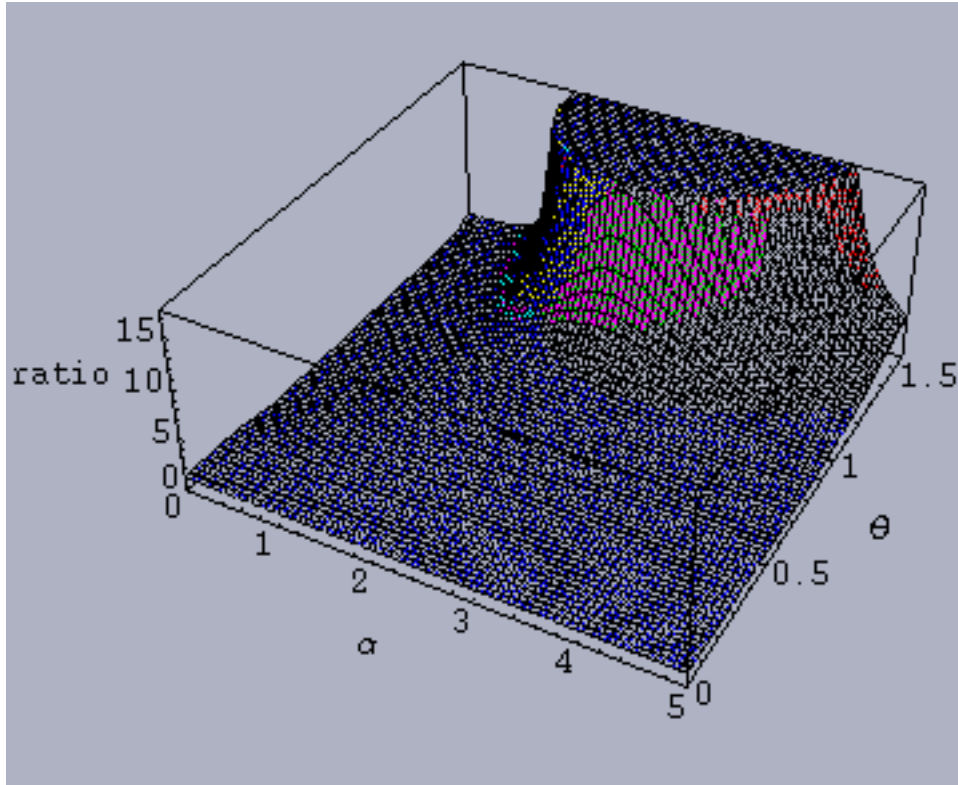


FIG. 105. Ratio of the Sjöqvist *et al* visibility (Fig. 96) to the Uhlmann visibility (Fig. 20) for the *eleven*-level Gibbsian systems

## X. SUMMARY

We have reported an in-depth study here of two different methodologies for determining geometric phases for *mixed* states [1,2]. The analysis has been framed in terms of rotations ( $O(3)$ -orbits) of  $n$ -level Gibbsian systems, as originally proposed by Uhlmann [3].

There are, of course, many features in these results. One of these is that the Sjöqvist *et al* geometric phases (sec. VI) appear to be less sensitive to the inverse temperature parameter ( $\alpha$ ) than do the Uhlmann geometric phases (sec. II).

In particular, we have found (sec. IV) that as the number of levels of the Gibbsian density matrices increases (in the sample we have studied) from  $n = 2$  to 11, the Uhlmann methodology often yields simple monotonic behavior. On the other hand, this seems to be largely absent using the Sjöqvist *et al* methodology (sec. VIII), which appears among other things to be sensitive to the bosonic (odd  $n$ ) or fermionic (even  $n$ ) character of the system under consideration,

It is certainly important to note that if one sets the parameter  $a$  — given in (4) — equal to zero in the approach of Uhlmann (sec. I), the resulting holonomy invariant (7) is simply *equal* to  $(-1)^{n+1}$  times the holonomy invariant of Sjöqvist *et al* [1, eq. (15)]. This would appear to help to explain the added complexity of the plots of the Uhlmann geometric phases (sec. II) vis-à-vis those of the Sjöqvist *et al* plots (sec. VI).

We have found compelling numerical evidence that for odd  $n$  the central ( $\lceil \frac{n}{2} \rceil$ -th) of the  $n$  eigenvalues (ordered in terms of absolute value) of the Uhlmann holonomy invariant (7) is always a real number (sec. V C). (By the fundamental theorem of algebra, for odd  $n$ , one of the  $n$  eigenvalues must of course be real — since complex roots come in conjugate pairs — but clearly not necessarily the centrally located eigenvalue.) Also, the ( $\lceil \frac{n}{2} \rceil, \lceil \frac{n}{2} \rceil$ )-entry of the Uhlmann holonomy invariant (7) is itself real, for odd  $n$ . In terms of absolute values, the diagonal entries of the invariant (7) appear to be always monotonically decreasing from the (upper left) (1,1)-entry to the (lower right) ( $n, n$ )-entry. (We note that the angular momentum operator  $J_z$  — entering in our equations (2), (4) and (15) — itself has declining [real] diagonal entries, that is,  $n - 1/over2, \dots, -\frac{n-1}{2}$ .)

## ACKNOWLEDGMENTS

I would like to express appreciation to the Institute for Theoretical Physics for computational support in this research.

- 
- [1] E. Sjöqvist, A. K. Pati, A. Ekert, J. S. Anandan, M. Ericsson, D. K. L. Oi and V. Vedral, Phys. Rev. Lett. 85, 2845 (2000).
  - [2] A. Uhlmann, in Nonlinear, Dissipative, Irreversible Quantum Systems, edited by H.-D. Doebner, V. K. Dobrev and P. Nattermann, (Clausthal, 1994).
  - [3] A. Uhlmann, in *Symmetries in Science VI*, edited by B. Gruber, (Plenum, New York, 1993), p. 741.
  - [4] P. B. Slater, e-print, math-ph/0111014.
  - [5] J. Dittmann and A. Uhlmann, J. Math. Phys. 40, 3246-67 (1999).
  - [6] R. Jackiw, Intl. J. Mod. Phys. A 3, 285-297 (1989).

## List of Figures

1	Uhlmann geometric phase for Gibbsian spin- $\frac{1}{2}$ systems . . . . .	3
2	Uhlmann geometric phase for Gibbsian spin-1 systems . . . . .	4
3	Uhlmann geometric phase for Gibbsian spin- $\frac{3}{2}$ systems . . . . .	4
4	Uhlmann geometric phase for Gibbsian spin-2 systems . . . . .	5
5	Uhlmann geometric phase for Gibbsian spin- $\frac{5}{2}$ systems . . . . .	5
6	Uhlmann geometric phase for Gibbsian spin-3 systems . . . . .	6
7	Uhlmann geometric phase for Gibbsian spin- $\frac{7}{2}$ systems . . . . .	6
8	Uhlmann geometric phase for Gibbsian spin-4 systems . . . . .	7
9	Uhlmann geometric phase for Gibbsian spin- $\frac{9}{2}$ systems . . . . .	7
10	Uhlmann geometric phase for Gibbsian spin-5 systems . . . . .	8
11	Uhlmann visibility for Gibbsian spin- $\frac{1}{2}$ systems . . . . .	8
12	Uhlmann visibility for Gibbsian spin-1 systems . . . . .	9
13	Uhlmann visibility for Gibbsian spin- $\frac{3}{2}$ systems . . . . .	9
14	Uhlmann visibility for Gibbsian spin-2 systems . . . . .	10
15	Uhlmann visibility for Gibbsian spin- $\frac{5}{2}$ systems . . . . .	10
16	Uhlmann visibility for Gibbsian spin-3 systems . . . . .	11
17	Uhlmann visibility for Gibbsian spin- $\frac{7}{2}$ systems . . . . .	11
18	Uhlmann visibility for Gibbsian spin-4 systems . . . . .	12
19	Uhlmann visibility for Gibbsian spin- $\frac{9}{2}$ -systems . . . . .	12
20	Uhlmann visibility for Gibbsian spin-5 systems . . . . .	13
21	Uhlmann geometric phases for $n$ -level Gibbsian systems ( $n = 2, \dots, 11$ ) holding $\alpha = 1$ . The curve for $n = 2$ dominates that for $n = 3$ , which dominates that for $n = 4, \dots$ . . . . .	14
22	Uhlmann geometric phases for $n$ -level Gibbsian systems ( $n = 2, \dots, 11$ ) holding $\theta$ fixed at $\frac{\pi}{10}$ . The curve for $n = 2$ dominates that for $n = 3$ , which dominates that for $n = 4, \dots$ . . . . .	14
23	Uhlmann visibilities for $n$ -level Gibbsian systems ( $n = 2, \dots, 11$ ) holding $\alpha$ fixed at 2. The curve for $n = 2$ dominates that for $n = 3$ , which dominates that for $n = 4, \dots$ . . . . .	15
24	Uhlmann geometric phases for $n$ -level Gibbsian systems ( $n = 2, \dots, 11$ ) holding $\alpha = 2$ . Only below $\theta \approx .65$ does the curve for $n = 2$ dominate that for $n = 3$ , which dominates that for $n = 4, \dots$ . . . . .	15
25	Uhlmann geometric phases for $n$ -level Gibbsian systems ( $n = 2, \dots, 11$ ) holding $\theta = \frac{\pi}{5}$ . Only below $\alpha \approx 2$ does the curve for $n = 2$ dominate that for $n = 3$ , which dominates that for $n = 4, \dots$ . . . . .	16
26	Uhlmann visibilities for $n$ -level Gibbsian systems ( $n = 2, \dots, 11$ ) fixing $\theta = \frac{\pi}{2}$ . At $\alpha = 2.1$ , the values of $\nu$ monotonically decline as $n$ increases. The highest peak belongs to $n = 2$ . . . . .	16
27	Argument of the trace of the <i>second</i> power of the holonomy invariant (7) for the two-level Gibbsian systems ( $n = 2$ ) . . . . .	17
28	Absolute value of the trace of the <i>second</i> power of the holonomy invariant (7) for the <i>two</i> -level Gibbsian systems ( $n = 2$ ) . . . . .	17

29	Argument of the trace of the <i>second</i> power of the holonomy invariant (7) for the <i>three</i> -level Gibbsian systems ( $n = 3$ ) . . . . .	18
30	Absolute value of the trace of the <i>second</i> power of the holonomy invariant (7) for the <i>three</i> -level Gibbsian systems ( $n = 3$ ) . . . . .	18
31	Argument of the trace of the <i>third</i> power of the holonomy invariant (7) for the <i>three</i> -level Gibbsian systems ( $n = 3$ ) . . . . .	19
32	Absolute value of the trace of the <i>third</i> power of the holonomy invariant (7) for the <i>three</i> -level Gibbsian systems ( $n = 3$ ) . . . . .	19
33	Argument of the trace of the <i>second</i> power of the holonomy invariant (7) for the <i>four</i> -level Gibbsian systems ( $n = 4$ ) . . . . .	20
34	Absolute value of the trace of the <i>second</i> power of the holonomy invariant (7) for the <i>four</i> -level Gibbsian systems ( $n = 4$ ) . . . . .	20
35	Argument of the trace of the <i>third</i> power of the holonomy invariant (7) for the <i>four</i> -level Gibbsian systems ( $n = 4$ ) . . . . .	21
36	Absolute value of the trace of the <i>third</i> power of the holonomy invariant (7) for the <i>four</i> -level Gibbsian systems ( $n = 4$ ) . . . . .	21
37	Argument of the trace of the <i>fourth</i> power of the holonomy invariant (7) for the <i>four</i> -level Gibbsian systems ( $n = 4$ ) . . . . .	22
38	Absolute value of the trace of the <i>fourth</i> power of the holonomy invariant (7) for the <i>four</i> -level Gibbsian systems ( $n = 4$ ) . . . . .	22
39	Argument of the trace of the <i>second</i> power of the holonomy invariant (7) for the <i>five</i> -level Gibbsian systems ( $n = 5$ ) . . . . .	23
40	Absolute value of the trace of the <i>second</i> power of the holonomy invariant (7) for the <i>five</i> -level Gibbsian systems ( $n = 5$ ) . . . . .	23
41	Argument of the trace of the <i>third</i> power of the holonomy invariant (7) for the <i>five</i> -level Gibbsian systems ( $n = 5$ ) . . . . .	24
42	Absolute value of the trace of the <i>third</i> power of the holonomy invariant (7) for the <i>five</i> -level Gibbsian systems ( $n = 5$ ) . . . . .	24
43	Argument of the trace of the <i>fourth</i> power of the holonomy invariant (7) for the <i>five</i> -level Gibbsian systems ( $n = 5$ ) . . . . .	25
44	Absolute value of the trace of the <i>fourth</i> power of the holonomy invariant (7) for the <i>five</i> -level Gibbsian systems ( $n = 5$ ) . . . . .	25
45	Argument of the trace of the <i>fifth</i> power of the holonomy invariant (7) for the <i>five</i> -level Gibbsian systems ( $n = 5$ ) . . . . .	26
46	Absolute value of the trace of the <i>fifth</i> power of the holonomy invariant (7) for the <i>five</i> -level Gibbsian systems ( $n = 5$ ) . . . . .	26
47	Argument of the trace of the <i>second</i> power of the holonomy invariant (7) for the <i>six</i> -level Gibbsian systems ( $n = 6$ ) . . . . .	27
48	Absolute value of the trace of the <i>second</i> power of the holonomy invariant (7) for the <i>six</i> -level Gibbsian systems ( $n = 6$ ) . . . . .	27
49	Argument of the trace of the <i>third</i> power of the holonomy invariant (7) for the <i>six</i> -level Gibbsian systems ( $n = 6$ ) . . . . .	28
50	Absolute value of the trace of the <i>third</i> power of the holonomy invariant (7) for the <i>six</i> -level Gibbsian systems ( $n = 6$ ) . . . . .	28
51	Argument of the trace of the <i>fourth</i> power of the holonomy invariant (7) for the <i>six</i> -level Gibbsian systems ( $n = 6$ ) . . . . .	29
52	Absolute value of the trace of the <i>fourth</i> power of the holonomy invariant (7) for the <i>six</i> -level Gibbsian systems ( $n = 6$ ) . . . . .	29
53	Argument of the trace of the <i>fifth</i> power of the holonomy invariant (7) for the <i>six</i> -level Gibbsian systems ( $n = 6$ ) . . . . .	30
54	Absolute value of the trace of the <i>fifth</i> power of the holonomy invariant (7) for the <i>six</i> -level Gibbsian systems ( $n = 6$ ) . . . . .	30
55	Ratio of the argument of the trace of the second power of the holonomy invariant (7) to the argument of the trace of the first power for the <i>eight</i> -level Gibbsian systems . . . . .	31
56	Ratio of the absolute value of the trace of the second power of the holonomy invariant (7) to the absolute value of the trace of the first power for the <i>eight</i> -level Gibbsian systems . . . . .	31



57	Ratio of the argument of the trace of the third power of the holonomy invariant (7) to the argument of the trace of the second power for the <i>eight</i> -level Gibbsian systems . . . . .	32
58	Ratio of the absolute value of the trace of the third power of the holonomy invariant (7) to the absolute value of the trace of the second power for the <i>eight</i> -level Gibbsian systems . . . . .	32
59	Argument of the dominant eigenvalue of the Uhlmann holonomy invariant (7) for the <i>two</i> -level Gibbsian density matrices . . . . .	33
60	Argument of the subordinate eigenvalue of the Uhlmann holonomy invariant (7) for the <i>two</i> -level Gibbsian density matrices . . . . .	33
61	Absolute value of the dominant eigenvalue of the Uhlmann holonomy invariant (7) for the <i>two</i> -level Gibbsian density matrices . . . . .	34
62	Absolute value of the subordinate eigenvalue of the Uhlmann holonomy invariant (7) for the <i>two</i> -level Gibbsian density matrices . . . . .	34
63	Argument of the dominant eigenvalue of the Uhlmann holonomy invariant (7) for the <i>three</i> -level Gibbsian density matrices . . . . .	35
64	Argument of the subordinate eigenvalue of the Uhlmann holonomy invariant (7) for the <i>three</i> -level Gibbsian density matrices . . . . .	35
65	Absolute value of the dominant eigenvalue of the Uhlmann holonomy invariant (7) for the <i>three</i> -level Gibbsian density matrices . . . . .	36
66	Intermediate eigenvalue of the Uhlmann holonomy invariant (7) for the <i>three</i> -level Gibbsian density matrices . . . . .	36
67	Absolute value of the subordinate eigenvalue of the Uhlmann holonomy invariant (7) for the <i>three</i> -level Gibbsian density matrices . . . . .	37
68	Argument of the leading eigenvalue of the Uhlmann holonomy invariant (7) for the <i>five</i> -level Gibbsian density matrices . . . . .	37
69	Argument of the second leading eigenvalue of the Uhlmann holonomy invariant (7) for the <i>five</i> -level Gibbsian density matrices . . . . .	38
70	Argument of the second smallest eigenvalue of the Uhlmann holonomy invariant (7) for the <i>five</i> -level Gibbsian density matrices . . . . .	38
71	Argument of the last eigenvalue of the Uhlmann holonomy invariant (7) for the <i>five</i> -level Gibbsian density matrices . . . . .	39
72	Absolute value of the leading eigenvalue of the Uhlmann holonomy invariant (7) for the <i>five</i> -level Gibbsian density matrices . . . . .	39
73	Absolute value of the second leading eigenvalue of the Uhlmann holonomy invariant (7) for the <i>five</i> -level Gibbsian density matrices . . . . .	40
74	Central eigenvalue of the Uhlmann holonomy invariant (7) for the <i>five</i> -level Gibbsian density matrices . . . . .	40
75	Absolute value of the second smallest eigenvalue of the Uhlmann holonomy invariant (7) for the <i>five</i> -level Gibbsian density matrices . . . . .	41
76	Absolute value of the last eigenvalue of the Uhlmann holonomy invariant (7) for the <i>five</i> -level Gibbsian density matrices . . . . .	41
77	Sjöqvist <i>et al</i> geometric phase for Gibbsian spin- $\frac{1}{2}$ systems . . . . .	42
78	Sjöqvist <i>et al</i> geometric phase for Gibbsian spin-1 systems . . . . .	43
79	Sjöqvist <i>et al</i> geometric phase for Gibbsian spin- $\frac{3}{2}$ systems . . . . .	43
80	Sjöqvist <i>et al</i> geometric phase for Gibbsian spin-2 systems . . . . .	44
81	Sjöqvist <i>et al</i> geometric phase for Gibbsian spin- $\frac{5}{2}$ systems . . . . .	44
82	Sjöqvist <i>et al</i> geometric phase for Gibbsian spin-3 systems . . . . .	45
83	Sjöqvist <i>et al</i> geometric phase for Gibbsian spin- $\frac{7}{2}$ systems . . . . .	45
84	Sjöqvist <i>et al</i> geometric phase for Gibbsian spin-4 systems . . . . .	46
85	Sjöqvist <i>et al</i> geometric phase for Gibbsian spin- $\frac{9}{2}$ systems . . . . .	46
86	Sjöqvist <i>et al</i> geometric phase for Gibbsian spin-5 systems . . . . .	47
87	Sjöqvist <i>et al</i> visibility for Gibbsian spin- $\frac{1}{2}$ systems . . . . .	48
88	Sjöqvist <i>et al</i> visibility for Gibbsian spin-1 systems . . . . .	49
89	Sjöqvist <i>et al</i> visibility for Gibbsian spin- $\frac{3}{2}$ systems . . . . .	49
90	Sjöqvist <i>et al</i> visibility for Gibbsian spin-2 systems . . . . .	50
91	Sjöqvist <i>et al</i> visibility for Gibbsian spin- $\frac{5}{2}$ systems . . . . .	50
92	Sjöqvist <i>et al</i> visibility for Gibbsian spin-3 systems . . . . .	51
93	Sjöqvist <i>et al</i> visibility for Gibbsian spin- $\frac{7}{2}$ systems . . . . .	51

94	Sjöqvist <i>et al</i> visibility for Gibbsian spin-4 systems . . . . .	52
95	Sjöqvist <i>et al</i> visibility for Gibbsian spin- $\frac{9}{2}$ systems . . . . .	52
96	Sjöqvist <i>et al</i> visibility for Gibbsian spin-5 systems . . . . .	53
97	Sjöqvist <i>et al</i> geometric phases for $n$ -level Gibbsian systems ( $n = 2, \dots, 11$ ) holding $\alpha = 1$ . At $\theta = .25$ , the curve for $n = 2$ is dominant, followed in order by those for $n = 4, 6, 8, 10$ , (all having <i>positive</i> values at $\theta = .25$ ) and $n = 3, 5, 7, 9, 11$ (all having <i>negative</i> values at $\theta = .25$ ), cf. Fig. 21 . . . . .	53
98	Sjöqvist <i>et al</i> geometric phases for $n$ -level Gibbsian systems ( $n = 2, \dots, 11$ ) holding $\theta$ fixed at $\frac{\pi}{10}$ . In monotonically decreasing order are the curves for (the even) $n = 2, 4, 6, 8, 10$ , followed by those for (the odd) $n = 3, 5, 7, 9, 11$ , cf. Fig. 22 . . . . .	54
99	Sjöqvist <i>et al</i> visibilities for $n$ -level Gibbsian systems ( $n = 2, \dots, 11$ ) holding $\alpha$ fixed at 2. The curve for $n = 2$ stands out from the other nine, cf. Fig. 23 . . . . .	54
100	Sjöqvist <i>et al</i> geometric phases for $n$ -level Gibbsian systems ( $n = 2, \dots, 11$ ) holding $\alpha = 2$ . In order of decreasing dominance at $\theta = .25$ are the curves for (the even) $n = 2, 4, 6, 8, 10$ , followed by those for (the odd) $n = 3, 5, 7, 9, 11$ , cf. Fig. 24 . . . . .	54
101	Sjöqvist <i>et al</i> geometric phases for $n$ -level Gibbsian systems ( $n = 2, \dots, 11$ ) holding $\theta = \frac{\pi}{5}$ . At $\alpha = 2$ , in order of decreasing dominance are the curves for $n = 7, 2, 9, 4, 11, 6, 8, 3, 10, 5$ , cf. Fig. 25 . . . . .	55
102	Ratio of the Sjöqvist <i>et al</i> geometric phase (Fig. 81) to the Uhlmann geometric phase (Fig. 5) for <i>six</i> -level Gibbsian systems . . . . .	55
103	Ratio of the Sjöqvist <i>et al</i> geometric phase (Fig. 86) to the Uhlmann geometric phase (Fig. 10) for the <i>eleven</i> -level Gibbsian systems . . . . .	56
104	Ratio of the Sjöqvist <i>et al</i> visibility (Fig. 91) to the Uhlmann visibility (Fig. 15) for the <i>six</i> -level Gibbsian systems . . . . .	56
105	Ratio of the Sjöqvist <i>et al</i> visibility (Fig. 96) to the Uhlmann visibility (Fig. 20) for the <i>eleven</i> -level Gibbsian systems . . . . .	57